

**IN-MILL CORROSION MONITORING  
IN KRAFT WHITE LIQUOR**

**Project 3556**

**Report Four  
A Progress Report  
to  
MEMBERS OF THE INSTITUTE OF PAPER CHEMISTRY**

**November 15, 1985**

#### NOTICE & DISCLAIMER

The Institute of Paper Chemistry (IPC) has provided a high standard of professional service and has exerted its best efforts within the time and funds available for this project. The information and conclusions are advisory and are intended only for the internal use by any company who may receive this report. Each company must decide for itself the best approach to solving any problems it may have and how, or whether, this reported information should be considered in its approach.

IPC does not recommend particular products, procedures, materials, or services. These are included only in the interest of completeness within a laboratory context and budgetary constraint. Actual products, procedures, materials, and services used may differ and are peculiar to the operations of each company.

In no event shall IPC or its employees and agents have any obligation or liability for damages, including, but not limited to, consequential damages, arising out of or in connection with any company's use of, or inability to use, the reported information. IPC provides no warranty or guaranty of results.

THE INSTITUTE OF PAPER CHEMISTRY

Appleton, Wisconsin

IN-MILL CORROSION MONITORING IN KRAFT WHITE LIQUOR

Project 3556

Report Four

A Progress Report

to

MEMBERS OF THE INSTITUTE OF PAPER CHEMISTRY

November 15, 1985

## TABLE OF CONTENTS

	Page
ABSTRACT	1
SUMMARY FOR THE NONSPECIALIST	2
INTRODUCTION	3
EXPERIMENTAL PROCEDURES	6
RESULTS	11
Linear Polarization Resistance	11
Electrical Resistance	18
Polarization Behavior	20
DISCUSSION	23
Electrical Resistance	23
Linear Polarization Resistance	23
Liquor Effects	28
Materials Comparison	29
Industrial Significance	30
CONCLUSIONS	33
ACKNOWLEDGMENT	34
REFERENCES	35
APPENDIX I: CORROSION RATE AND CORROSION POTENTIAL DURING LPR TESTS	37
APPENDIX II: POLARIZATION CURVES	95

THE INSTITUTE OF PAPER CHEMISTRY

Appleton, Wisconsin

IN-MILL CORROSION MONITORING IN KRAFT WHITE LIQUOR

ABSTRACT

Corrosion rates in white liquor tanks and clarifiers at four pulp mills have been monitored during exposure periods of approximately one month by means of weight loss coupons, the electrical resistance technique, and an electrochemical method called the linear polarization resistance technique. Polarization curves also were obtained in the mills. Four grades of carbon steel were studied. They were, in order of decreasing corrosion rate: 1018, A285C, A283, and A285-SPECIAL. Liquor samples were obtained when the corrosion rate exceeded a set level, but high corrosion rate did not correlate with significant change in the liquor composition. Differences in liquor composition accounted for some of the difference between mills. Liquor velocity was observed to significantly affect corrosion rates.

## SUMMARY FOR THE NONSPECIALIST

Corrosion by kraft white liquor is recognized to be a costly problem, resulting in decreased lifetime of operating equipment and unexpected failures. Replacement costs for white liquor clarifiers can be as high as \$200,000. There is a need to identify the factors which increase the corrosion rates. Plant monitoring can help to determine the sources of increased corrosion rates. This is the first step toward eventual control of high corrosion rates.

The objective of the present work was to validate corrosion monitoring methods for use in mills, to use these for a study of the effects of liquor changes on relative corrosion rates of four carbon steels, and to test the monitoring equipment in the mill.

Corrosion rates measured in the field by weight loss coupon and electrical resistance methods showed satisfactory agreement. Measurements by the linear polarization resistance technique were in reasonable agreement with weight loss and electrical resistance results if an appropriate correction factor was applied. There was considerable variation in corrosion rate between mills, which could be partly explained by differences in liquor composition. Velocity differences may have had a significant influence on differences; corrosion rates were much higher in storage tanks, as compared to clarifiers, where flow velocities are lower. Temperature and unidentified liquor constituents may have had significant effects, also.

Corrosion rates were determined for four test materials. In order of decreasing corrosion rate, the materials were 1018, A285C, A283, and A285-SPECIAL.

## INTRODUCTION

Corrosion studies in mill white liquors have been conducted in the past using weight loss coupons in mills<sup>1,2</sup> and by testing in the laboratory.<sup>3-5</sup> Continuous corrosion monitoring methods have not been described, although they are used frequently in other industries.

In an effort to qualify monitoring techniques for use in white liquors, Yeske<sup>6</sup> described the validation of the linear polarization resistance and electrical resistance techniques for corrosion measurements in white liquors. A brief explanation of these methods is in order.

In the linear polarization resistance (LPR) technique, the electrode is displaced from its rest potential by  $\pm 10$  mV by means of a potential controller called a potentiostat. The applied potential is measured with respect to a reference electrode. The ratio of current required to apply this potential and the applied potential itself is proportional to the corrosion rate (C.R.) in mils per year (mpy) according to:

$$\text{C.R.} = 1/(2.3F) (\beta/z) (\text{MW/d}) (\Delta i/\Delta E) \quad (1)$$

where  $F$  is Faraday's constant (96,500 coulombs/mole of electrons),  $\Delta E$  is applied potential,  $\Delta i$  is induced current density,  $z$  is the number of electrons released when a metal atom is dissolved,  $\text{MW}$  is the molecular weight (g/mol),  $d$  is the density ( $\text{g/cm}^3$ ) of the steel. The factor  $\beta$  is given by:

$$\beta = \beta_A * \beta_C / (\beta_A + \beta_C) \quad (2)$$

where  $\beta_A$  and  $\beta_C$  are Tafel constants which are measured from polarization curves and describe the anodic and cathodic reaction processes. The name 'linear polarization resistance' arises from the last term in Eq. (1),  $(\Delta i/\Delta E)$ , which

has the units of electrical resistance. Yeske<sup>6</sup> has described the derivation of Eq. (1) in more detail. The linear polarization resistance technique has been reviewed by others.<sup>7,8</sup>

Both  $\beta$  and  $z$  are unknown and must be assigned values. Yeske used a value of  $z = 2$  but indicated that  $z$  may be 3 if  $\text{NaFeS}_2$  is formed as a corrosion product in white liquors containing large amounts of thiosulfate. Often, in the absence of proper data,  $\beta_A$  and  $\beta_C$  are assigned values of 100 mV. The instrument used in the present study, a Petrolite M1010, uses hardwired values of  $\beta = 83.3$  and  $z = 2$ . For linear polarization resistance measurements in simulated white liquor, Singbeil and Tromans<sup>9</sup> assumed  $\beta_C$  to be 145 mV, a value published for hydrogen evolution.<sup>10</sup> They adopted a value of 72 mV for  $\beta_A$  for iron dissolution.<sup>11</sup> In a large number of polysulfide liquors, average values of  $\beta_A = 64$  mV and  $\beta_C = 128$  mV were measured.<sup>12</sup> The accuracy of the linear polarization measurement depends on the values assigned to the ratio  $\beta/z$  in the corrosion rate equation. Empirically derived values of  $\beta/z$  parameters were obtained by Yeske<sup>6</sup> for evaluating corrosion rates in several simulated white liquors. The empirical factor was applicable in stagnant liquor, but was not appropriate in high flow situations.<sup>6</sup> Significant errors in measured corrosion rates were associated with sulfide oxidation in the liquor above 100 mV(SSSE) (vs. the silver/silver sulfide reference electrode<sup>13</sup>). Thick iron sulfides on the surface had little effect. The empirical factor was supported by measurements of anodic and cathodic Tafel slopes ( $\beta_A = 49$  and  $\beta_C = 118$ , giving  $\beta = 34.6$  mV). For  $z = 2$ ,  $\beta/z$  equaled 17.3 mV, which agreed well with values required to bring LPR results into agreement with weight loss measurements. It was suggested that higher values would be required in vigorously stirred liquors. Despite this difficulty with unknown constants in the corrosion rate equation, the LPR



technique is very useful because it can provide a measurement of the instantaneous corrosion rate.

The electrical resistance (ER) technique is an alternative electrical method which measures cumulative corrosion. A wire element of the steel of interest is exposed in solution and an electrical current is passed through it. As corrosion reduces the wire's cross section, the resistance increases in proportion to loss of material due to corrosion. The measured resistance may be affected by temperature fluctuations and by build-up of conductive corrosion products. A dummy element in the probe is designed to correct for temperature fluctuations. One drawback of the (ER) method is that it is not an instantaneous measurement of corrosion rate and thus cannot indicate occurrence of brief fluctuations in corrosion rate associated with process upsets. This disadvantage is offset by the ease of operation which makes this method most acceptable to mill personnel.

These corrosion measurement methods have been applied in mills and compared with results from weight loss tests of coupons as described in this report. Corrosion rates of four materials were examined. These were compared with the results of Wensley and Charlton,<sup>2</sup> which showed that steels containing Cu, Cr, and Ni had lower corrosion rates in white liquors, but that Si was detrimental. It is worth noting that they found the effect of steel composition to be small compared to the effect of liquor composition in determining the corrosion rate.

The present study was aimed at obtaining corrosion data in white liquors on a continuous basis in operating equipment to identify the reasons for periods of high corrosion rate (presumably due to liquor changes) and was to demonstrate the use of various methods for corrosion monitoring.

## EXPERIMENTAL PROCEDURES

Weight loss coupons were cylindrical specimens 3/8-inch in diameter with a surface area of 9 cm<sup>2</sup>. Prior to testing, they were polished to 120 grit, degreased and weighed. The coupons were threaded onto glass-to-metal seals on a probe as shown in Fig. 1, with Hypalon gaskets between the samples and seals. The probe contained ten electrodes: eight for linear polarization resistance (LPR) and weight loss testing, two silver/silver sulfide (SSSE) reference electrodes, and two additional weight loss specimens. Testing was performed on 1018, A285C, A283, and A285-SPECIAL steels of composition as listed in Table 1. During testing, the probe was suspended through a manhole in the roof of the tank or clarifier. After the test, the specimens were carefully blasted clean (glass beads) and weighed (as described in a previous report.<sup>12</sup>

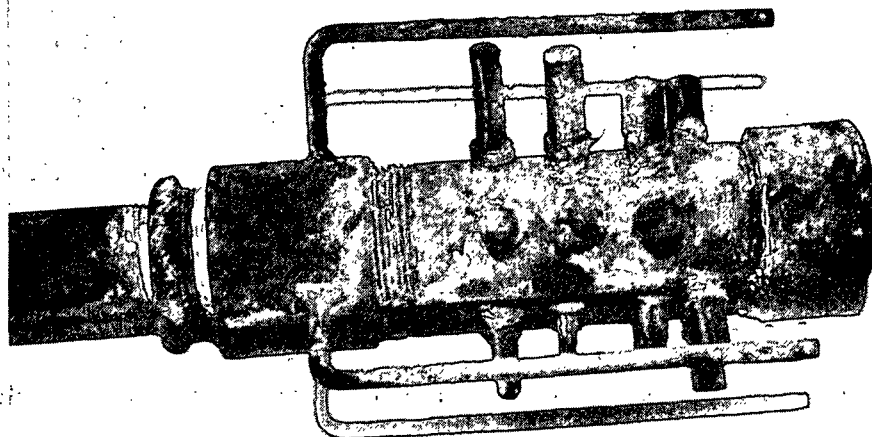


Figure 1. Probe used for LPR and weight loss electrodes. The three arms on the side are to protect the electrodes.

Table 1. Composition of steels tested.

Steel	C	Mn	P	S	Si	Ni	Cr	Cu	Fe
1018	0.16	0.69	0.018	0.031	0.26	0.03	0.10	0.15	bal
A285C	0.20	0.43	0.010	0.021					bal
A283	0.16	0.49	0.012	0.023	0.02	0.01	0.01	0.01	bal
A285SPEC	0.18	0.65	0.019	0.020	0.02	0.01	0.01	0.27	bal

All measured potentials have been quoted with respect to the silver/silver sulfide electrode, V(SSSE). These may be converted to the standard hydrogen scale, V(SHE), via the empirical equation:

$$V(SHE) = V(SSSE) - 0.7125 - 0.039 \log([Na_2S]/858) \quad (2)$$

where  $[Na_2S]$  is the sodium sulfide concentration in g/L, as described previously.<sup>13</sup>

The linear polarization resistance measurements were recorded by a 10-channel Petrolite M1010 instrument. It is programmed to impose alternate +/- 10 mV polarizations of 15-minute duration on each of eight electrodes. Measurements were made of polarization resistance for both the anodic and cathodic directions. A sample of the output is illustrated in Fig. 2. The current required to maintain the 10-mV polarization at the end of each 15-minute polarization cycle was converted by the instrument into an electrical signal proportional to the corrosion rate in mils per year (mpy) according to Eq. (1). This long polarization period was required to ensure that the current had stabilized. The  $\beta/z$  value hardwired into the Petrolite instrument (41.65 mV) was considered to be inappropriate for white liquor, and an adjustment was required. The correction factor for white liquor was determined previously<sup>6</sup> to be:

$$C.R.(actual) = C.R.(measured)/2.8$$

(4)

where C.R. is corrosion rate measured in mpy (mils per year). A different conversion may be required for brands of instruments other than Petrolite. These measurements of corrosion rate were plotted vs. time. Electrodes were of the same design as for the weight loss test and were prepared in the same way. The LPR results were recorded on charts, and data were input manually to a computer file for subsequent use.

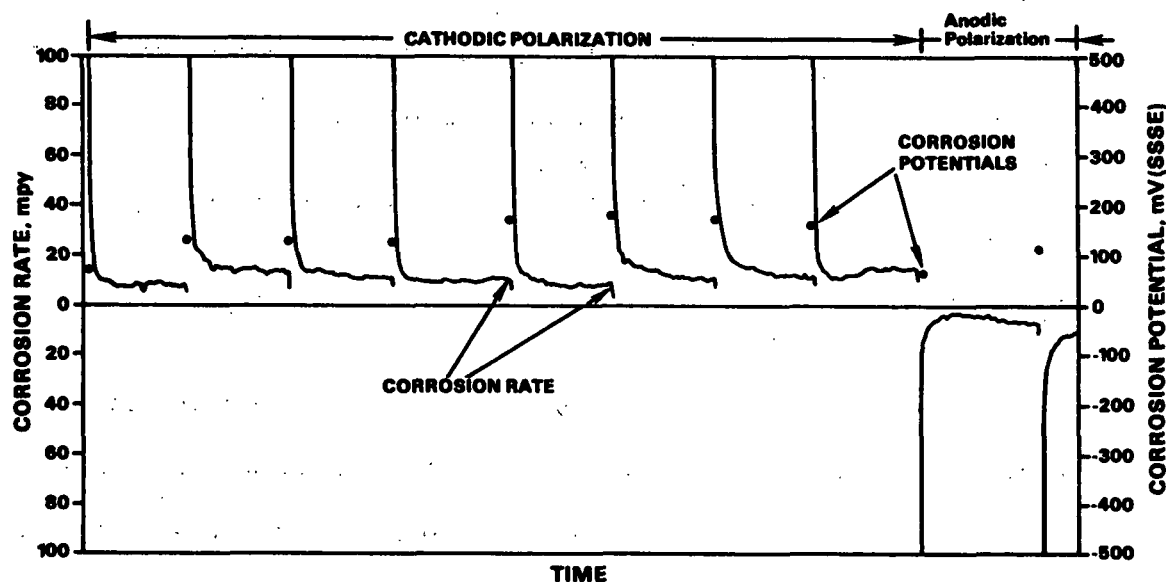


Figure 2. Sample of linear polarization resistance output from the Petrolite M1010.

The electrical resistance instrument was a Rohrbach Corrosometer 4000. Figure 3 illustrates the test element of this probe, which was a single loop of 1020 steel wire (probe Type W80). The Corrosometer provided a continuous digital indication of the normalized loss of wire cross section due to corrosion. The measurement of electrical resistance was recorded daily by mill personnel. These measurements were converted to an average corrosion rate by calculating the loss of wire thickness divided by the total exposure time according to the equation:

$$\text{mpy} = \frac{\Delta R (365) P}{\Delta t (1000)} \quad (5)$$

where  $\Delta R$  is the change in dial reading and  $\Delta t$  is the exposure time in days. The factor  $P$  is a probe range multiplier factor. Electrical resistance (ER) tests were performed at the last two mills only (T3 and C4).

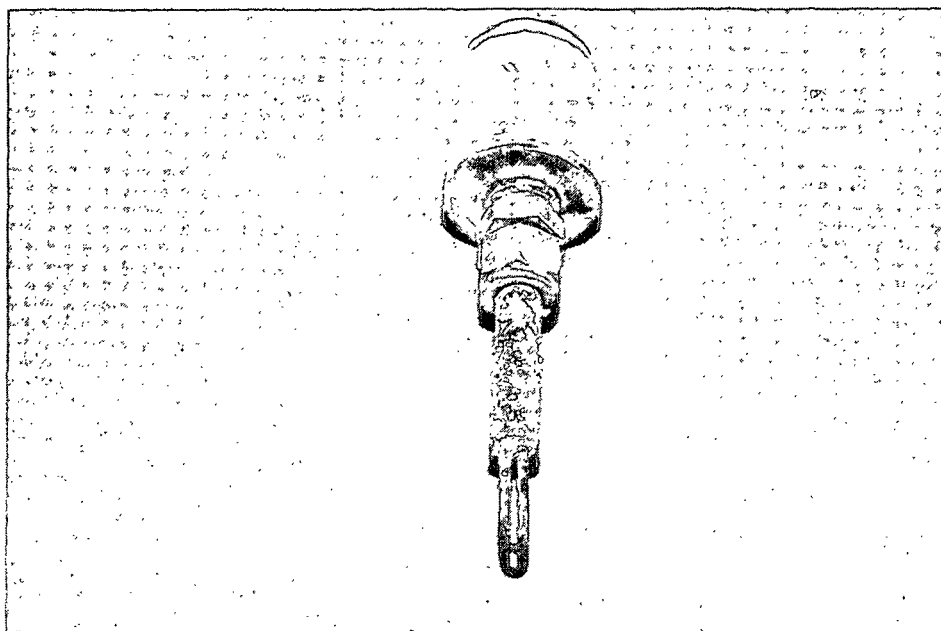


Figure 3. The electrical resistance test element.

An automatic liquor sampling device was installed to obtain liquors for analysis in the event of an excursion in corrosion rate. Liquor was pumped from the tank and circulated through a valved sample bottle via the system illustrated schematically in Fig. 4. When the corrosion rate exceeded a set point (75 mpy) on one of the 1018 electrodes used for LPR measurements, the valves automatically operated, and a sample of the liquor was retained in the sample bottle. Samples were returned to the Institute for acidimetric analysis of NaOH, Na<sub>2</sub>S, and Na<sub>2</sub>CO<sub>3</sub>, potentiometric titration of Na<sub>2</sub>S<sub>x</sub>, and ion chromatographic analysis of Na<sub>2</sub>SO<sub>3</sub>, Na<sub>2</sub>S<sub>2</sub>O<sub>3</sub>, and Na<sub>2</sub>SO<sub>4</sub> to determine whether high corrosion rate was

associated with any liquor constituents. Concentrations of dissolved metals were measured by emission spectrographic analysis.

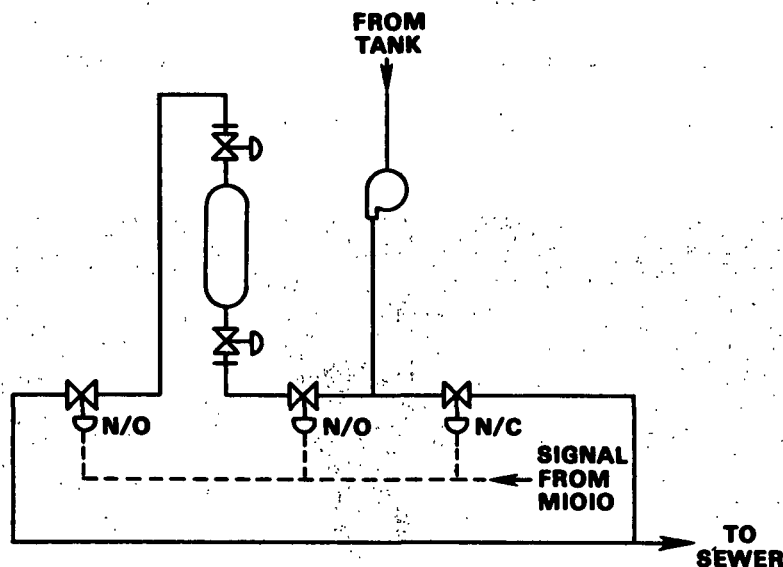


Figure 4. Schematic diagram of liquor sampling apparatus.

Polarization curves were obtained with a Petrolite Potentiodyne portable potentiostat. Scan rates of 0.1 mV/s were employed at mills B1 and W2, and a rate of 0.60 V/hour was adopted at mill C4. The 0.6 V/h scan rate was the standard value chosen by N.A.C.E. Task Group T5H-11 for polarization testing in kraft pulping liquor. All measured potentials are quoted with respect to the silver/silver sulfide electrode (SSSE).

Mill B1 tests were performed in a white liquor tank where level fluctuated by as much as 16 feet. Tests at the second mill, W2, were performed in a clarifier which was always full and quiescent. Mill T3 tests were done in a white liquor day tank, under fairly turbulent conditions. Relatively quiet conditions were encountered at the last mill, C4, in a clarifier.

## RESULTS

## LINEAR POLARIZATION RESISTANCE

Figure 5 illustrates the fluctuation of corrosion rate which was measured by the linear polarization resistance method. The corrosion potential is plotted on the figures for comparison and is seen to vary considerably with time. The results of all other LPR tests are contained in Appendix I. The measured values have been corrected with a factor of 2.8 according to Eq. (4).<sup>6</sup>

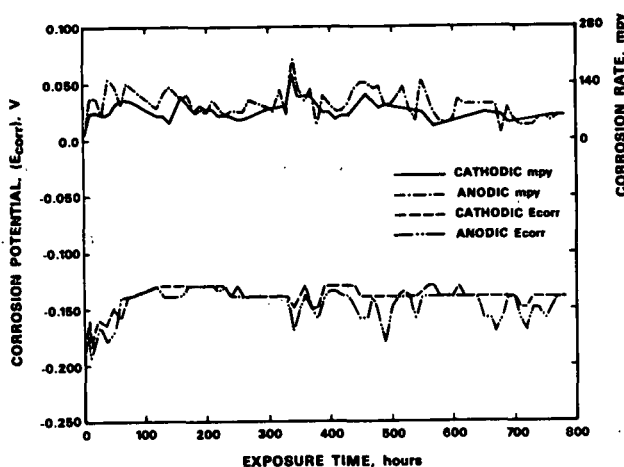


Figure 5. Corrosion rate (by LPR) during exposure at mill B1, 1018 Steel, Electrode 1.

At mill B1, the rate of corrosion of 1018 steel as determined by LPR ranged from 1 to 75 mpy and the corrosion potential ( $E_{\text{corr}}$ ) varied from -200 to -120 mV(SSSE). The A285C and A285-SPEC showed much less variation, lower corrosion rate, and  $E_{\text{corr}}$  ranging from -130 to -100 mV(SSSE). The electrodes did not all show excursions in corrosion rate at the same time. Both A283 electrodes had an excursion to 75 mpy for several hours during which the  $E_{\text{corr}}$  became active. Samples of liquor obtained during periods of high corrosion rate did not reveal any differences in composition, as summarized in Table 2.

Table 2. Liquor Analyses.

Mill	No.	NaOH	Na <sub>2</sub> S	Na <sub>2</sub> CO <sub>3</sub>	Na <sub>2</sub> S <sub>2</sub> O <sub>3</sub>	Na <sub>2</sub> SO <sub>3</sub>	Na <sub>2</sub> SO <sub>4</sub>	NaCl	Al	Mg	Fe	Cu	Si	Mn	Ca	Na
B1	1	92.0	39.2	32.5	4.9	7.1	4.0	14.8								
B1	2 <sup>a</sup>	93.9	38.8	32.0	5.4	3.8	3.3	8.5								
B1	3 <sup>a</sup>	92.9	39.6	32.5	5.3	4.4	5.1	14.8								
B1	4 <sup>a</sup>	98.7	35.7	30.0	2.9	2.9	3.2	6.2								
B1	5 <sup>a</sup>	93.4	37.8	27.2	4.5	4.9	4.3	7.3								
B1	6 <sup>a</sup>				5.0	6.2	4.4	13.0								
W2	1	92.3	41.4	26.9	3.5	3.8	3.4	1.3								
T3	1	92.9	31.5	45.1	8.0	3.36	3.76	2.24								
T3	2	91.9	44.5	41.8	7.2	7.44	7.76	—	0.18	0.0054	0.071	0.0042	0.62			100
T3	3	97.3	46.8	40.6	6.66	6.56	4.10		0.20	0.0045	0.042	0.0075	0.44			100
T3	4	100.3	39.8	24.6	4.29	3.20	5.32	1.24								
C4	1	87.1	21.7	24.9	2.38	2.32	5.24	1.20	0.0096	0.01	0.024	0.024	0.24	0.0039	0.34	81
C4	2 <sup>b</sup>	126.2	30.8	14.0	3.32	4.12	2.84	1.0								
C4	3 <sup>b</sup>	124.3	36.0	15.3	6.2	6.42	4.34	2.3								

<sup>a</sup>During a period of high corrosion rate.  
<sup>b</sup>Last week of test.

Corrosion rates at mill W2 were about one half of those at mill B1, and there was much less variation with time. The tests lasted only 400 hours due to a spill of liquor onto the Petrolite M1010 instrument. Two of the electrodes were not tested because of a poor electrical connection (probably the glass-to-metal seals). The corrosion rate rose slightly and corrosion potential fell after 250 hours for unknown reasons. The A283 steel showed less variation than in mill B1, even though the corrosion potential was variable. The 1018 showed a significant decrease in fluctuation and corrosion rate compared to mill B1. This may have been due to the reduced turbulence in mill W2 or more stable liquor chemistry.

Instrumentation difficulties at mill T3 (from damage due to the liquor spill at mill W2) resulted in loss of data for long periods (100-225 h and 475-600 h). Both corrosion rates and corrosion potential fluctuated during the tests. Corrosion potential increased during the test.



Mill C4, with a fairly quiet clarifier, experienced low corrosion rates. Gaps in the data from 225-295 h, 310-355 h, 360-475 h, and 525-700 h precluded a good understanding of the fluctuations. The corrosion potential generally increased during the test, presumably due to passivation.

Tables 3-6 summarize average LPR weight loss and corrosion potential at each mill for each electrode and weight loss measurements for the electrodes. In the LPR results, 'x' is the average LPR corrosion rate or  $E_{\text{corr}}$ , 's' is the standard deviation of the readings, and 'n' is the number of measurements. The LPR measurements from the Petrolite instrument were divided by 2.8 as recommended by Yeske.<sup>6</sup> The average corrosion potentials are tabulated to provide information on the condition of the electrode. The figures in Appendix I should be consulted for a more accurate idea of variations. Weight loss results obtained during previous tests at mill T3 were included.

The agreement between the weight loss and the average LPR corrosion rate is generally poor when a correction factor of 2.8 is used. This was especially true at mill T3 for 1018 steel, where the weight loss measurements were approximately twice the values obtained from LPR. Results for A285C, A283, and A285-SPEC were similarly inaccurate. The measurements at W2 were only slightly better for 1018 and worse for A285C. The results for mill C2 showed poor agreement between weight loss and LPR. At mill T3,  $E_{\text{corr}}$  was lower on electrodes 1-4 [-205 mV(SSSE)] than for electrodes 5-8 [-165 mV(SSSE)], but the corrosion rate was the same. Similar trouble was encountered at mill C4. The silver/silver sulfide reference electrode for electrodes 5-8 was inspected and found to be covered with a thick sulfide layer (80 % by volume of the electrode). Thus, it was probably defective, and the corrosion potentials for these electrodes are suspect.

Table 3. - Weight loss, average corrosion rates and corrosion potentials of 1018 steel exposed in the field.

Mill No.	Weight Loss, mpy		LPR Anod., mpy	LPR Cath., mpy	LPR Ave., mpy	LPR Anod., E <sub>corr</sub>	LPR Cath., E <sub>corr</sub>	LPR Ave., E <sub>corr</sub>
B1 1	29.7	x	30.3	24.9	27.6	-148	-141	-145
		s	12.0	8.5	10.3	16	13	
		n	67	43		74	73	
B1 5	34.9	x	37.7	28.8	33.3	-155	-147	-151
		s	15.0	12.4	13.7	16	14	
		n	58	27		72	70	
W2 1	15.6							
W2 5	25.0	x	19.4	8.2	13.8	-159	-169	-164
		s	9.7	5.5	7.6	15	19	
		n	30	34		34	34	
T3 1	44.2	x	22.1	12.5	17.3	-215	-213	-214
		s	9.5	6.1	7.8	51	52	
		n	79	73		91	92	
T3 5	41.2	x	20.9	13.6	17.3	-163	-164	-163
		s	10.1	6.3	8.2	43	43	
		n	79	71		90	88	
T3 <sup>a</sup>	29.4							
a	25.7							
a	30.9							
C4 1	5.8	x	3.2	3.5	3.4	-31	-27	-29
		s	1.6	1.1	1.4	20	20	
		n	63	64		64	64	
C4 5	9.2	x	4.1	3.6	3.9	-125	-126	-126
		s	1.9	1.3	1.6	20	21	
		n	62	63		62	63	

<sup>a</sup>These results are from a test program a few months earlier.

Table 4. Weight loss, average corrosion rates and corrosion potentials of A285C steel exposed in the field.

Mill No.	Weight Loss, mpy		LPR Anod., mpy	LPR Cath., mpy	LPR Ave., mpy	LPR Anod., E <sub>corr</sub>	LPR Cath., E <sub>corr</sub>	LPR Ave., E <sub>corr</sub>
B1 2	23.2	x	24.8	19.1	22	-127	-126	-126
		s	9.5	7.6	8.6	25	26	
		n	47	43		74	73	
B1 6	27.1	x	27.1	19.1	23.1	-129	-127	-128
		s	8.5	6.5	7.5	23	23	
		n	73	71		73	72	
W2 2	16.5							
W2 6	19.5	x	5.8	8.3	7.1	-164	-165	-164
		s	8.1	4.6	6.4	19	20	
		n	34	34		34	34	
T3 2	44.0	x	20.4	13.5	17.0	-207	-206	-206
		s	7.9	6.9	7.4	46	48	
		n	76	71		91	91	
T3 6	41.1	x	23.3	13.7	18.5	-160	-161	-160
		s	10.7	6.5	8.6	42	41	
		n	80	75		92	89	
T3 <sup>a</sup>	30.4							
C4 2	6.4	x	5.1	4.7	4.9	-72	-70	-71
		s	2.1	2.0	2.1	33	32	
		n	62	63		64	63	
C4 6	5.8	x	4.1	3.9	4.0	-138	-137	-138
		s	1.7	1.3	1.5	21	21	
		n	61	64		63	63	

<sup>a</sup>These results are from a test program a few months earlier.

Table 5: Weight loss, average corrosion rates and corrosion potentials of A283 steel exposed in the field.

Mill No.	Weight Loss, mpy		LPR Anod., mpy	LPR Cath., mpy	LPR Ave., mpy	LPR Anod., E <sub>corr</sub>	LPR Cath., E <sub>corr</sub>	LPR Ave., E <sub>corr</sub>
B1 3	25.8	x	25.5	19.6	22.6	-137	-137	-137
		s	16	16.8	16.4	28	25	
		n	74	68		74	73	
B1 7	29.0	x	28	21.7	24.9	-142	-139	-140
		s	14	15.2	14.6	23	24	
		n	68	61		74	70	
B1	25.2							
W2 3	18.5	x	9.3	10.1	9.7	-166	-164	-165
		s	3.7	4.1	3.9	17	19	
		n	34	34		34	34	
W2 7	18.8	x	12.7	9.4	11.1	-163	-163	-163
		s	8.4	4.8	6.6	18	19	
		n	34	34		34	34	
W2	16.7							
T3 3	29.3	x	18.5	10.2	14.4	-208	-209	-208
		s	10.7	5.4	8.1	46	49	
		n	86	81		92	91	
T3 7	26.5	x	17.1	10	13.6	-163	-163	-163
		s	10	6	8	43	45	
		n	89	81		94	90	
T3	23.7							
T3 <sup>a</sup>	18.1							
C4 3	7.5	x	3.9	3.6	3.8	-68	-71	-70
		s	1.9	1.1	1.5	32	33	
		n	60	63		62	64	
C4 7	7.1	x	3.9	3.8	3.9	-138	-138	-138
		s	1.5	1.4	1.5	18	19	
		n	63	64		63	64	
C4	7.3							

<sup>a</sup>These results are from a test program a few months earlier.

Table 6. Weight loss, average corrosion rates and corrosion potentials of A285-SPECIAL steel exposed in the field.

Mill No.	Weight Loss, mpy		LPR Anod., mpy	LPR Cath., mpy	LPR Ave., mpy	LPR Anod., E <sub>corr</sub>	LPR Cath., E <sub>corr</sub>	LPR Ave., E <sub>corr</sub>
B1 4	22.9	x	12.4	12.3	12.3	-150	-161	-155
		s	10	4.5	7	20	20	
		n	35	32		23	20	
B1 8	23.9	x	20.9	15.1	18	-137	-136	-136
		s	8.5	4.9	6.7	16	16	
		n	69	64		72	70	
B1	21.1							
W2 4	14.2	x	8.6	8.3	8.4	-151	-156	-153
		s	4.4	2.8	3.6	20	20	
		n	34	34		34	34	
W2 8	14.2	x	8.3	7.7	8.0	-154	-158	-156
		s	6.8	2.4	4.6	19	21	
		n	34	34		34	34	
W2	11.4							
T3 4	27.8	x	16.4	10.0	13.2	-209	-207	-208
		s	9	6	7.5	48	50	
		n	85	81		93	91	
T3 8	27.1	x	17.9	10.7	14.3	-163	-163	-163
		s	7.9	5.4	6.6	44	45	
		n	85	85		93	91	
T3	21.4							
T3 <sup>a</sup>	8.9							
C4 4	6.2	x	3.7	4.0	3.9	-70	-70	-70
		s	1.7	1.5	1.6	32	31	
		n	61	62		61	64	
C4 8	6.1	x	3.9	3.9	3.9	-136	-135	-136
		s	1.5	1.5	1.5	16	17	
		n	62	64		63	63	
C4	7.6							

<sup>a</sup>These results are from a test program a few months earlier.

Analyses of liquor composition at each mill are summarized in Table 2. It should be noted that thiosulfate concentration was low at mill W2, which may have been a factor in the lower corrosion rate there. Mill T3 had a high sulfide concentration and very high thiosulfate. Only sample 4 at mill T3 was obtained during LPR testing. The other samples at T3 had been obtained during previous weight loss tests. Mill C4 had the lowest thiosulfate concentration

and lower NaOH and Na<sub>2</sub>S concentrations (and the lowest corrosion rate). The analysis of metals in solution was performed to determine whether some of the variation in corrosion rates was due to differences in iron concentration. No significant difference was noted. There was a high aluminum concentration at mill T3. The temperature of the liquor in the tank was measured to be 208°F at mill T3 and 206°F at mill C4.

#### ELECTRICAL RESISTANCE

The electrical resistance method was evaluated in the laboratory prior to its use in the field. The corrosion rate was determined from the ER probe and compared with weight loss specimens after two weeks. Additions of thiosulfate increased the corrosion rate. There was some difference in the weight loss in tests D and E, but the ER values were almost identical. The corrosion rate in solutions containing polysulfide was low according to the ER and weight loss tests; apparently the accuracy of ER measurements was not affected (unlike LPR measurements). Table 7 summarizes the comparison between weight loss and ER results in the laboratory. The agreement is generally excellent.

Table 7. Electrical resistance.

Test	NaOH, g/L	Na <sub>2</sub> S, g/L	Na <sub>2</sub> S <sub>x</sub> (as S), g/L	Na <sub>2</sub> S <sub>2</sub> O <sub>3</sub> , g/L	ER, mpy	Ave. Weight Loss, mpy
A	100	33	--	--	13	13
B	100	33	--	25	44	42
C	100	33	10	--	3	5
D	100	33	--	5	20	23
E	100	33	--	5	23	12
F	100	33	5	--	1	3

Figures 6 and 7 illustrate the change of corrosion rate during exposure at mills T3 and C4. One of the curves at mill T3 (early test) shows a declining section reflecting a drop in the corrosion rate, which may have been associated with a shutdown.

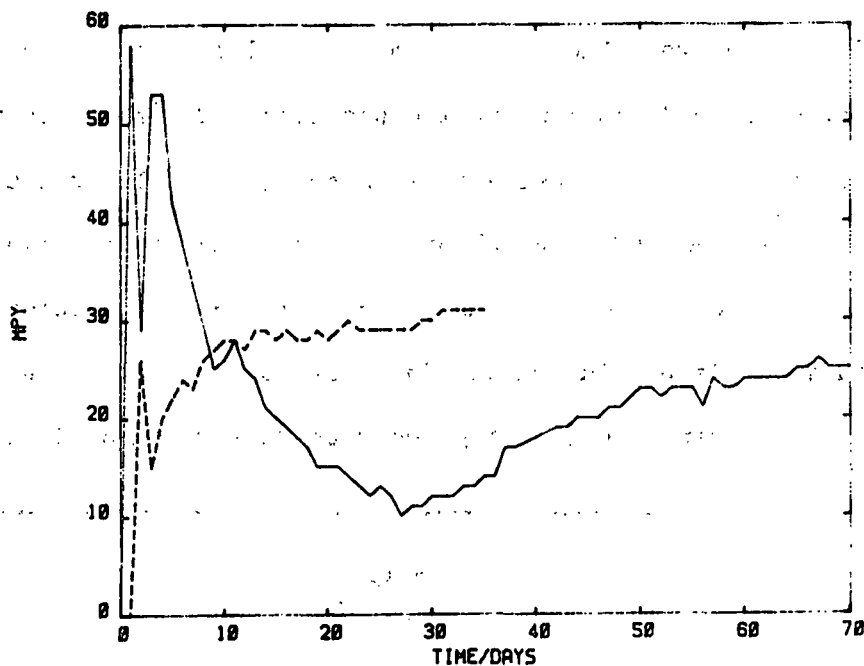


Figure 6. Electrical resistance measurements at mill T3.

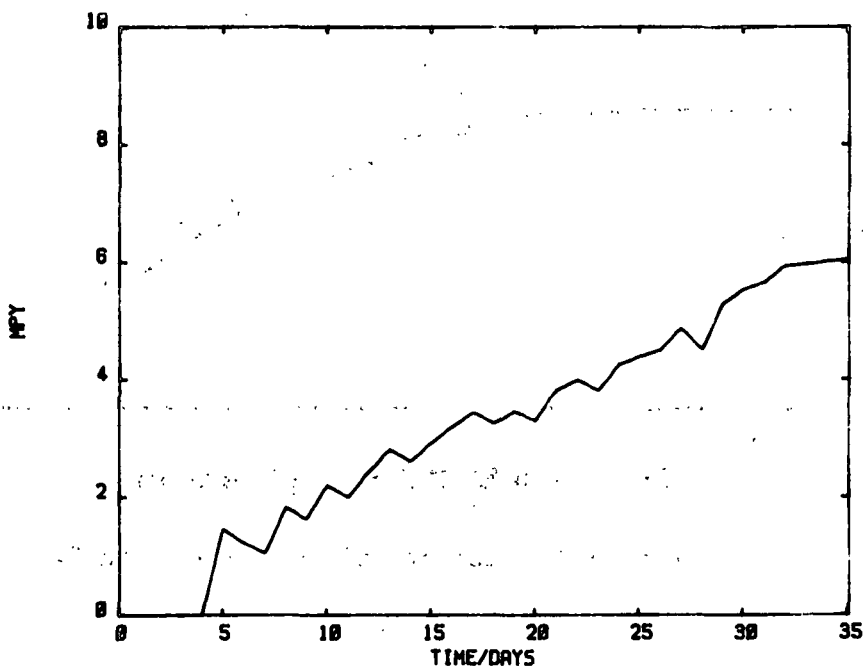


Figure 7. Electrical resistance measurements at mill C4.

## POLARIZATION BEHAVIOR

Polarization curves were generated on carbon steel electrodes in the mill liquors to characterize the electrochemistry of the corrosion process. Figures 8-10 are representative curves for three of the mills. Polarization curves for mill T3 were unavailable at the time of publication due to difficulties with glass-to-metal seals and instrumentation problems. The polarization curves obtained in the other mills are illustrated in Appendix II. The curves were the same general shape at all mills, although at mill C4 an active-passive transition was observed. Tafel slopes were measured from the polarization curves and are summarized in Table 8. The anodic Tafel region was short due to the adjacent active-passive transition, making accurate measurements difficult.

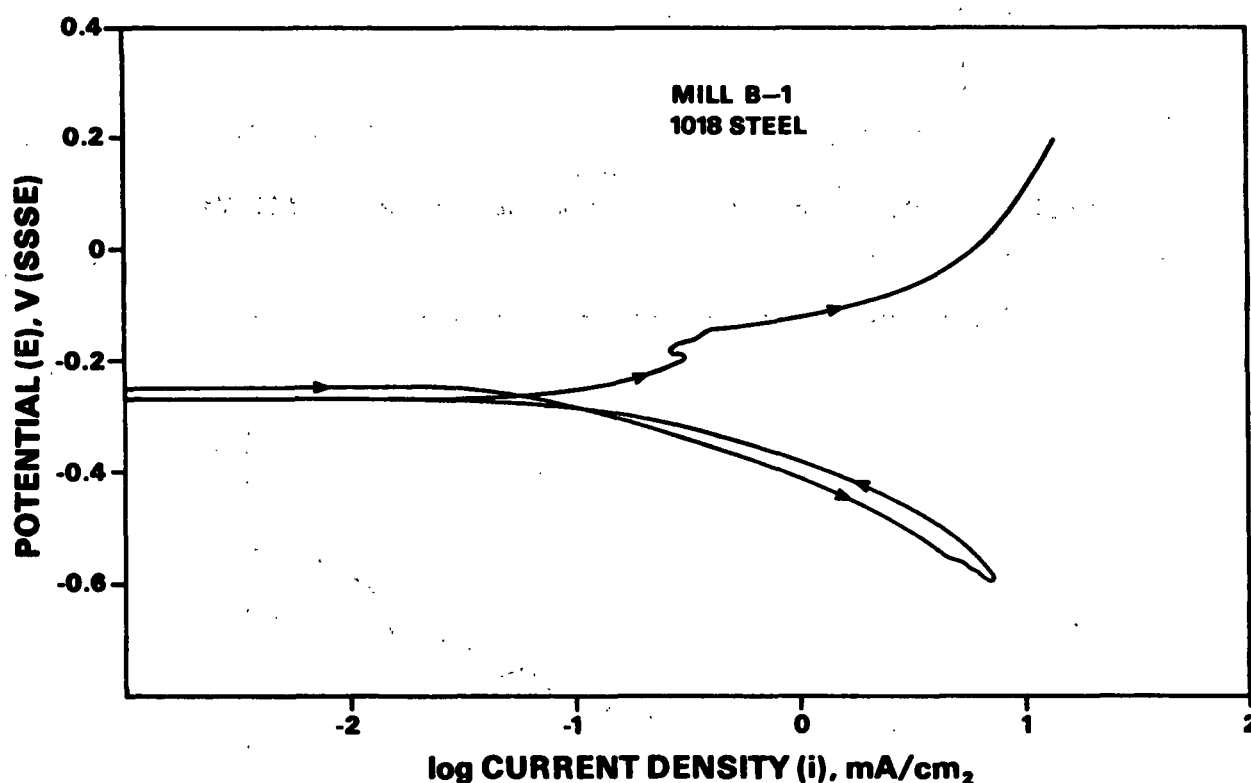


Figure 8. Polarization of 1018 steel at mill B1, scan rate 0.1 mV/s.



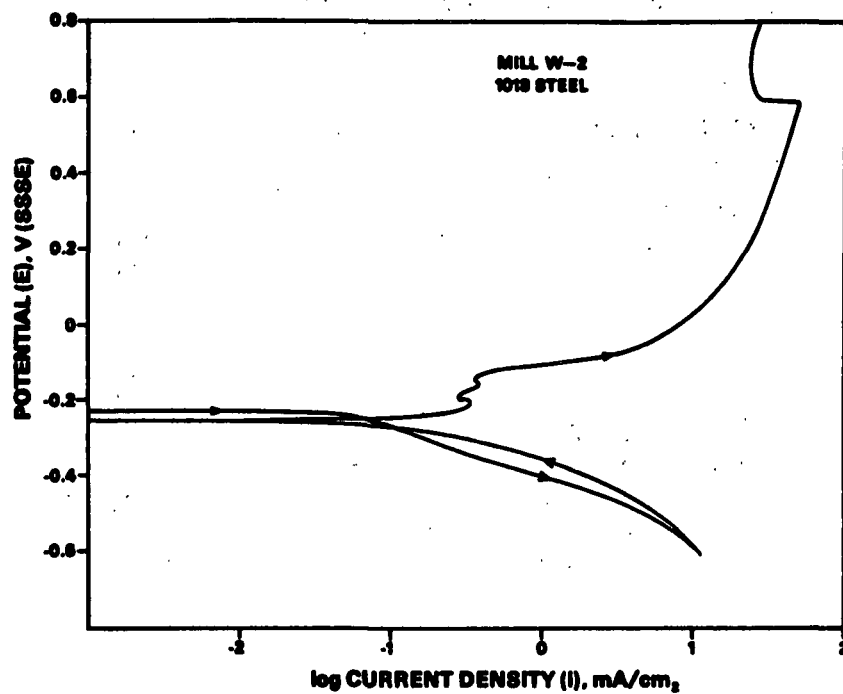


Figure 9. Polarization curve of 1018 steel at mill W2, scan rate 0.1 mV/s.

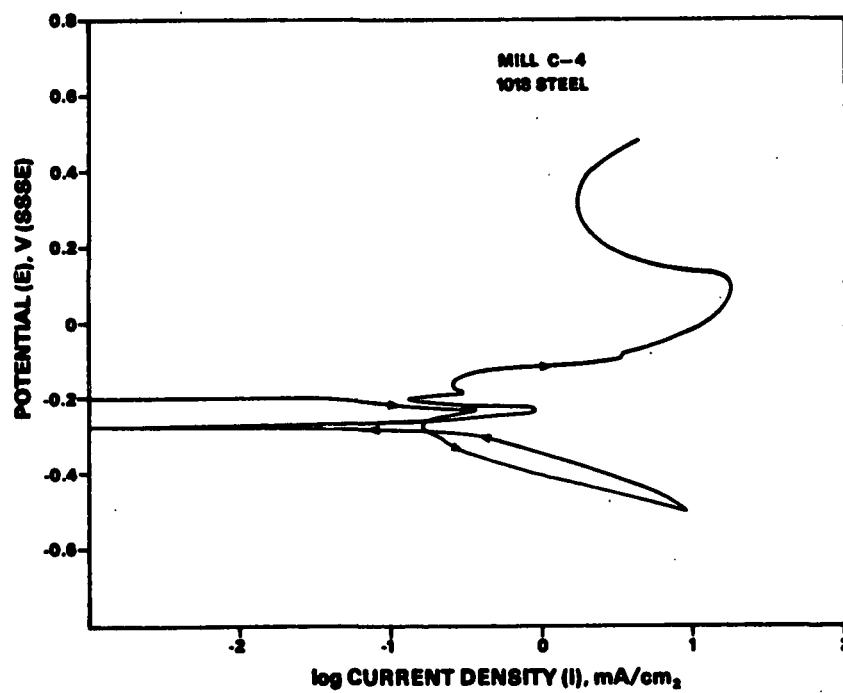


Figure 10. Polarization curve of 1018 steel at mill C4, 0.6 V/h.

Table 8. Tafel slopes measured from polarization curves.

Mill	Material	$\beta_A$	$\beta_C$
B1	1018	--	150
	A285C	60	140
	A283	60	130
	A285 SPEC	110	115
W2	1018	60	120
	A285C	65	120
	A283	60	110
	A285 SPEC	60	130
C4	1018	--	110
	A285C	--	130
	A283	70	140
	A285 SPEC	85	110

## DISCUSSION

## ELECTRICAL RESISTANCE

The electrical resistance technique agreed very well with weight loss results at mill T3 and C4. These results are summarized in Table 9. The curve of corrosion rate versus time did not level out until about 40-70 days as illustrated in Fig. 6 and 7. Thus these tests should be conducted for at least 30 days to obtain a stable measurement of corrosion rate in agreement with weight loss tests.

Table 9. Comparison of corrosion rates measured by electrical resistance and weight loss tests.

Mill No.	E.R. (1020 Steel), mpy	Weight Loss (1018 Steel), mpy
T3	25	29.4, 25.7, 30.9
T3	32	44.2, 41.2
C4	6	5.8, 9.2

The ER method has a number of advantages. It is useful where there is no information available on the Tafel slopes or the corrosion mechanism is not understood because the method does not require calibration or interpretation. Data are in a form which is easy for operating personnel to interpret. The ER method is also suitable for use in circumstances where the electrode is not continuously immersed, e.g., at liquid level lines. One drawback of this method is that it does not detect short-term fluctuations in corrosion rate which may be related to process upsets. Only an integrated measurement of corrosion rate is obtained. It should be capable of measuring changes in corrosion rate of 25% over a period of 2 weeks.

## LINEAR POLARIZATION RESISTANCE

The plots of corrosion rate (LPR) and corrosion potential vs. time (Fig. 5) illustrate the relationship between corrosion rate and corrosion potential. The corrosion rates were very high when the electrode was at active and active-passive potentials. Generally, the  $E_{\text{corr}}$  became more noble and the corrosion rate declined with exposure, presumably due to the formation of a passive film. This result confirms the importance of  $E_{\text{corr}}$  in determining the corrosion rate. It also indicates that chemical species in the liquor which place the corrosion potential in the active-passive range will cause increased corrosion rates. Fluctuations in corrosion rate may not be related to changes in liquor composition; similar fluctuations were observed in laboratory tests where liquor composition was stable.<sup>14</sup>

The poor agreement between weight loss coupons and the LPR corrosion rates (Table 3-6) suggests that the correction factor 2.8 was not appropriate for mill studies. The corrosion rate is underestimated. Table 10 lists weight loss and LPR measurements directly from the instrument. Calculated values of  $\beta/z$  which would be required to obtain agreement between the weight loss measurement and the LPR measurement are denoted  $(\beta/z)^*$ . Table 10 lists  $(\beta/z)^*$  values and correction factors for LPR measurements required to obtain agreement with weight loss results. Note that LPR measurements given in Table 10 have not been corrected with the 2.8 factor. In the table, the LPR measurements are the average of the values obtained directly from the Petrolite M1010 instrument. The correction factor,  $f$ , to make the LPR measurements agree with the weight loss tests is listed. The average of all values of correction factor is 1.7. The correction factor varied from mill to mill and from material to material. It did not seem to be related to corrosion potential or the amount of turbulence

Table 10. Tafel constants ratio ( $\beta/z$ )\* and correction factor for LPR measurements.

Material	Mill	Weight Loss, mpy	LPR Avg. mpy	$\frac{\text{LPR}}{\text{wt. loss}} = f$	$\frac{41.65}{f} = \frac{\beta^*}{z}$ mV	$\frac{\text{LPR}}{1.7}$ mpy
1018	B1	29.7	83.2	2.80	14.9	48.9
	B1	34.9	93.2	2.67	15.6	54.8
	W2	15.6				
	W2	25.0	38.6	1.54	27.1	22.7
	T3	44.2	48.4	1.10	37.9	28.5
	T3	41.2	48.4	1.17	35.6	28.5
	C4	5.8	9.5	1.64	25.4	5.6
	C4	9.2	10.9	1.18	35.3	6.4
A285C	B1	23.2	61.6	2.66	15.7	36.2
	B1	27.1	64.7	2.39	17.4	38.1
	W2	16.5				
	W2	19.5	19.9	1.02	40.8	11.7
	T3	44.0	47.6	1.08	38.6	28.0
	T3	41.1	51.8	1.26	33.1	30.5
	T3	30.4				
	C4	6.4	13.7	2.14	19.5	8.1
A283	C4	5.8	11.2	1.93	21.6	6.6
	B1	25.8	63.3	2.45	17.0	37.2
	B1	29.0	69.7	2.40	17.4	41.0
	B1	25.2				
	W2	18.5	27.2	1.47	28.3	16.0
	W2	18.8	31.1	1.65	25.2	18.3
	W2	16.7				
	T3	29.3	40.3	1.38	30.2	23.7
	T3	26.5	38.1	1.44	28.9	22.4
	T3	23.7				
	T3	18.1				
	C4	7.5	10.6	1.41	29.5	6.2
A285 SPEC	C4	7.1	10.9	1.54	27.0	6.4
	C4	7.3				
	B1	22.9	34.4	1.50	27.8	20.2
	B1	23.9	50.4	2.11	19.7	29.6
	B1	21.1				
	W2	14.2	23.5	1.65	25.2	13.8
	W2	14.2	22.4	1.58	26.4	13.2
	W2	11.4				
	T3	27.8	37.0	1.33	31.3	21.8
	T3	27.1	40.0	1.48	28.1	23.5
	T3	21.4				
	T3	8.9				
	C4	6.2	10.9	1.76	23.7	6.4
	C4	6.1	10.9	1.79	23.3	6.4
	C4	7.6				

in the liquors. The correction factors are divided into the value of  $\beta/z$  used by the instrument (41.65 mV) to obtain  $(\beta/z)^*$  values that would be required to make the LPR measurement agree with the weight loss. The average  $(\beta/z)^*$  value would be 25 mV. The Tafel slopes listed in Table 8, measured from the polarization curves obtained in the tanks and clarifiers, have average values of  $\beta_A = 70$  mV and  $\beta_C = 125$  mV. These values give a  $\beta/z$  value of 22.4 mV, assuming  $z = 2$ . This value is reasonably close to the average value of  $(\beta/z)^*$  required (25 mV) in Table 10 and confirms the practice of correcting the measured LPR values using Tafel slopes measured from the polarization curves. LPR measurements corrected with a factor of 1.7 (Table 10) agreed well with ER measurements and agreement with weight loss results was much better.

The different  $(\beta/z)^*$  values for the field study resulted from different Tafel slopes in mill liquors. Species not present in simulated white liquors may give rise to these differences. The actual kraft white liquors contain a multitude of minor constituents. These constituents may exert a strong influence on the electrode kinetics, reflected in the change in Tafel slopes. Moreover, they may affect the corrosion potential, and different reactions may predominate compared with the lab study. For example, polysulfide at intermediate concentration controls the corrosion potential in the active-passive range (and in the passive range when present in sufficient quantities). Thiosulfate impairs passivation and the corrosion potential remains in the active-passive range.<sup>12</sup> Other species may affect the corrosion potential and kinetics in ways that were not discovered in the study of simulated white liquor.

Weight loss of electrodes on which no LPR measurements were made was generally lower than for electrodes used for the LPR technique. The LPR

technique may disrupt the formation of the passive film or may cause some sloughing of corrosion products. This will be tested in the future by monitoring corrosion potential of weight loss coupons without polarizing them, to see if they passivate more quickly than LPR electrodes.

The corrosion rate determined by the cathodic polarization cycle of the M1010 LPR instrument was slightly more accurate than the anodic measurements because it was slightly lower. Bandy and Jones<sup>22</sup> have investigated the errors due to nonlinearity for some combinations of  $\beta_A$  and  $\beta_C$ , i.e., the error arising because the polarization curve is not linear in the range -10 to +10 mV. They found that the error was as high as -50% for the anodic polarization and +30% for the cathodic polarization. In the present study, the errors due to nonlinearity were minimized by averaging anodically and cathodically determined corrosion rates.

The LPR method possesses some important advantages in corrosion measurement. It responds instantaneously to changes in liquor corrosivity, and provides more information on the corrosion process. The method is suitable as a basis for automatic measurements in operating equipment. These advantages must be considered of sufficient value to justify the effort of measuring Tafel slopes and calibrating the LPR measurements with weight loss testing.

Mill personnel should be able to apply the LPR technique to measurement of corrosion rates in their white liquor systems. Good agreement of weight loss and LPR can be obtained by applying an appropriate correction factor based on Tafel slopes measured from polarization curves obtained in the mill. The correction factor may be checked by comparison of corrosion rates measured by LPR with corrosion rates measured by weight loss tests. Once this correction

factor is established, on-line monitoring could be started. Even without this calibration, the technique can be used to measure relative corrosion rates of different materials or changes over a period of time.

#### LIQUOR EFFECTS

The corrosion rates at mill T3 were highest, followed by mills B1, W2 and C4. Mills T3 and B1 had high flow rates, which is probably the major cause of their high corrosion rates. Mill T3 also had the highest thiosulfate concentration. There is a possibility that some of this thiosulfate results from turbulence which causes oxidation of sulfides by increasing contact with air. Mill C4, with the weakest liquor, lowest thiosulfate concentration, and a low flow rate had very low corrosion rates. The corrosion rates apparently were related to the thiosulfate concentrations. This confirms Roald's<sup>4</sup> claim that corrosion rate was directly related to the thiosulfate concentration. Studies at IPC<sup>12</sup> have shown thiosulfate to increase corrosion rates dramatically. The liquor composition was not significantly different during periods of high corrosion rate at mill B1. Some minor constituent may have placed  $E_{corr}$  in a range where high dissolution rates are encountered. The increase in NaOH and  $Na_2S$  concentration during the last week at mill C4 was thought to have had little effect on corrosion rate because the electrodes had reached corrosion potentials in the passive range by then.

Flow rates may also have a significant effect on corrosion rates. Studies in this laboratory have shown corrosion rates to increase dramatically in flowing white liquor. Mill B1 had considerable liquor motion associated with level cycling and experienced high corrosion rates. Mill T3 also had high corrosion rates and considerable liquor motion.



## MATERIALS COMPARISON

Wensley and Charlton<sup>2</sup> observed that coupons in a given test had similar corrosion rates ( $\pm 50\%$  of the mean), and that mean rates varied considerably from test to test. The rates for a given steel varied considerably but some steels had corrosion rates which always tended to be lower than the mean. To separate liquor corrosivity effects, they plotted corrosion rates of individual samples versus the liquor corrosivity. The liquor corrosivity was defined as the average corrosion rate of all coupons exposed during a specified period at a mill. By this means, it could be determined which materials were repeatedly above average in corrosion rate and which were below. A line through the data points was determined by the least squares method and the slope ( $m$ ) of the line was taken as an index of the relative corrosion rate. The results for a good material lie at corrosion rates below average ( $m < 1$ ) for the range of liquor corrosivities. The materials that performed worse than average had a line with slope  $m > 1$ . The weight loss results were analyzed in the same way as part of this study. The corrosion rates of individual steel coupons were plotted vs. corrosivity for that test, as illustrated in Fig. 11-14. The 1018 steel showed corrosion rates above average ( $m = 1.24$ ), and A285C was slightly above average ( $m = 1.15$ ). Lower corrosion rates were observed for A283 ( $m = 0.92$ ) and A285 SPEC ( $m = 0.78$ ). These results confirm that A285 SPECIAL steel is the best steel for use in white liquor and its corrosion rate is about two-thirds that of 1018 steel. This difference must be related to its low Si concentration and high Cu content.<sup>2</sup> Results calculated with the LPR data were similar (1018:  $m = 1.24$ , A285C:  $m = 1.01$ , A283:  $m = 0.99$ , A285 SPEC:  $m = 0.76$ ) demonstrating the reliability of the LPR technique in comparing relative corrosion rates of materials. The present results also confirm that the effect of steel composition is small compared to the effect of liquor corrosivity in determining corrosion rates.

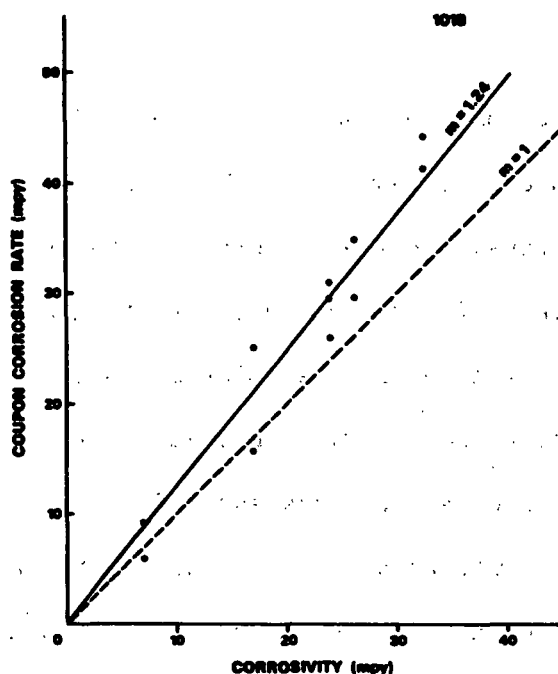


Figure 11. Corrosion rate of 1018 steel vs. liquor corrosivity.

The fluctuating corrosion rate observed for the 1018 steel suggested that passive film formation was poor. Fluctuations may have corresponded to spalling and reformation of the passive film. This effect may have been a factor in the generally poorer performance of 1018 compared with the other materials.

#### INDUSTRIAL SIGNIFICANCE

Implementation of corrosion monitoring techniques in-mill will aid in reducing the costs of corrosion by providing information on rates of damage to equipment which will assist personnel in maintenance and replacement programs. It will aid in material selection by providing data on relative corrosion rates of different materials. Continuous monitoring will be useful in determining how modifications to process and operations are affecting corrosion rates. Monitoring corrosion rates will assist operators in correcting problems of which they may be unaware. For example, higher corrosion rates may point to excessive

contact of the liquor with the atmosphere causing liquor oxidation. Poor recovery boiler operations may be reflected in higher corrosion rates caused by higher concentrations of oxidizing species.

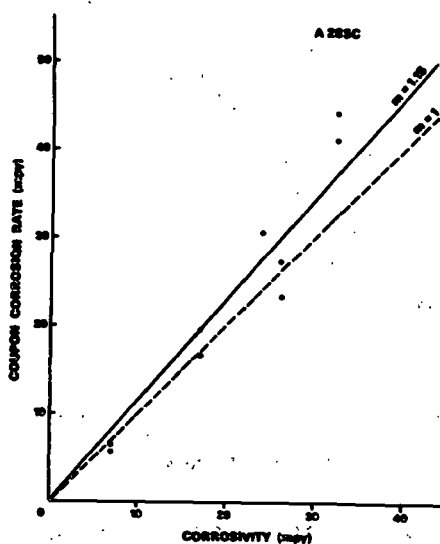


Figure 12. Corrosion rate of A285C steel vs. liquor corrosivity.

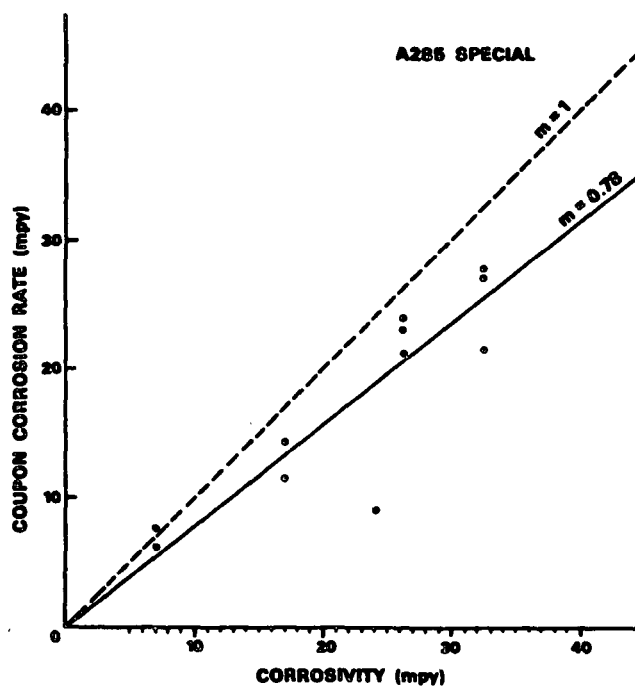


Figure 13. Corrosion rate of A283 steel vs. liquor corrosivity.

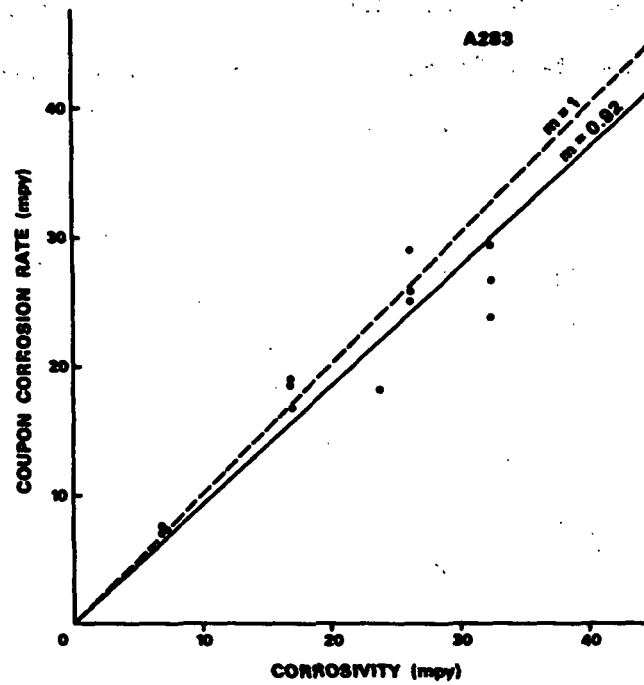


Figure 14. Corrosion rate of A285 SPEC steel vs. liquor corrosivity.

## CONCLUSIONS

1. The linear polarization resistance technique provided a good estimate of corrosion rates of carbon steel in white liquor if an appropriate correction factor was applied to the results. LPR is useful to measure effects of liquor changes or to obtain measurements of relative corrosion rates of materials.
2. Electrical resistance measurements agreed well with weight loss tests. A test period of about 30 days is required to obtain an accurate measurement. The results need no correction or interpretation.
3. Liquor composition was the most significant factor in determining corrosion rates. Higher corrosion rates were observed at mills with high thiosulfate concentrations. Higher hydroxide and sulfide concentrations also increased corrosion.
4. Liquor velocity was a significant factor in determining the corrosion rate.
5. The test steels, in order of increasing corrosion rate, were A285 SPEC, A283, A285C, and 1018. The resistance of the A285-SPECIAL was probably related to its high Cu content and low Si content.
6. The development of reliable corrosion monitoring methods for use in white liquors will aid in reducing the costs of corrosion by helping to identify the sources of increased corrosion rate.

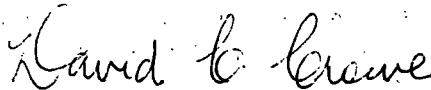
## ACKNOWLEDGMENT

The authors wish to acknowledge the experimental work performed by Mr. James Tierney. The cooperation and enthusiasm of the mill personnel with whom we worked was greatly appreciated.

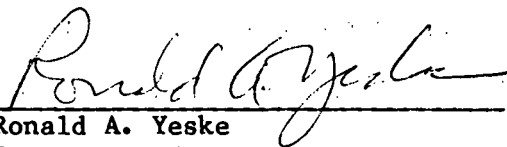
## REFERENCES

1. Christiansen, C. B.; Lathrop, J. B., Pulp Paper Mag. Can. 55(11):113-19 (1954).
2. Wensley, D. A. In: Pulp and Paper Industry Corrosion Problems, Vol. 3, N.A.C.E., Houston, 1981.
3. Kesler, R. B.; Bakken, J. F., Tappi 41(3):97-102(1958).
4. Roald, B., Norsk Skogind. 10(8):285-9(1956).
5. Wensley, D. A.; Charlton, R. S., Corrosion 36:385-9(1980).
6. Yeske, R. A. Corrosion rate measurements in kraft white liquor, Progress Report Two, Project 3556, The Institute of Paper Chemistry, Appleton, Wisconsin, 1984.
7. Mansfeld, F., Adv. Corr. Sci. and Tech. 6:163-262(1976).
8. Barnartt, S. Electrochemical techniques for corrosion, R. Baboian, Ed., NACE, Houston (1977):1-10.
9. Singbell, D.; Tromans, D., J. Electrochem. Soc. 129:2669-73(1982).
10. Vetter, K. J., Electrochemical Kinetics, Academic Press, New York (1967).
11. Doig, P.; Flewitt, P. E. J., Corr. Sci. 17:369(1977).
12. Crowe, D. C.; Yeske, R. A. Liquor composition effects on corrosion rates in kraft white liquors, Progress Report Three, Project 3556, The Institute of Paper Chemistry, Appleton, Wisconsin, Sept., 1985.
13. Yeske, R. A. The silver/silver sulfide reference electrode for use in corrosion studies in kraft white liquor, Progress Report One, Project 3556, The Institute of Paper Chemistry, Appleton, Wisconsin, Feb., 1984.
14. Yeske, R. A. Proc. Symposium on Corrosion Monitoring and Nondestructive Testing, Montreal 1984, ASTM, to be published.
15. Bandy, R.; Jones, D. A. Corrosion 32:126-34(1976).

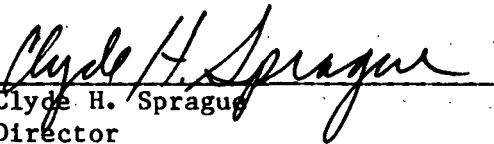
THE INSTITUTE OF PAPER CHEMISTRY



David C. Crowe  
Research Fellow  
Corrosion and Materials  
Engineering Section  
Engineering Division



Ronald A. Yeske  
Section Leader  
Corrosion and Materials  
Engineering Section  
Engineering Division



Clyde H. Sprague  
Director  
Engineering Division



## APPENDIX I

## CORROSION RATE AND CORROSION POTENTIAL DURING LPR TESTS

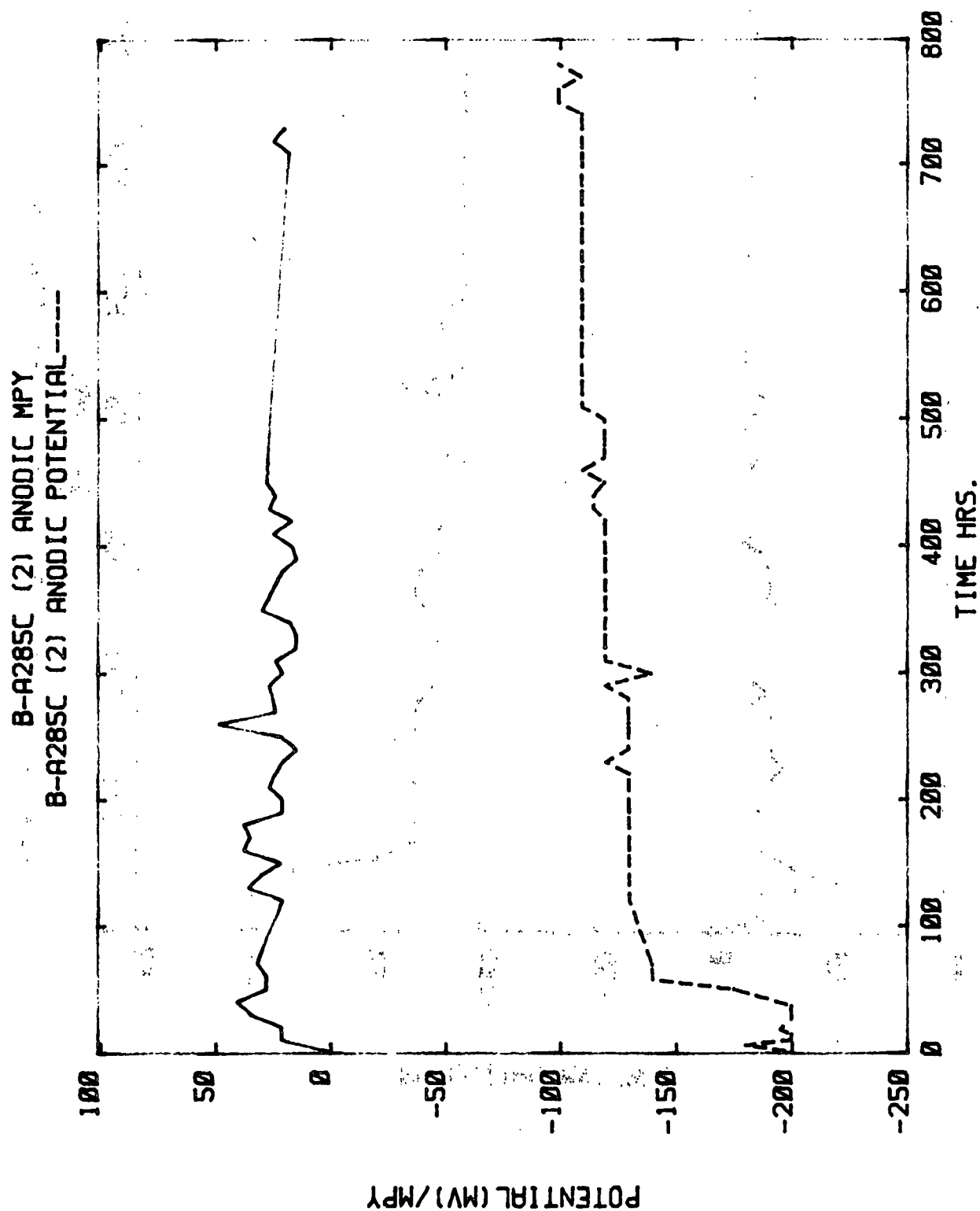


Figure 15. Mill B1. A285C. Anodic LPR. Electrode 2.

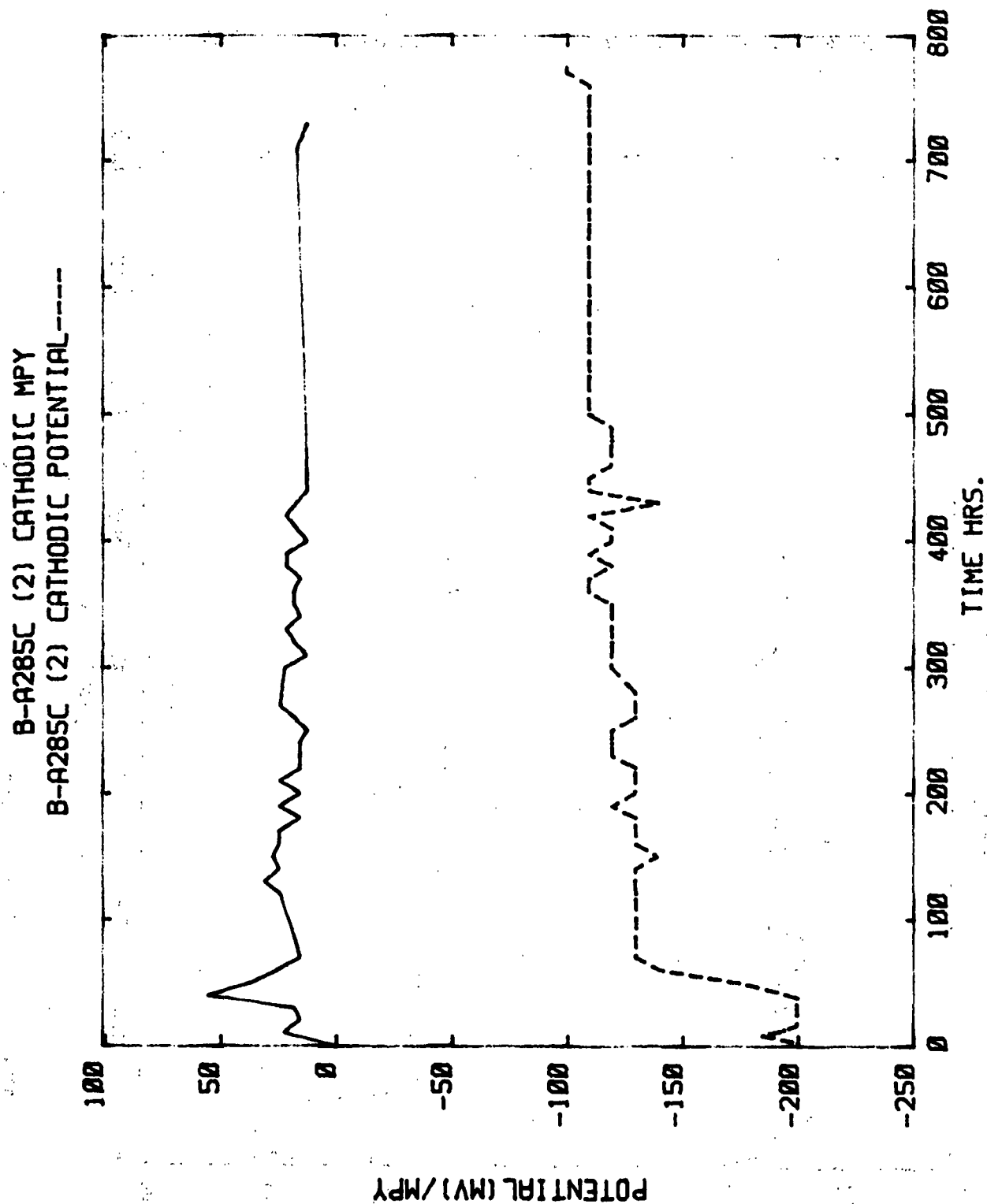


Figure 16. Mill Bl. A285C. Cathodic LPR. Electrode 2.

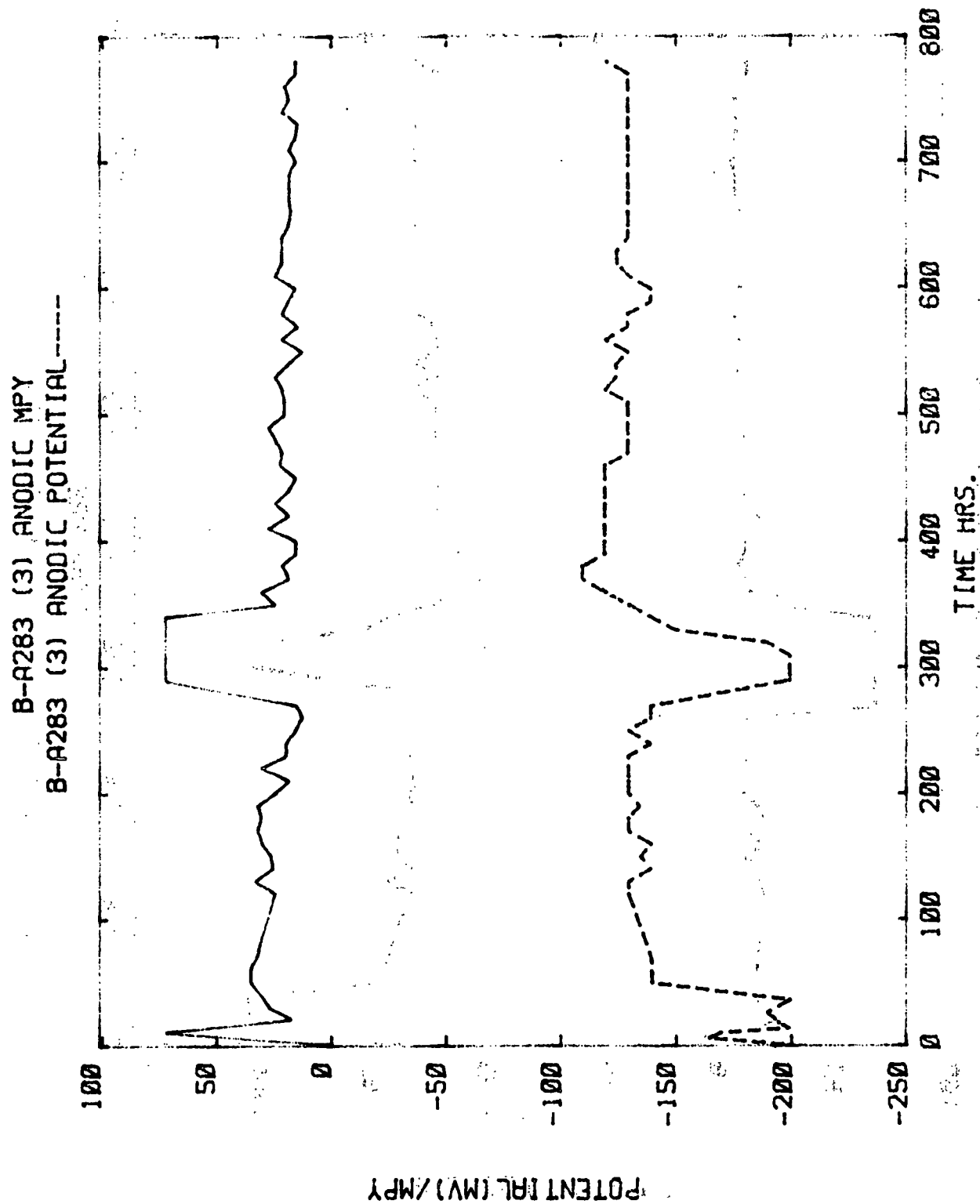


Figure 17. Mill B1, A283. Anodic LPR. Electrode 3.

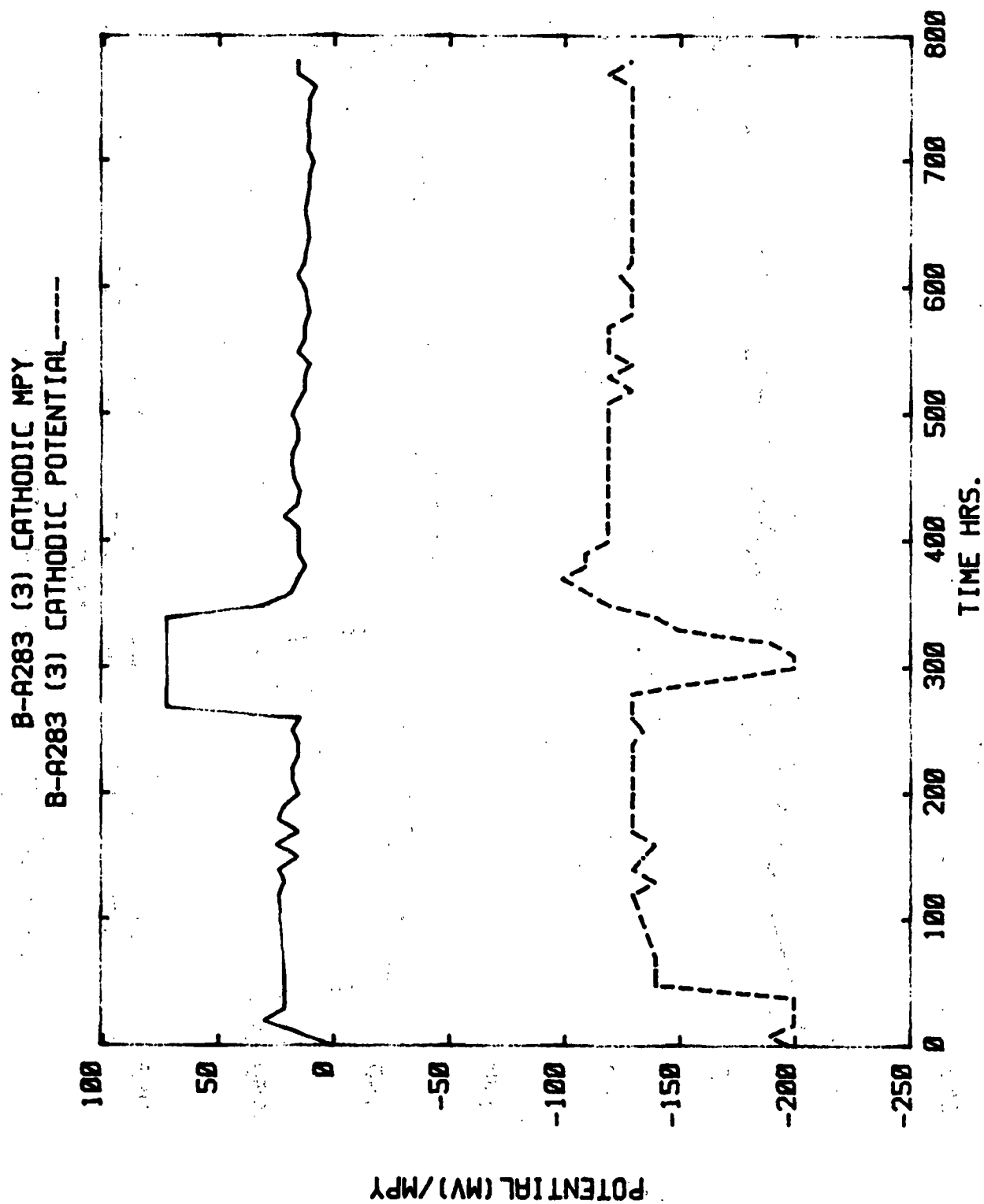


Figure 18. Mill Bl. A283. Cathodic LPR. Electrode 3.

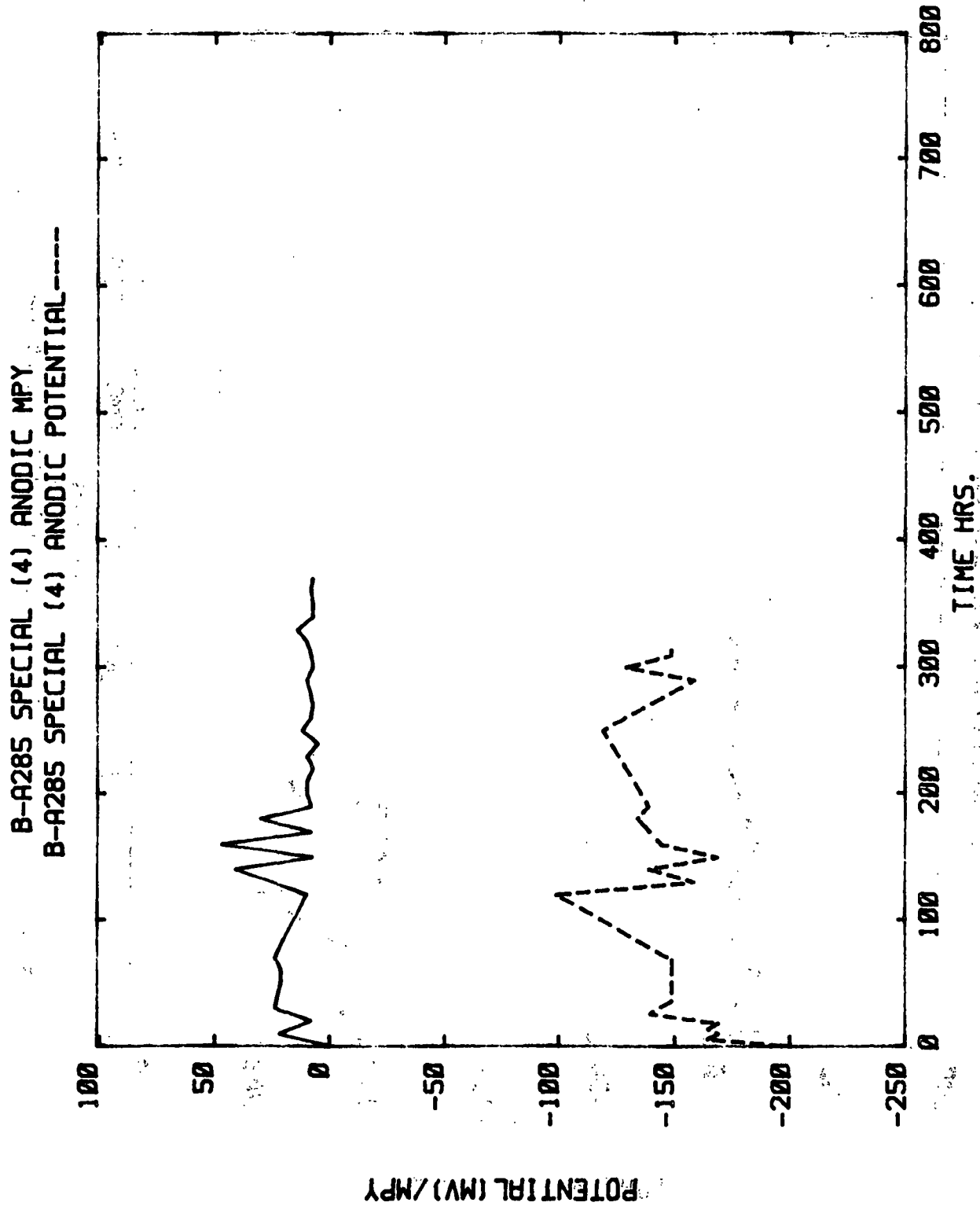


Figure 19. Mill-B1. A285-SPEC. Anodic LPR. Electrode 4.

B-A285 SPECIAL (4) CATHODIC MPY  
B-A285 SPECIAL (4) CATHODIC POTENTIAL-----

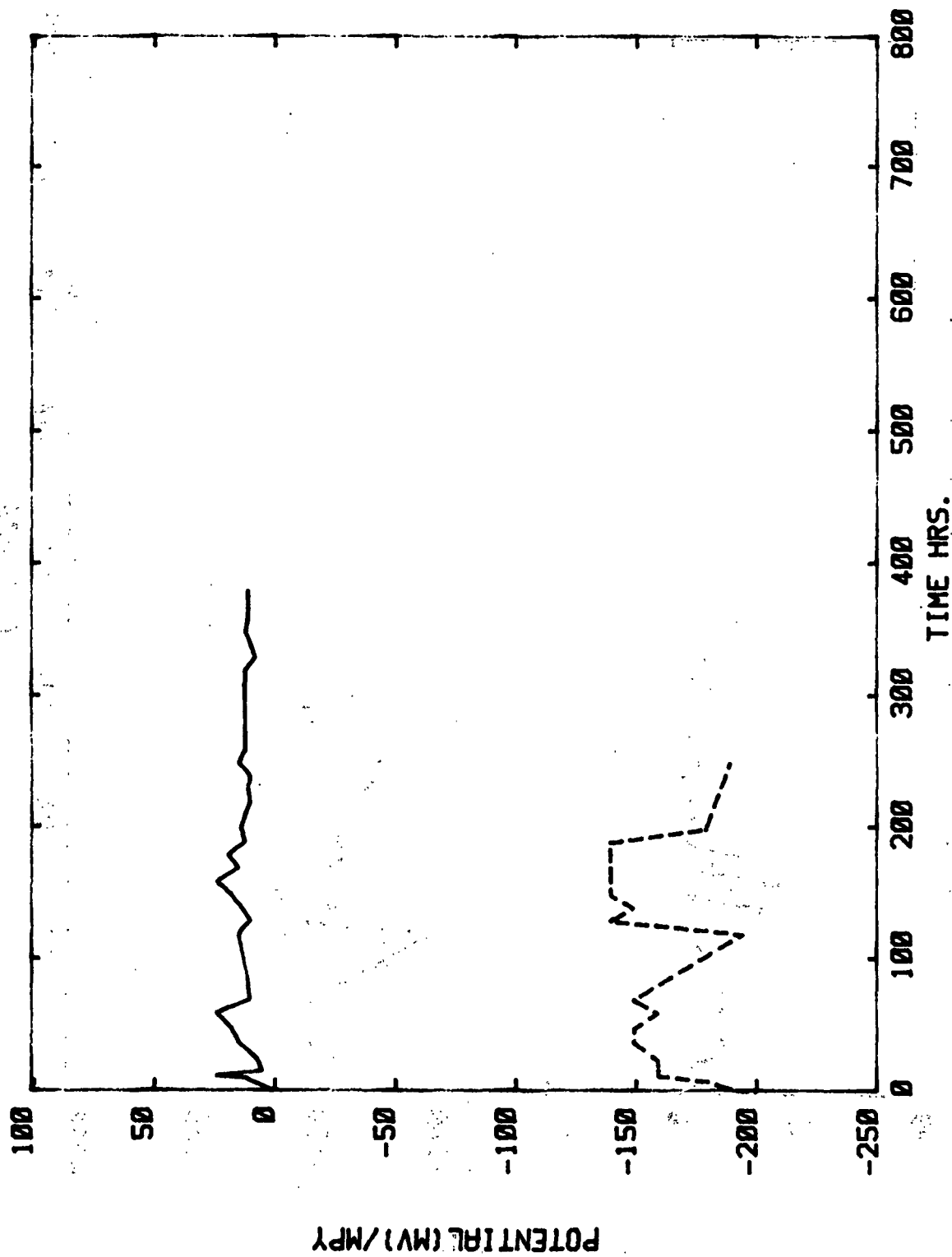


Figure 20. Mill B1. A285-SPEC. Cathodic LPR. Electrode 4.

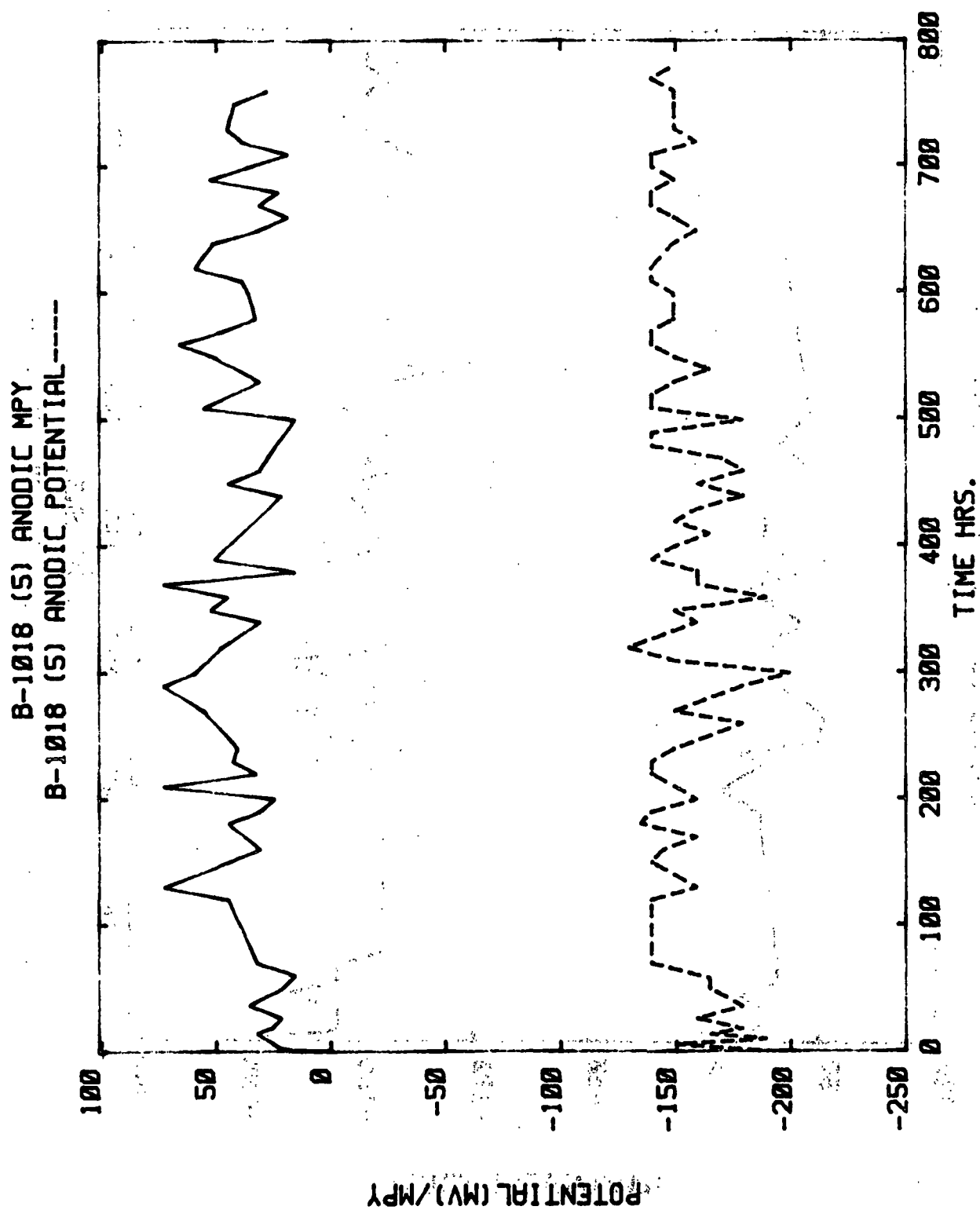


Figure 21. Mill Bl. 1018. Anodic LPR. Electrode 5.

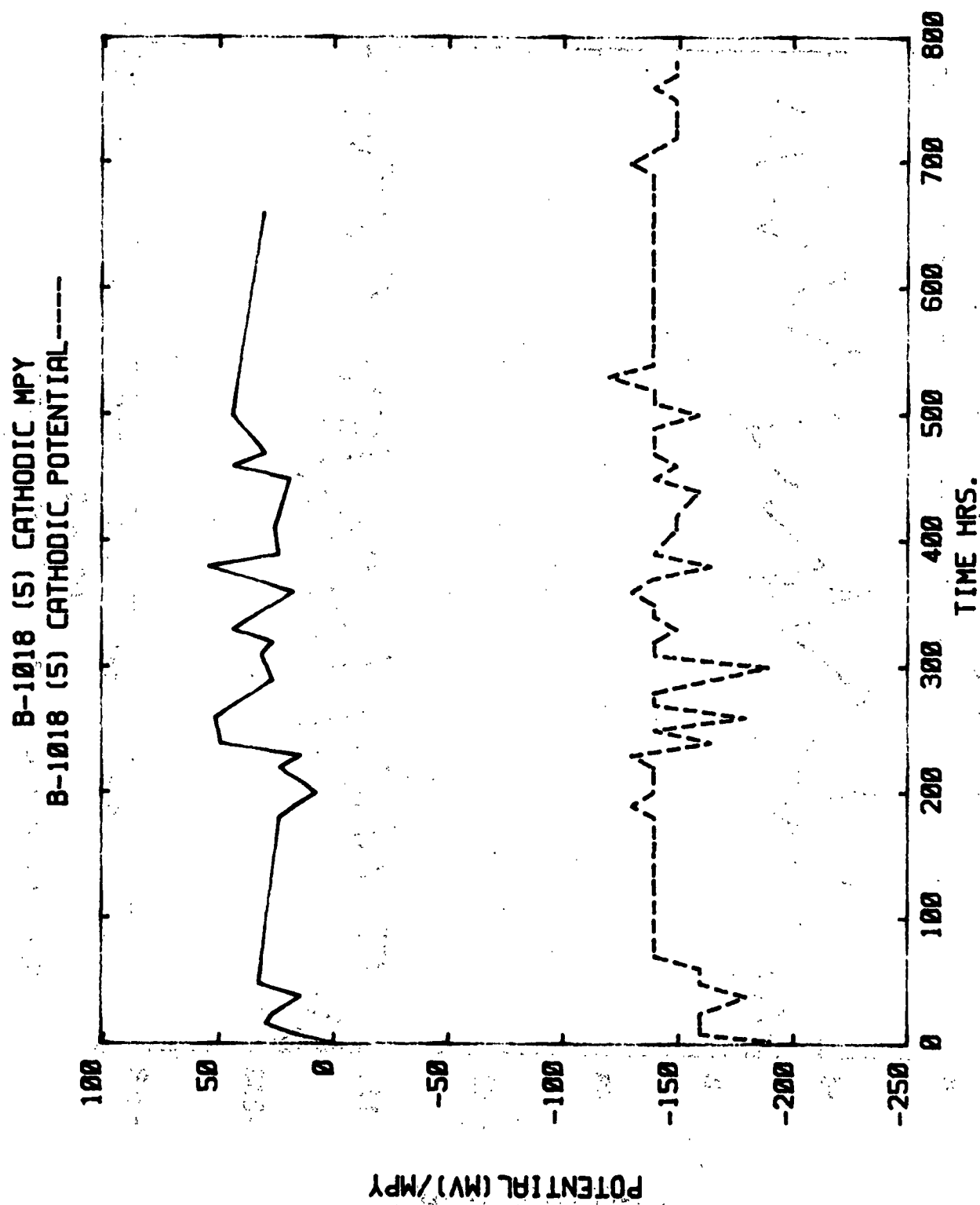


Figure 22. Mill Bl. 1018. Cathodic LPR. Electrode 5.



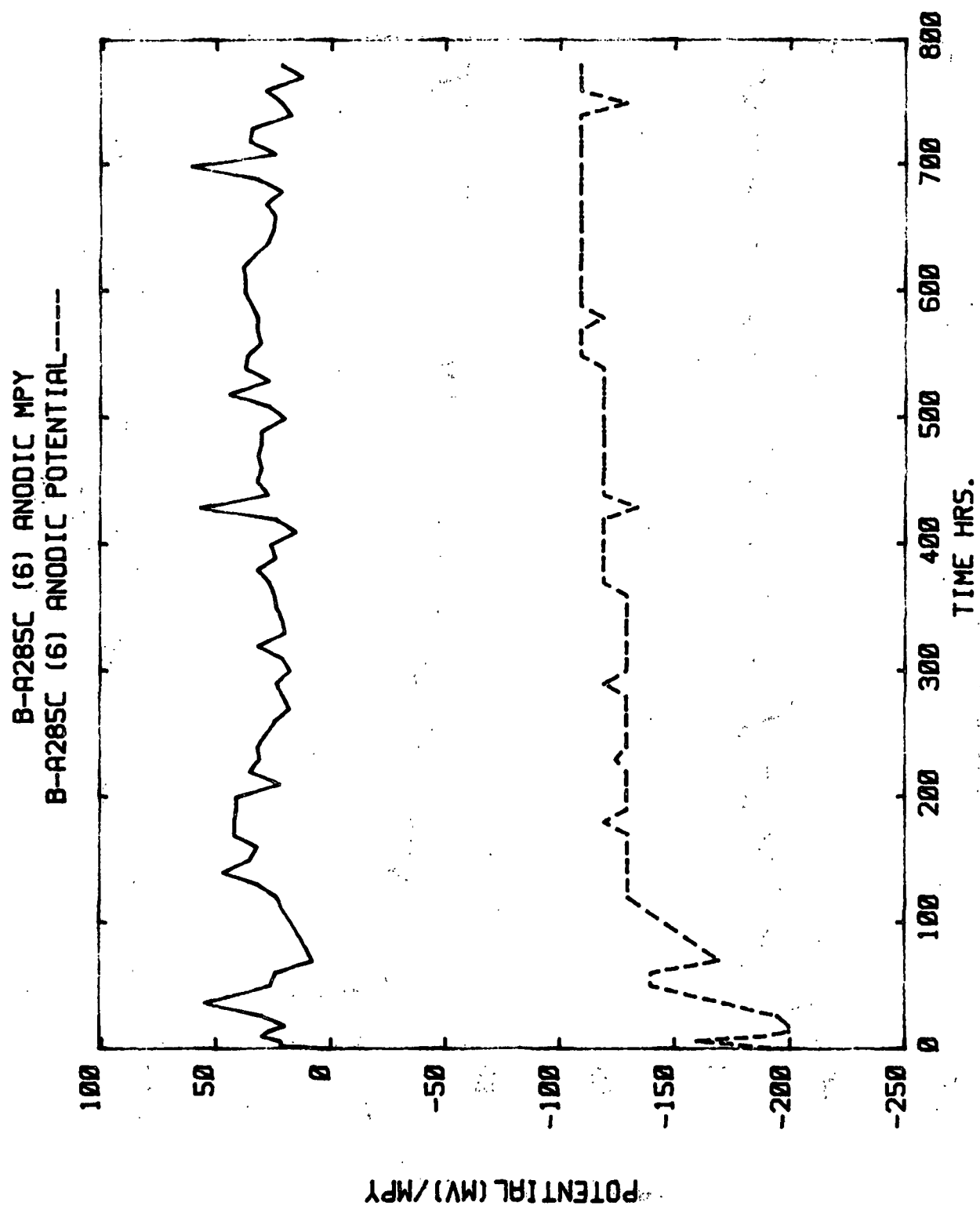


Figure 23. Mill B1. A285C. Anodic LPR. Electrode 6.

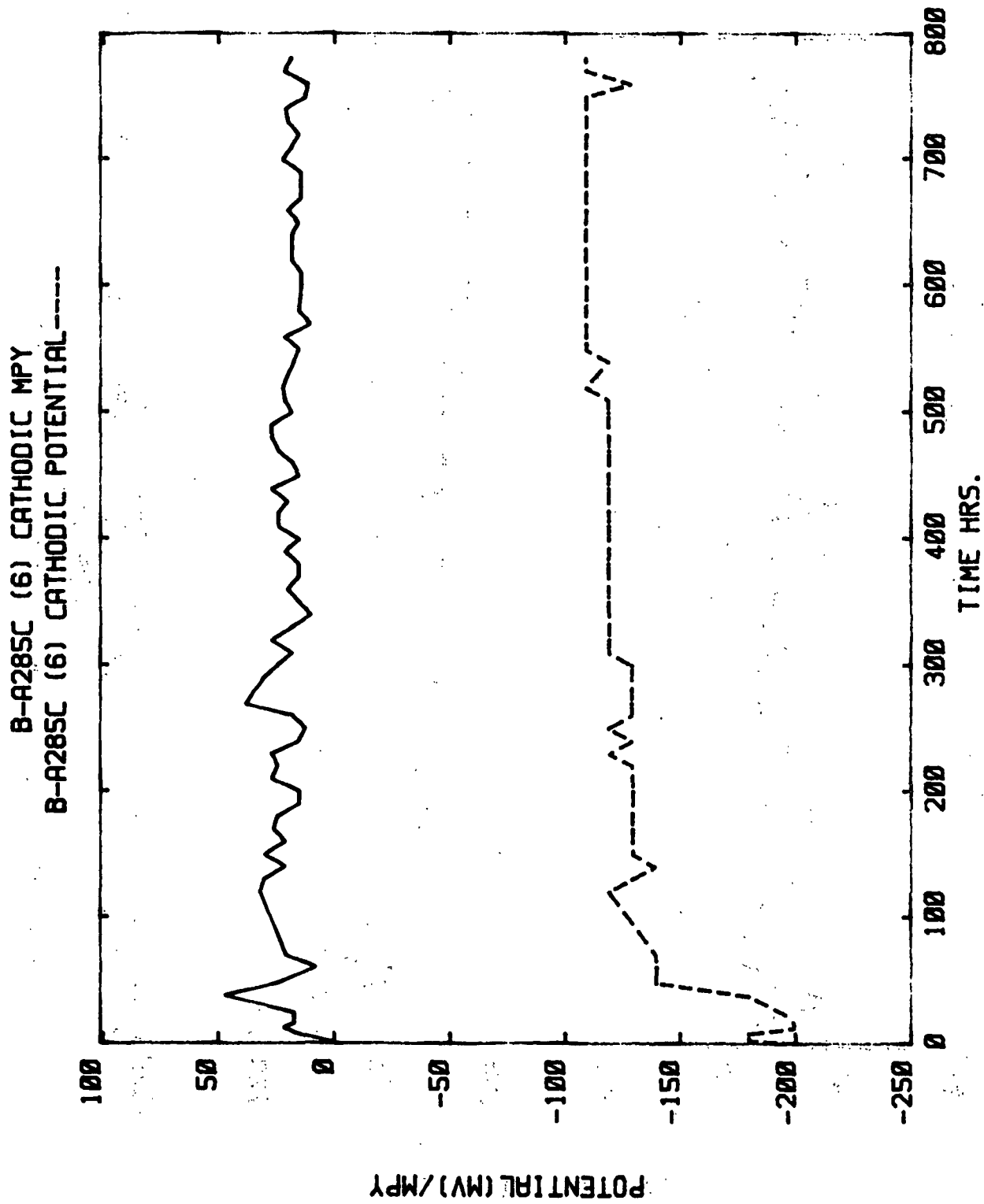
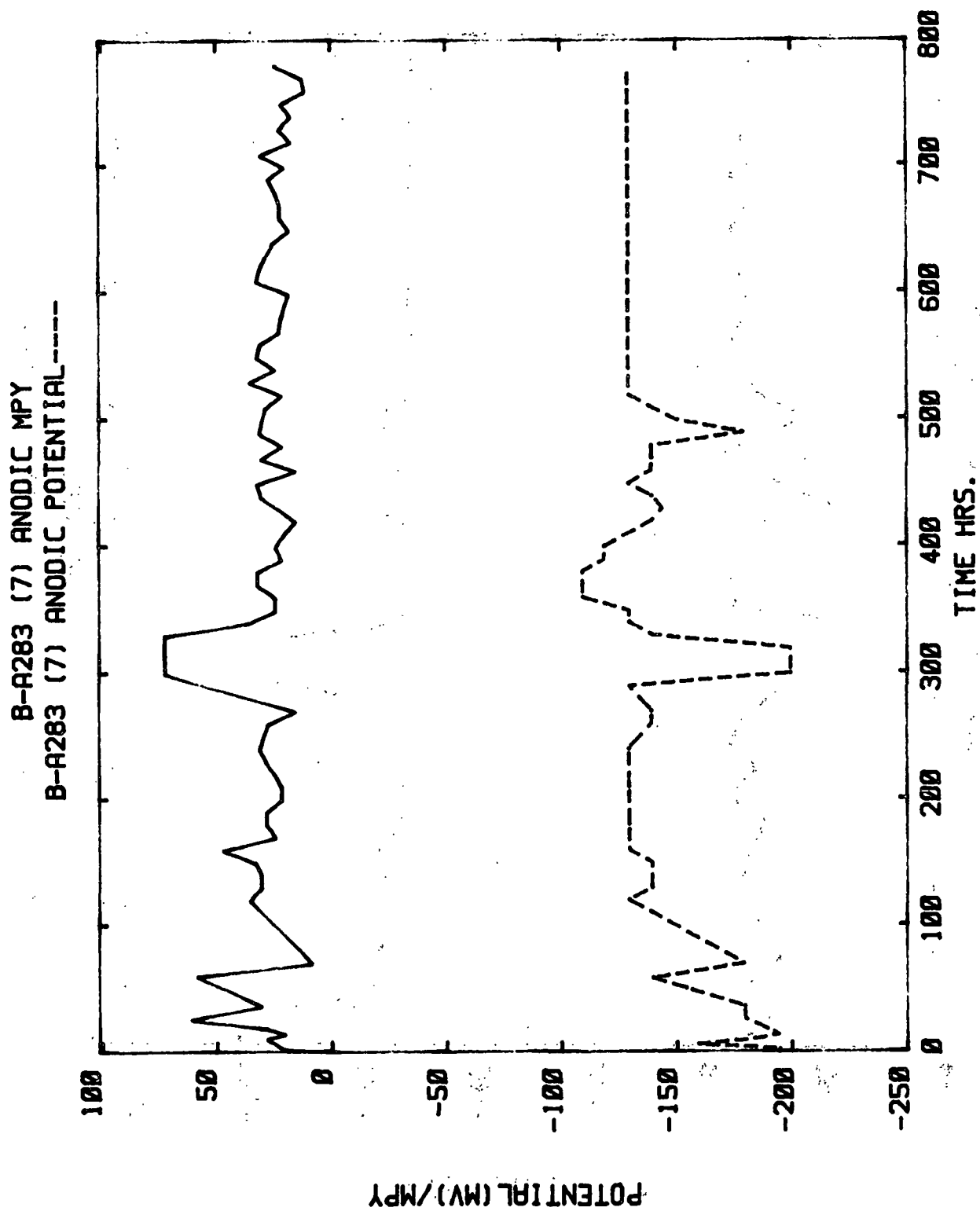


Figure 24. Mill B1. A285C. Cathodic LPR. Electrode 6.



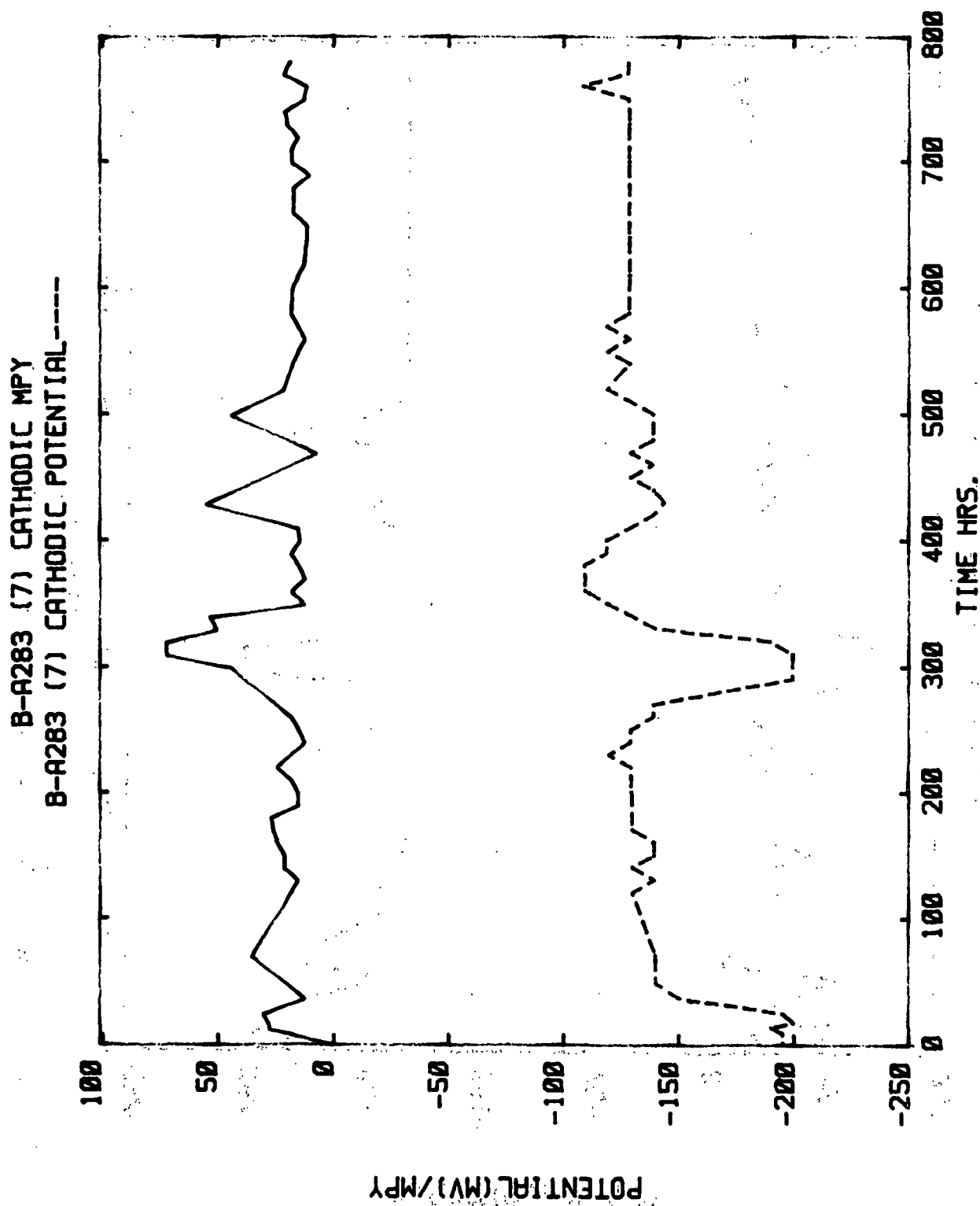


Figure 26. Mill B1. A283. Cathodic LPR. Electrode 7.

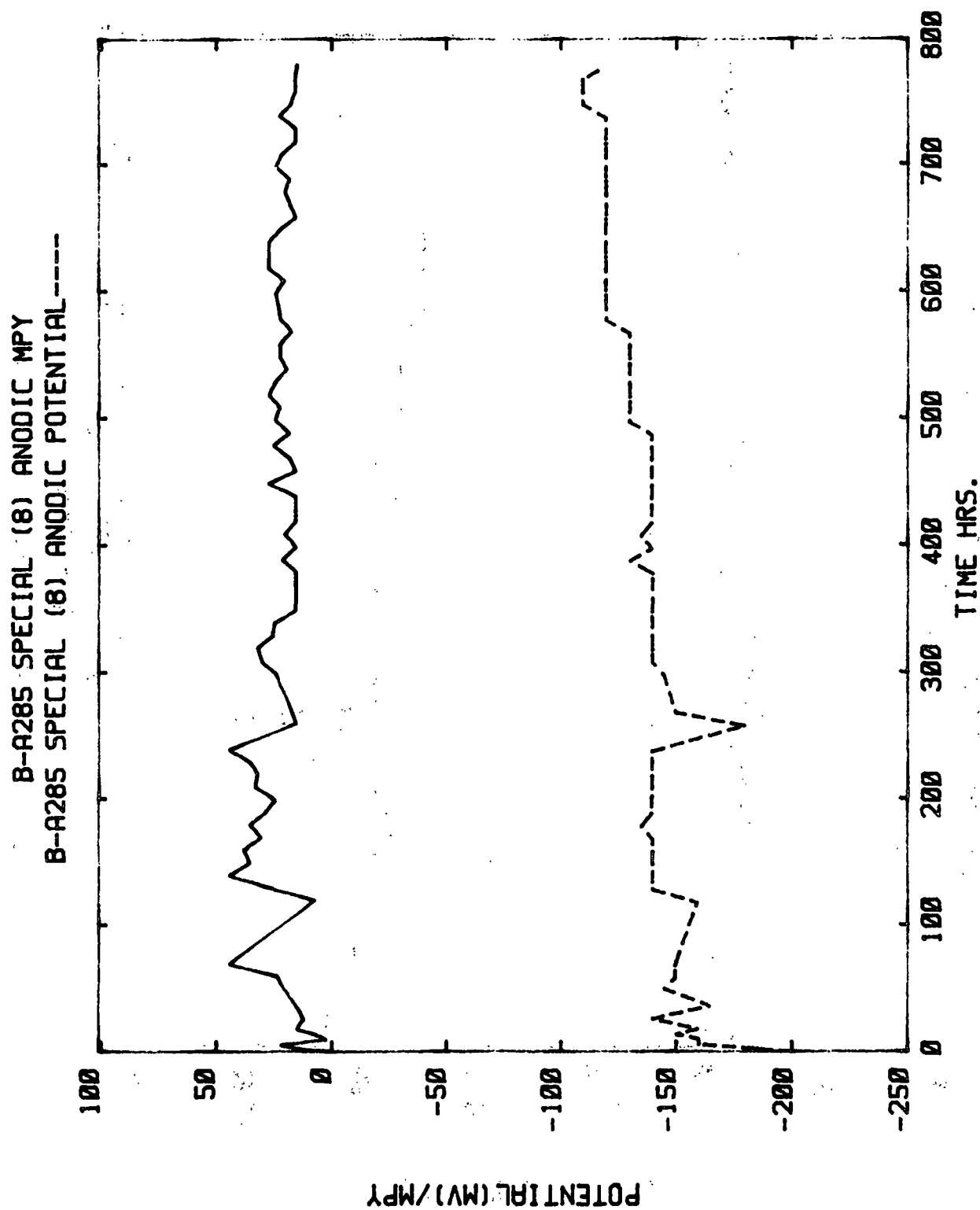


Figure 27. Mill Bl. A285-SPEC. Anodic LPR. Electrode 8.

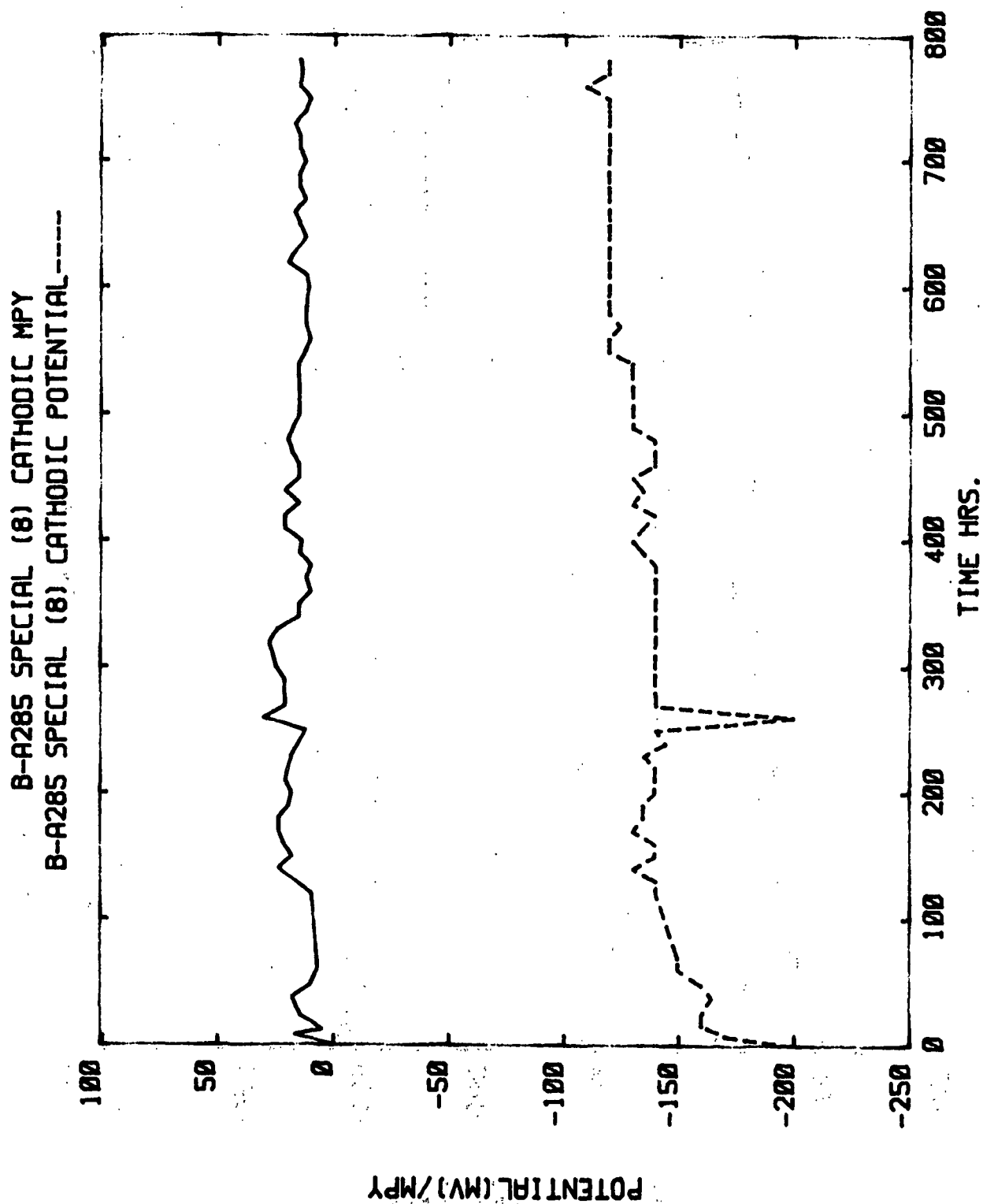


Figure 28. Mill B1. A285-SPEC. Cathodic LPR. Electrode 8.

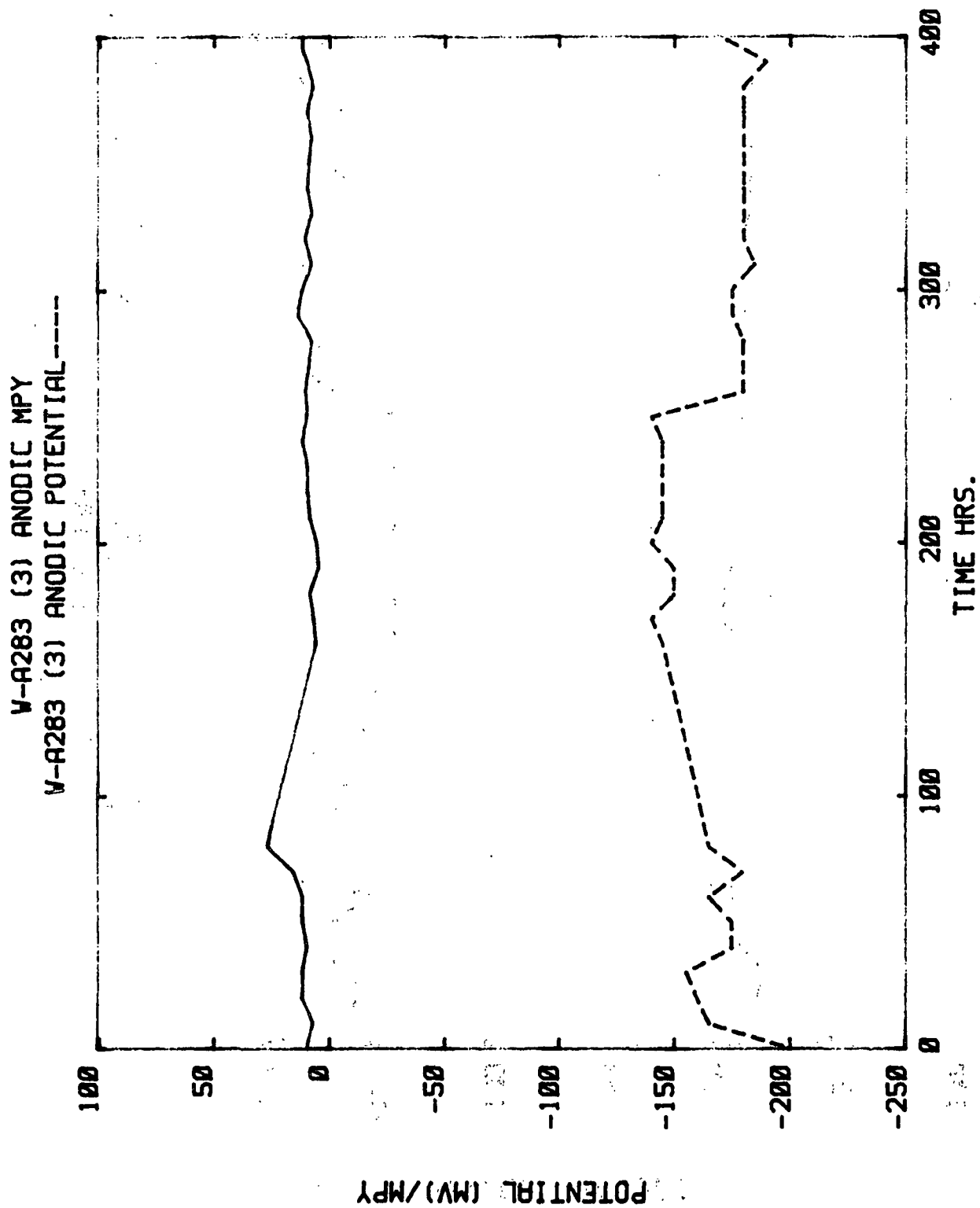


Figure 29. Mill W2. A283. Anodic LPR. Electrode 3.

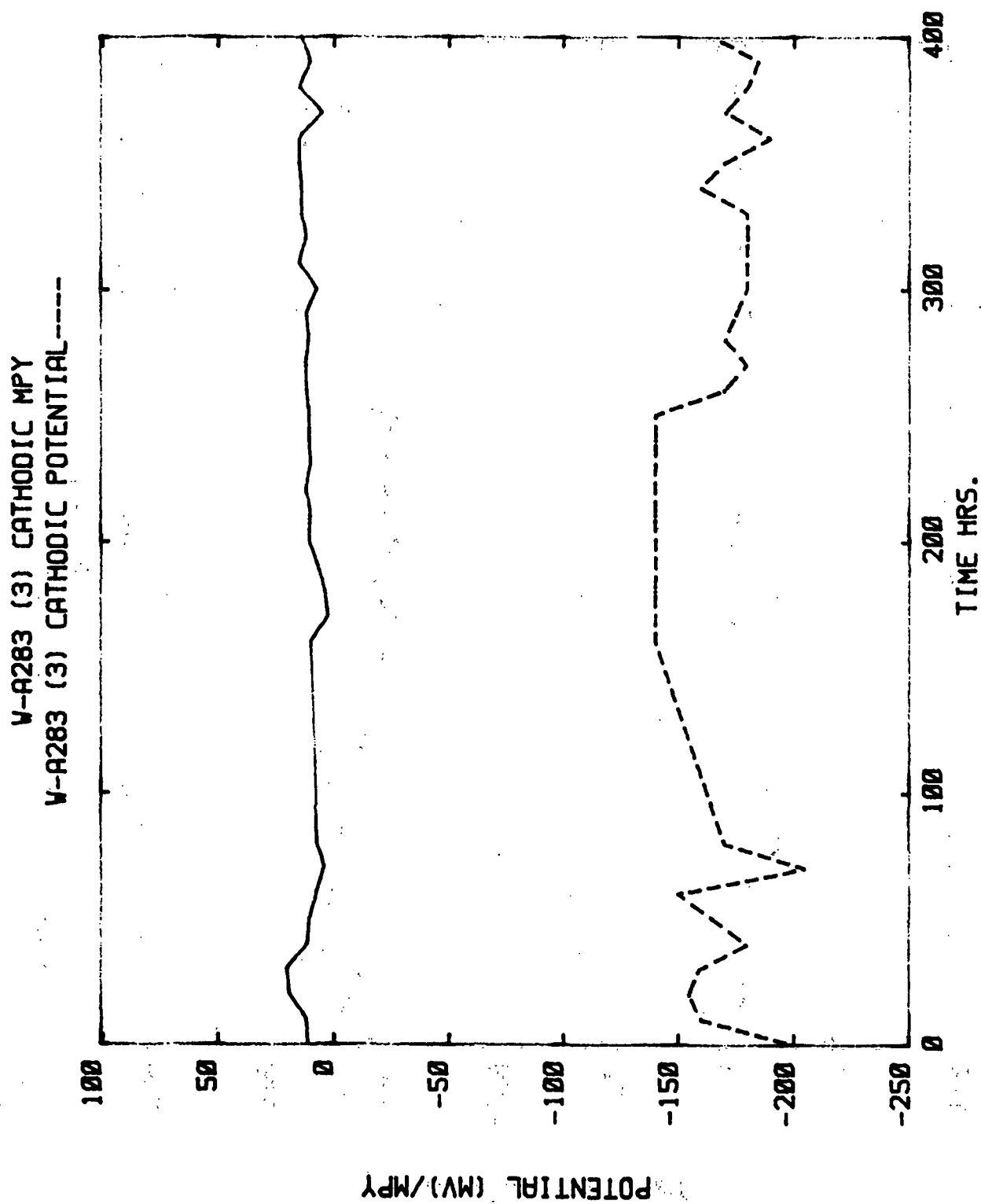


Figure 30. Mill W2. A283. Cathodic LPR. Electrode 3.



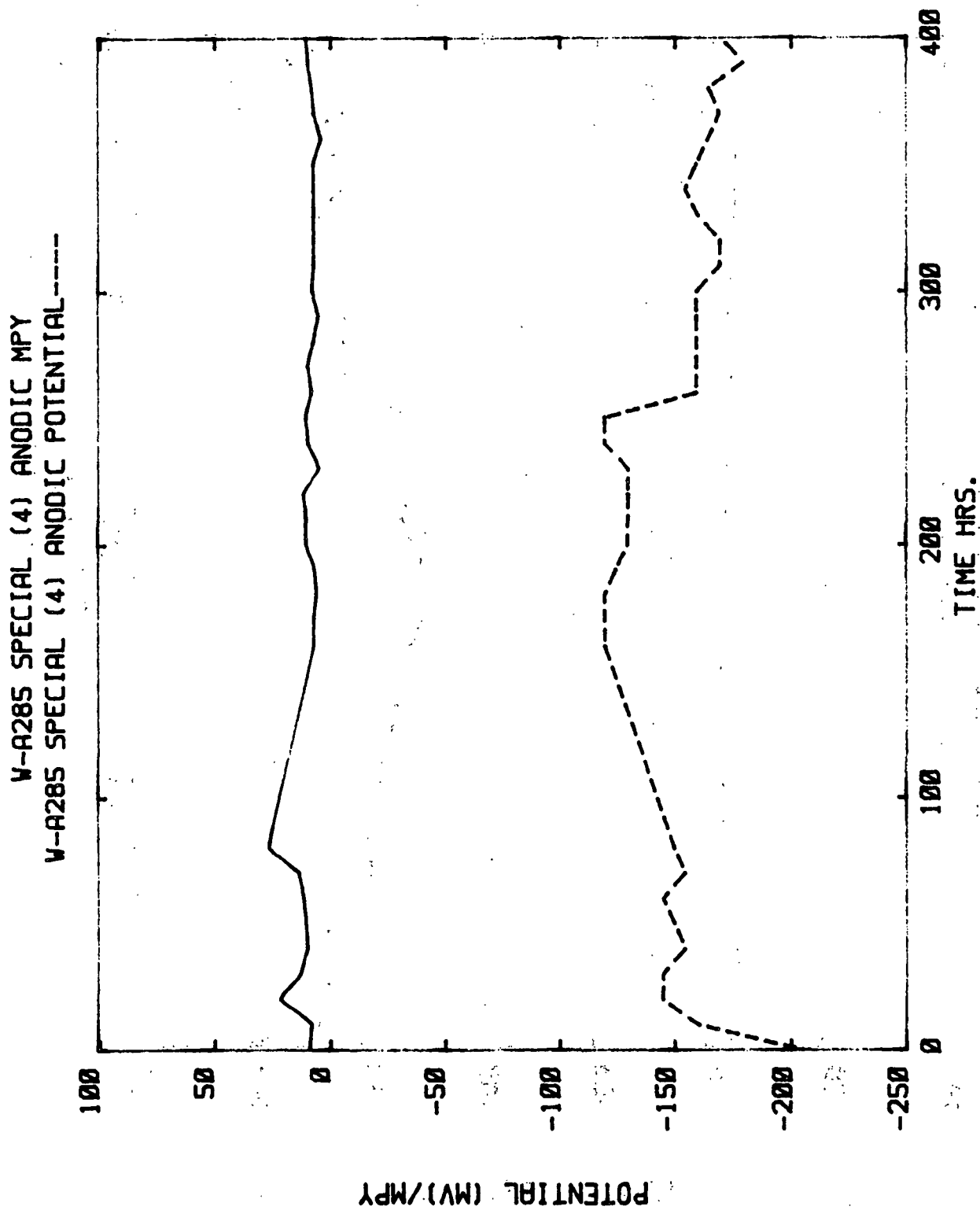


Figure 31. Mill W2. A285-SPEC. Anodic LPR. Electrode 4.

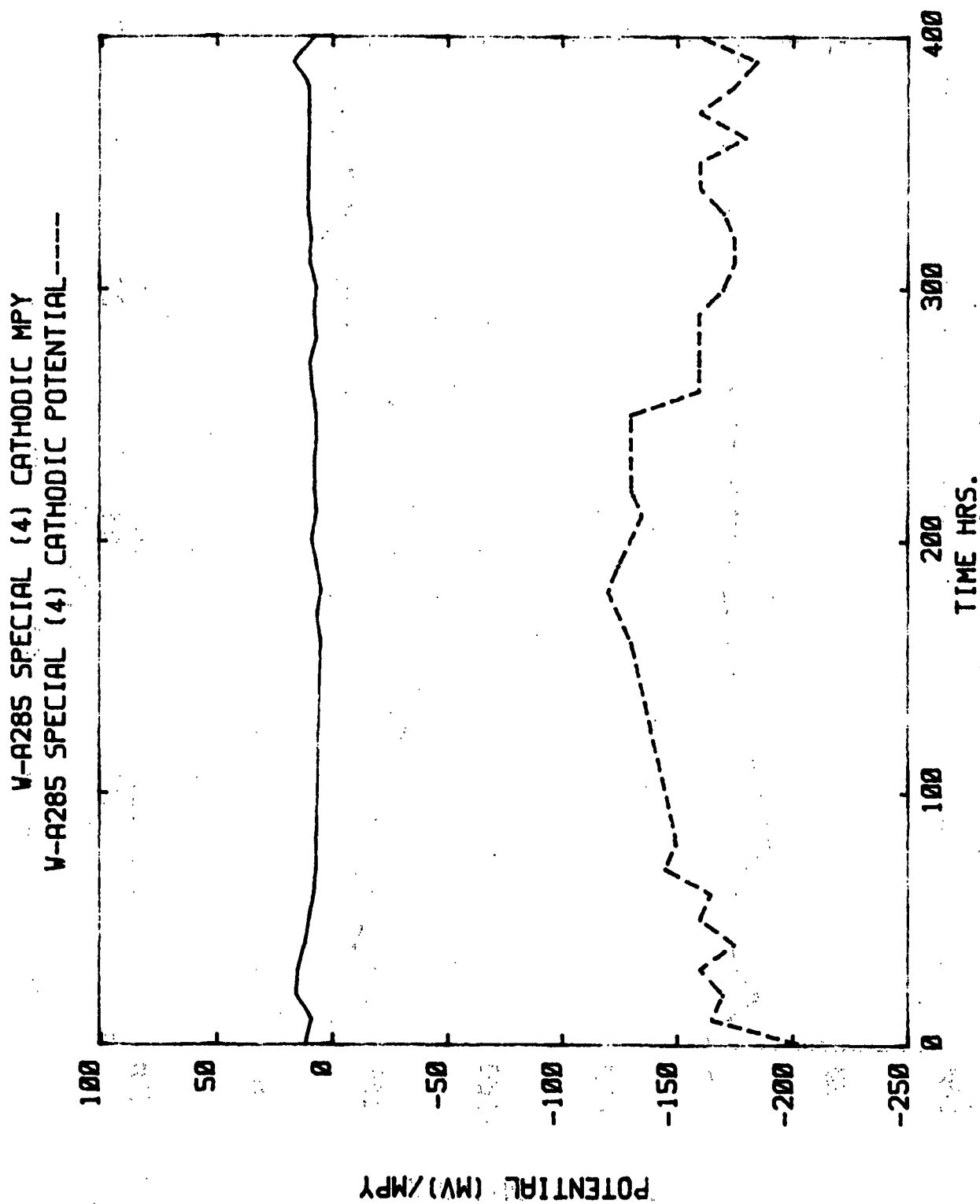


Figure 32. Mill W2. A285-SPEC. Cathodic LPR. Electrode 4.

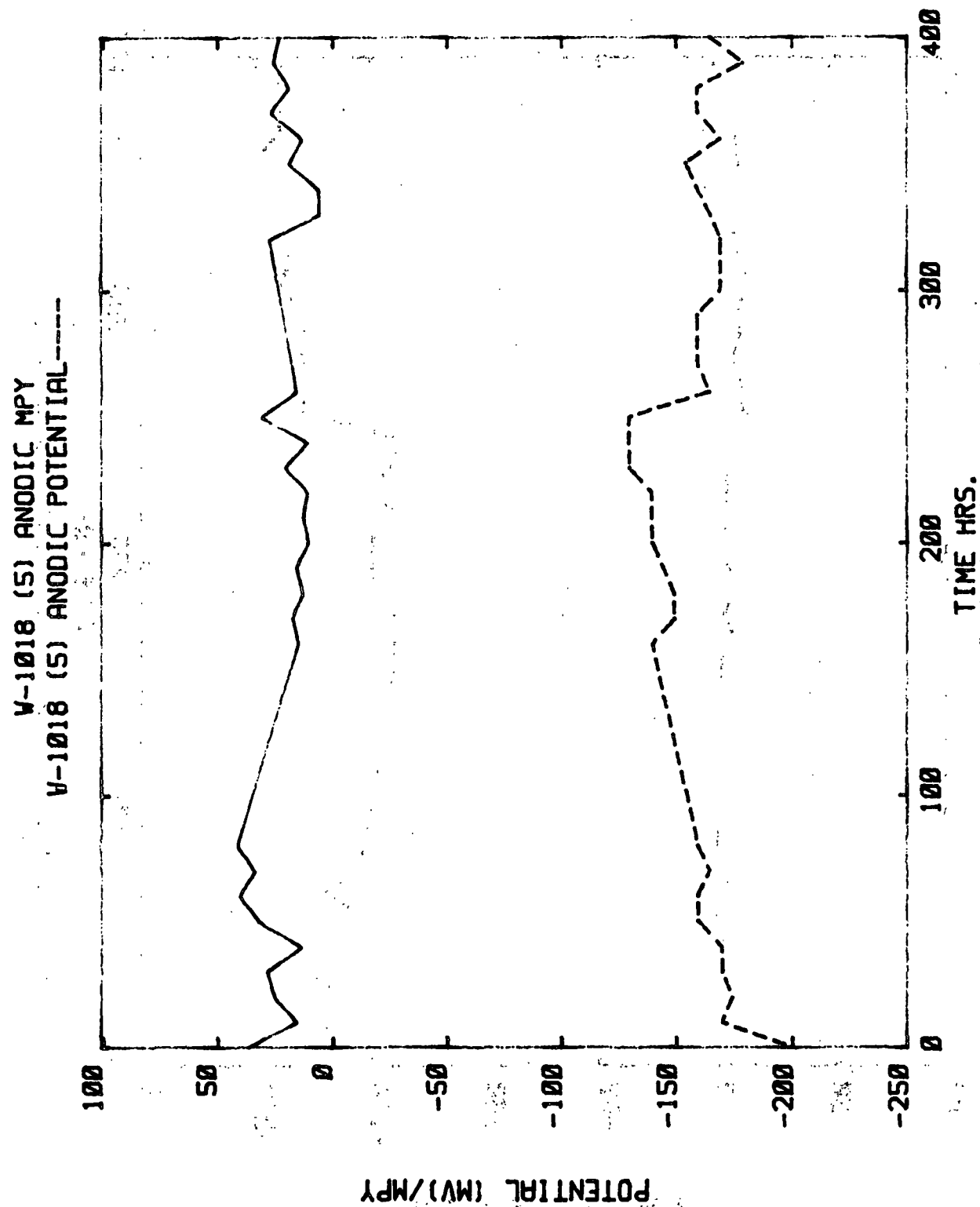


Figure 33. Mill W2. 1018. Anodic LPR. Electrode 5.

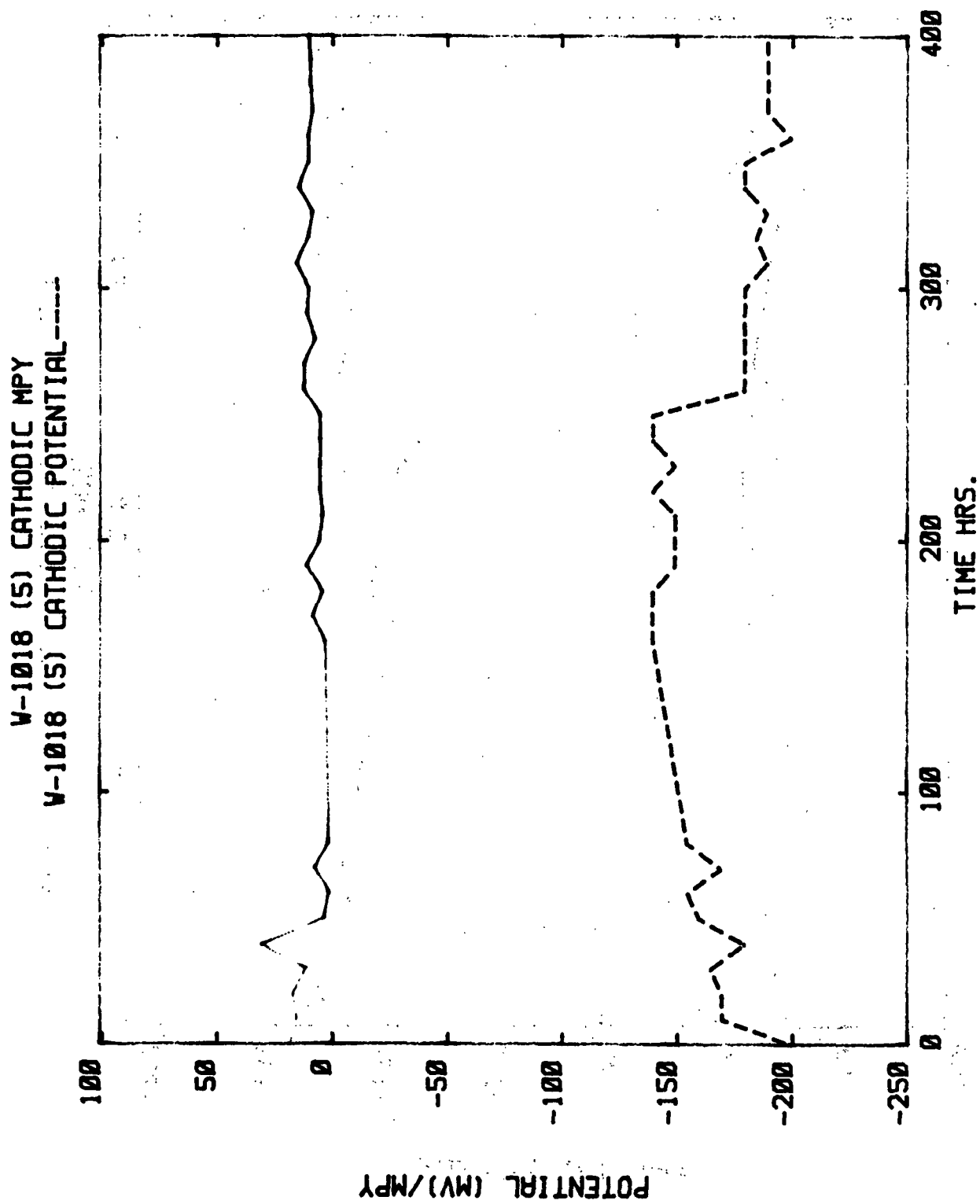


Figure 34. Mill W2. 1018. Cathodic LPR. Electrode 5.

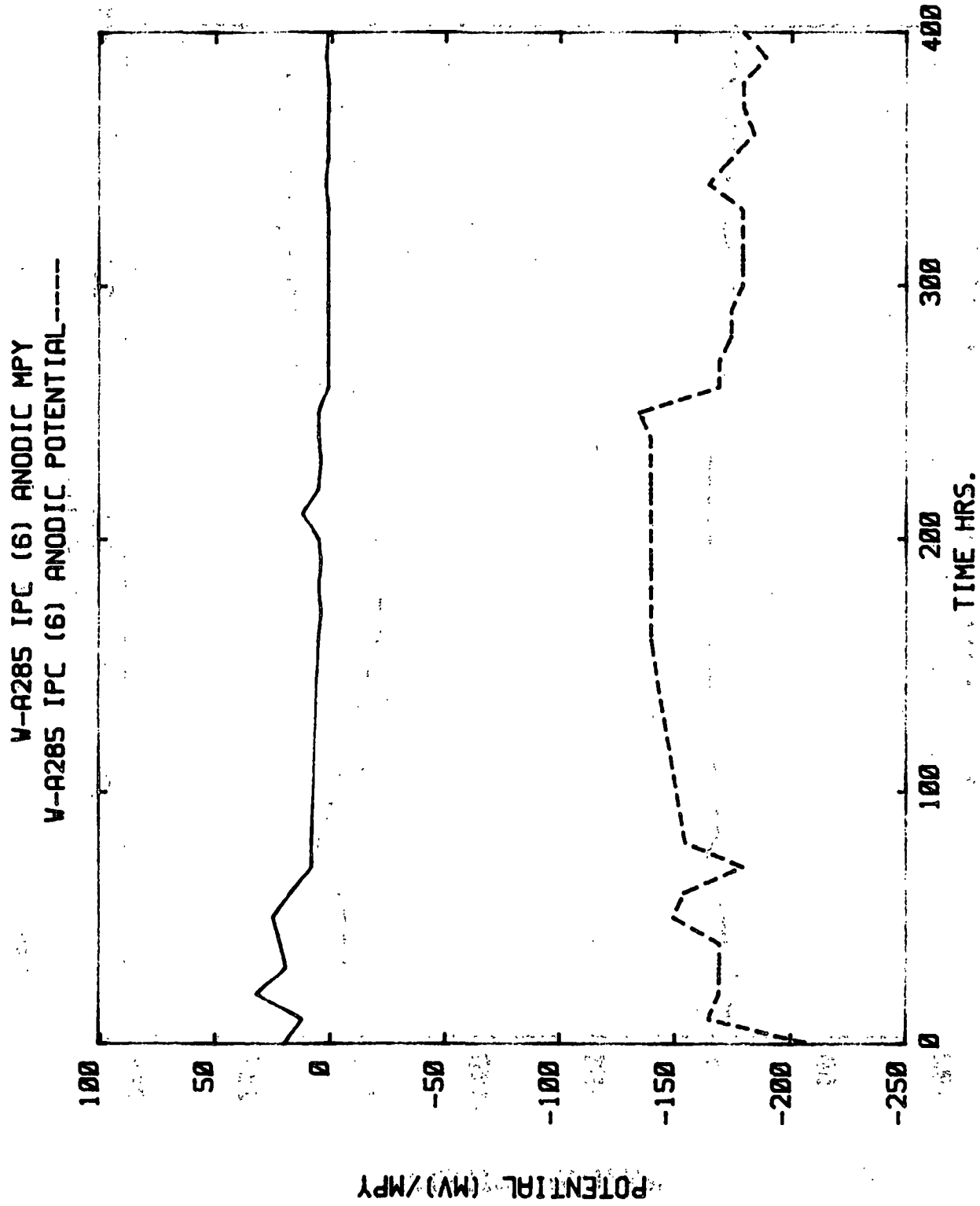


Figure 35. Mill W2-A285C. Anodic LPR. Electrode 6.

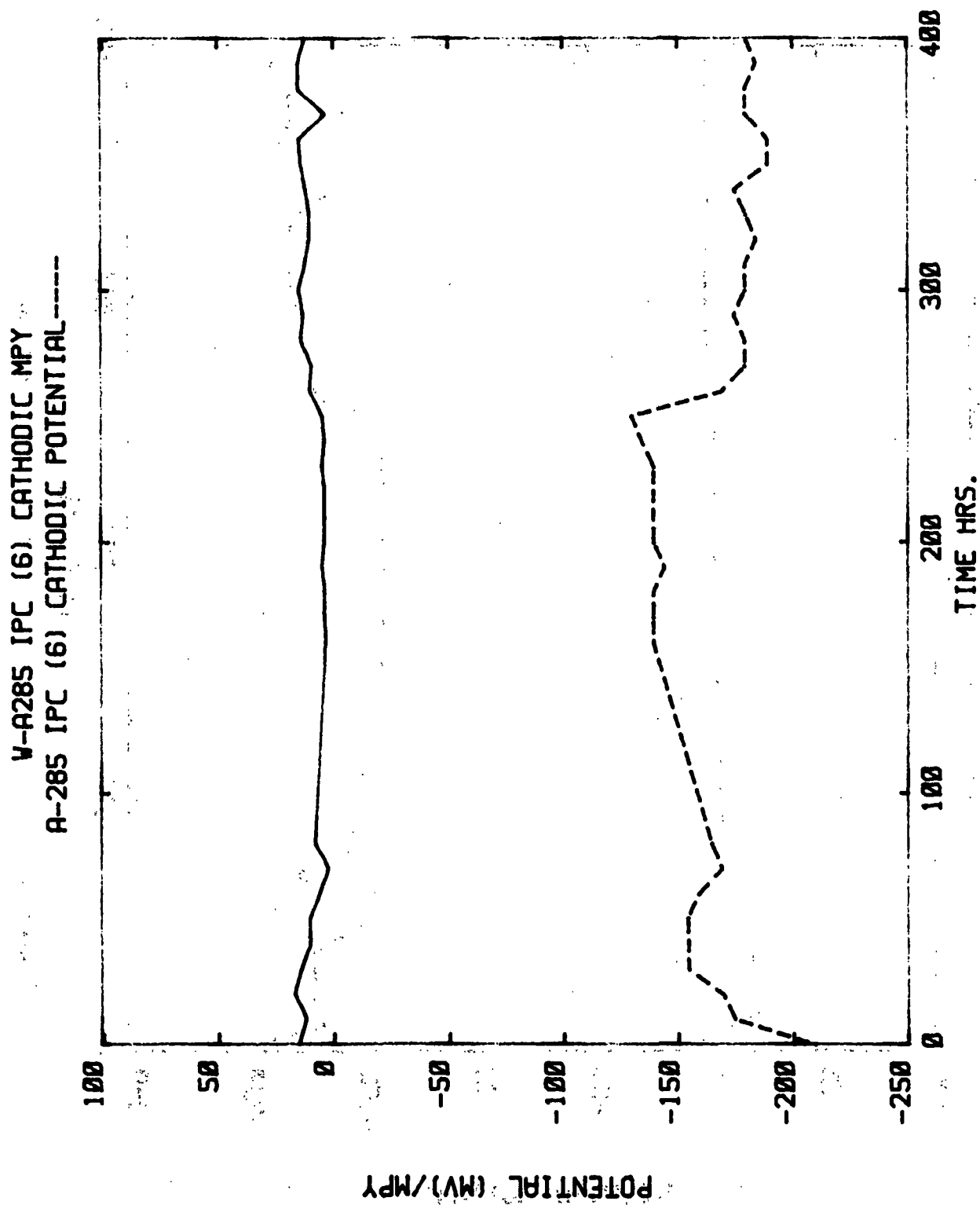


Figure 36. Mill W2. A285C. Cathodic LPR. Electrode 6.

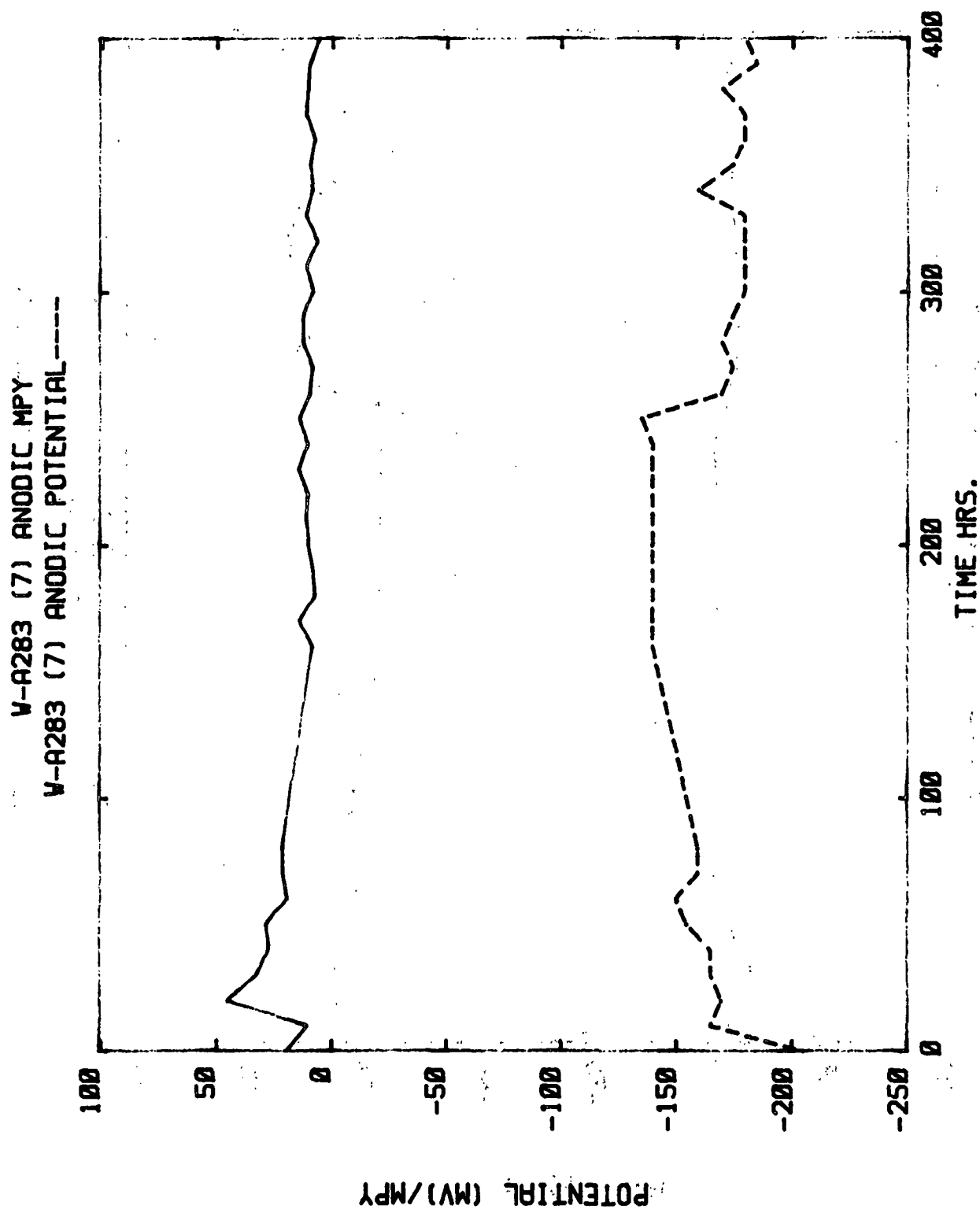


Figure 37. Mill W2. A283. Anodic LPR. Electrode 7.

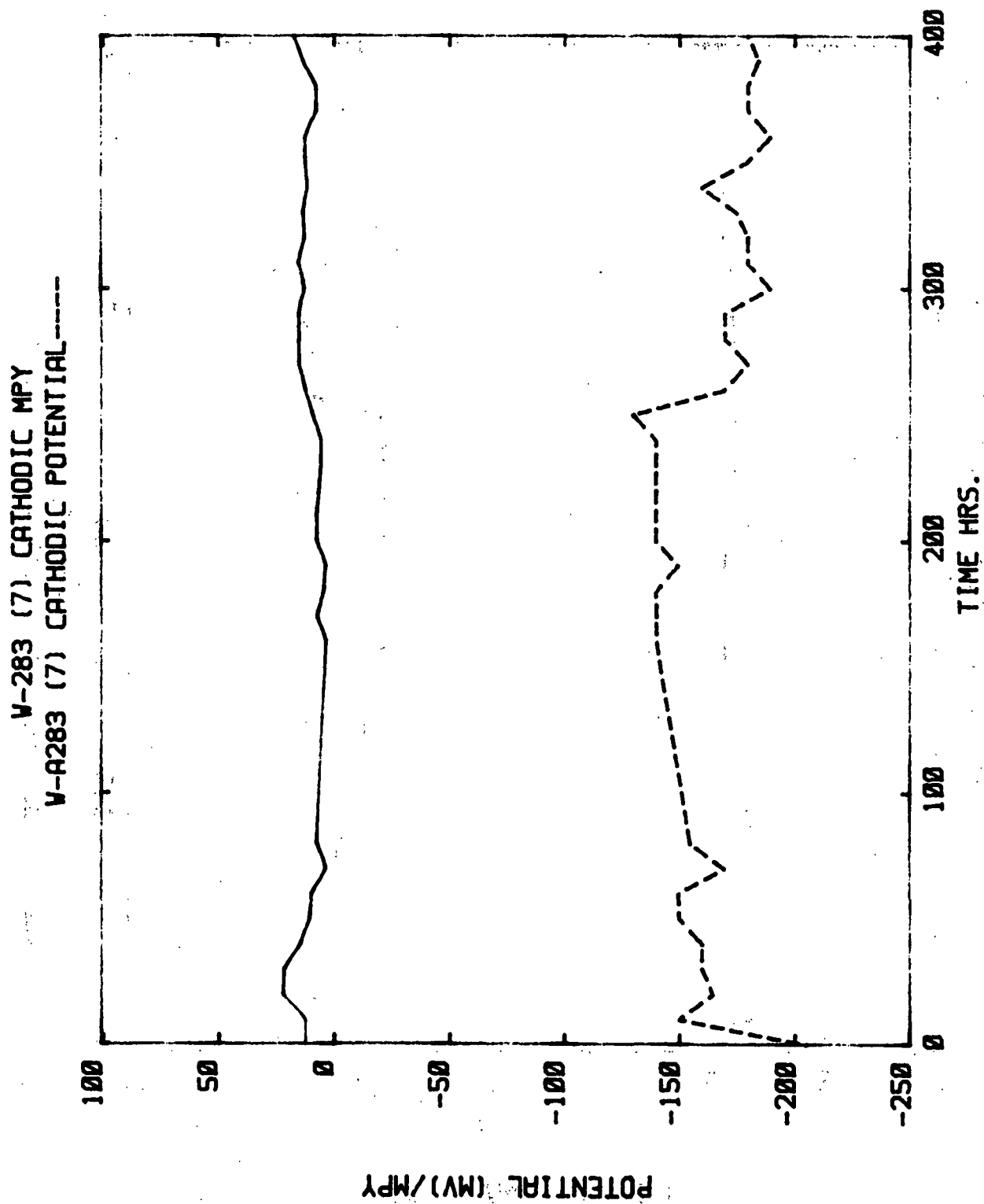


Figure 38. Mill W2. A283. Cathodic LPR. Electrode 7.



V-A285 SPECIAL (8) ANODIC MPY  
V-A285 SPECIAL (8) ANODIC POTENTIAL----

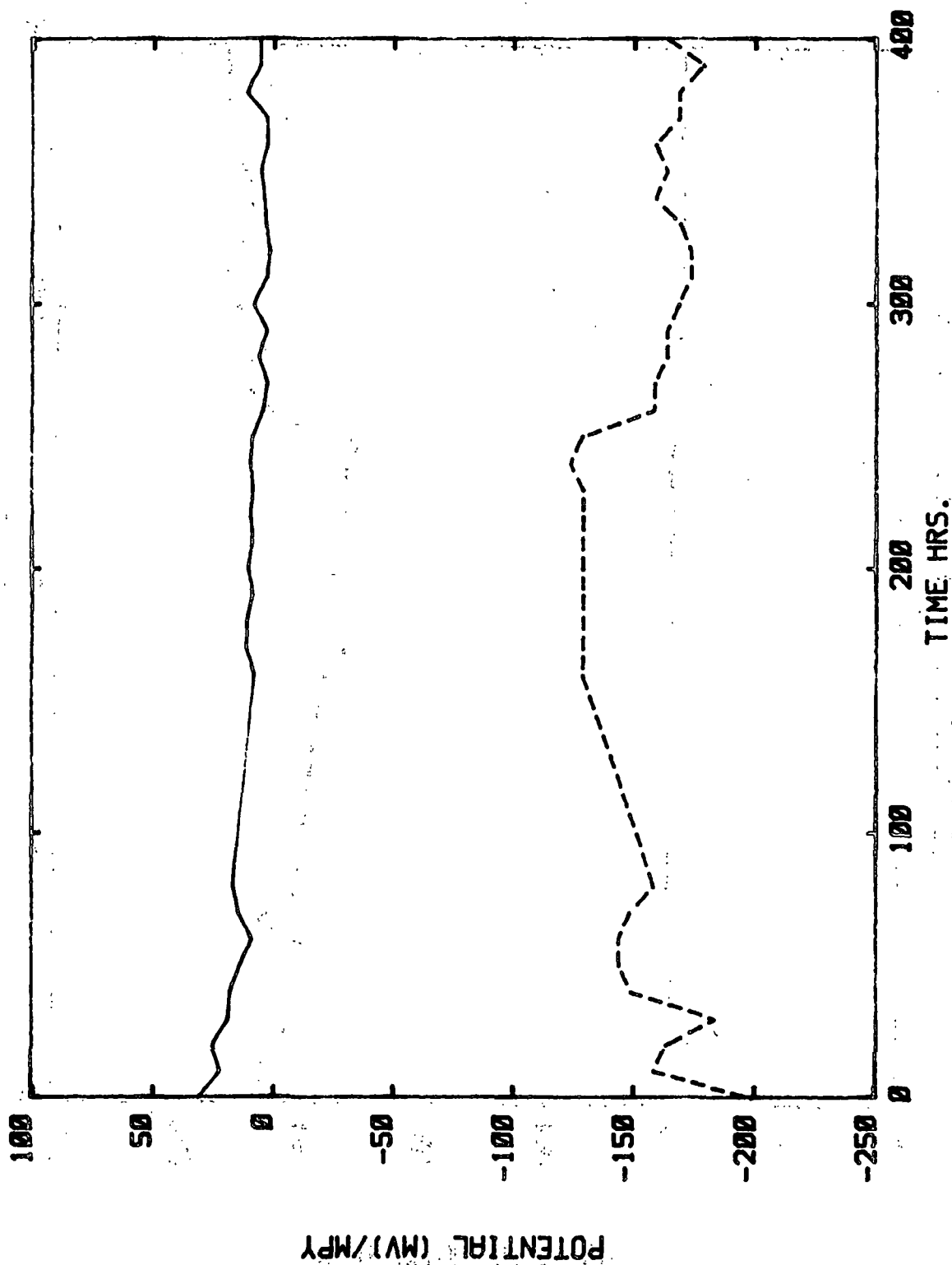


Figure 39. Mill W2. A285-SPEC. Anodic LPR. Electrode 8.

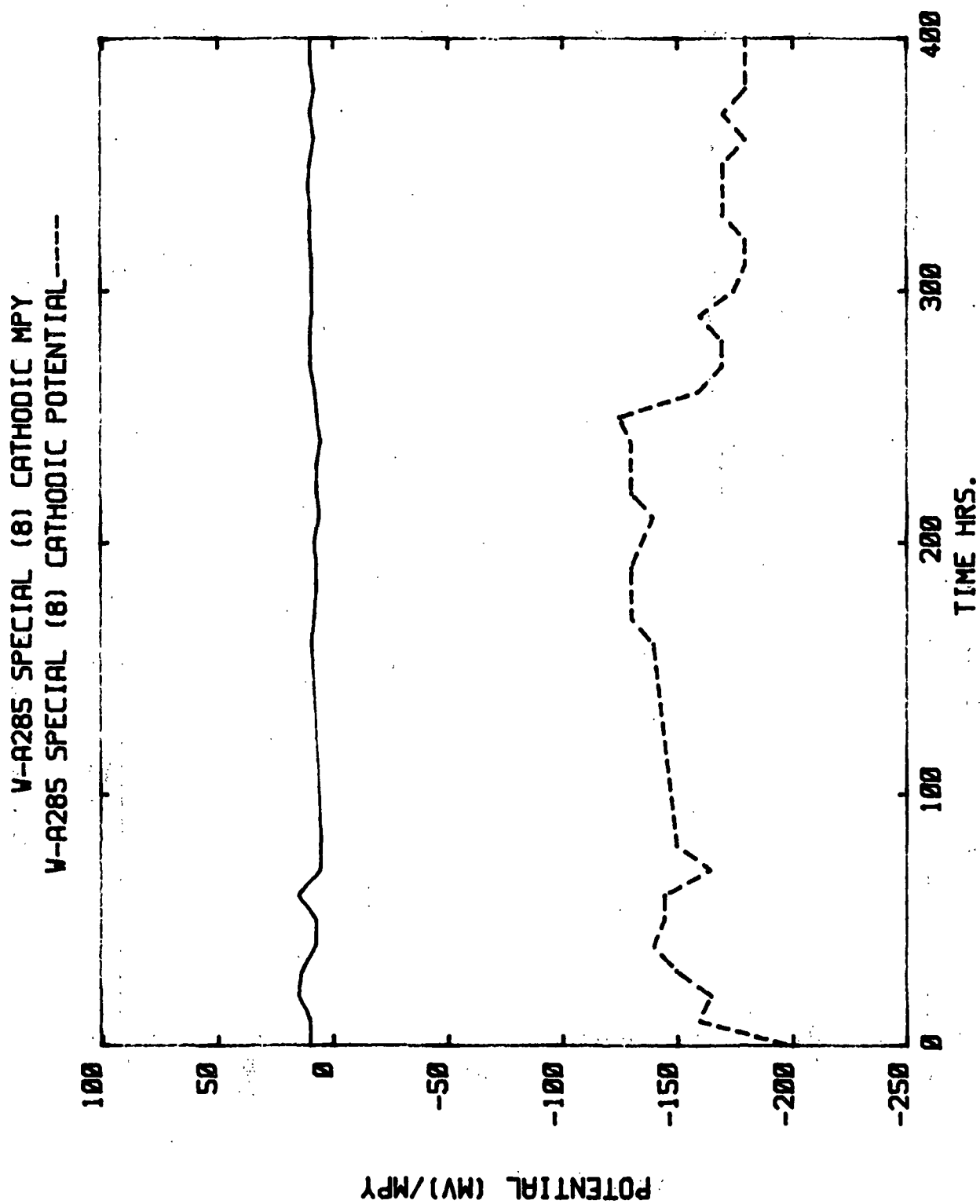


Figure 40. Mill W2. A285-SPEC. Cathodic LPR. Electrode 8.

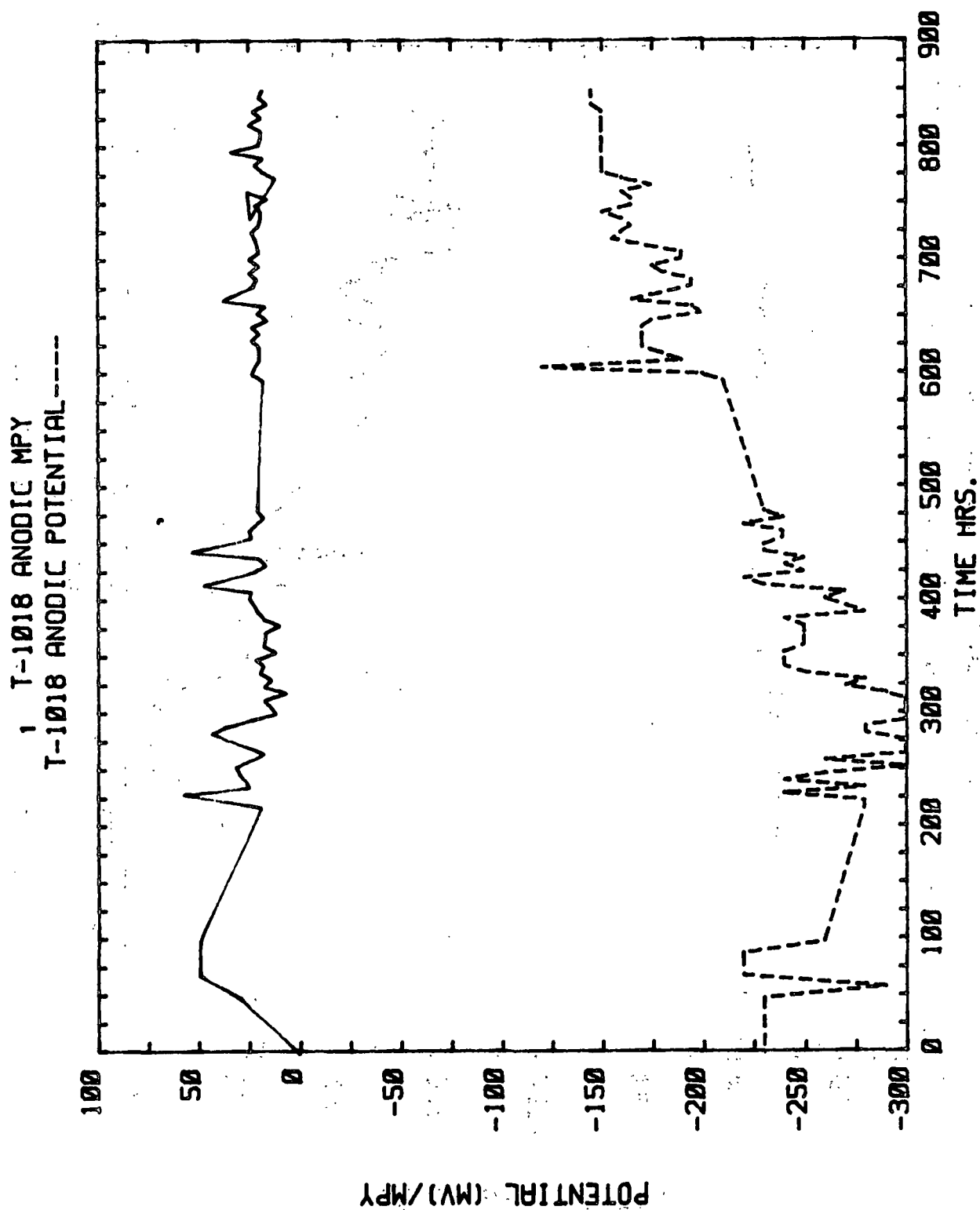


Figure 41. Mill T3. 1018. Anodic LPR. Electrode 1.

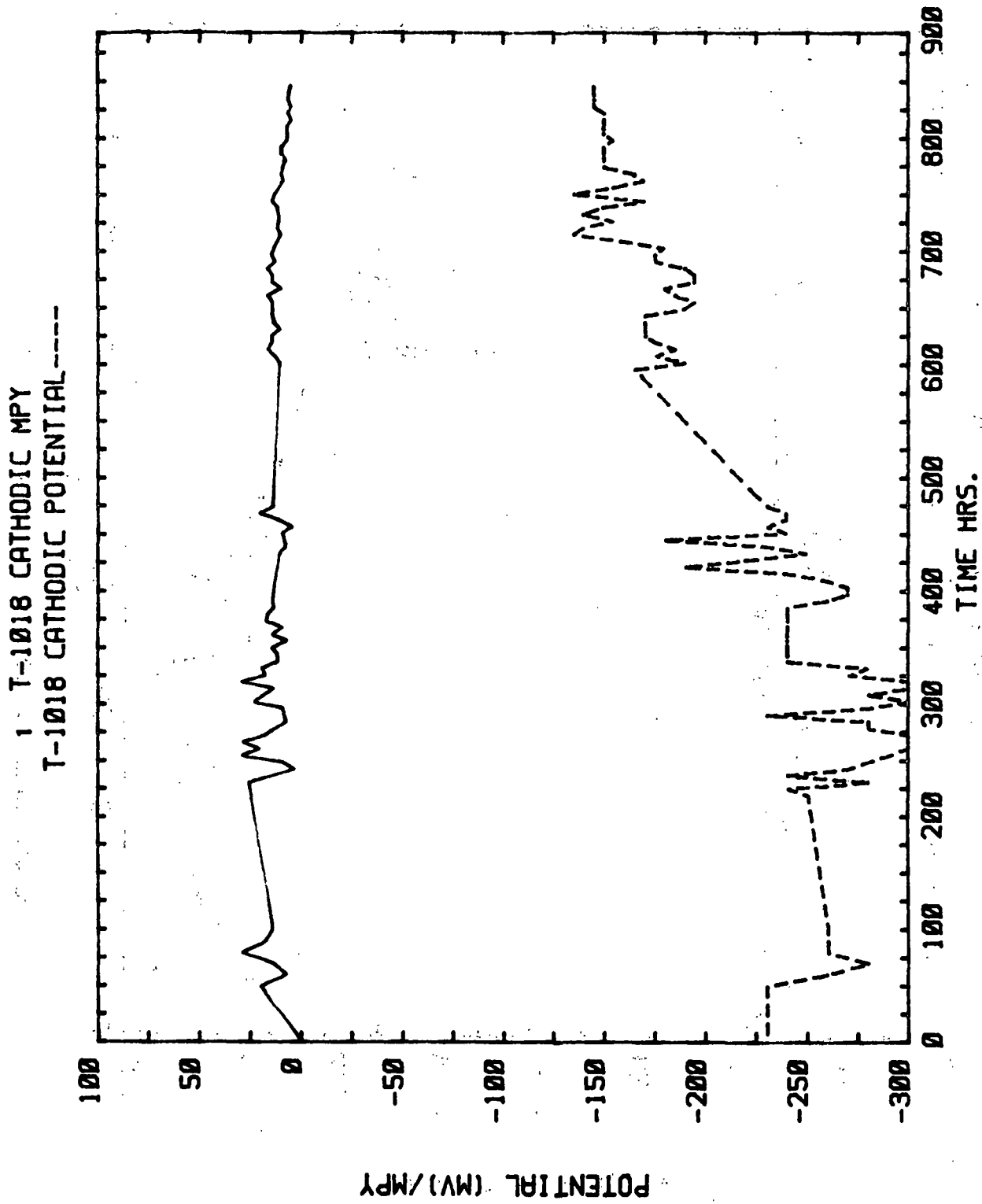


Figure 42. Mill T3. 1018. Cathodic LPR. Electrode 1.

2 T-A285 ANODIC MPY  
T-A285 ANODIC POTENTIAL-----

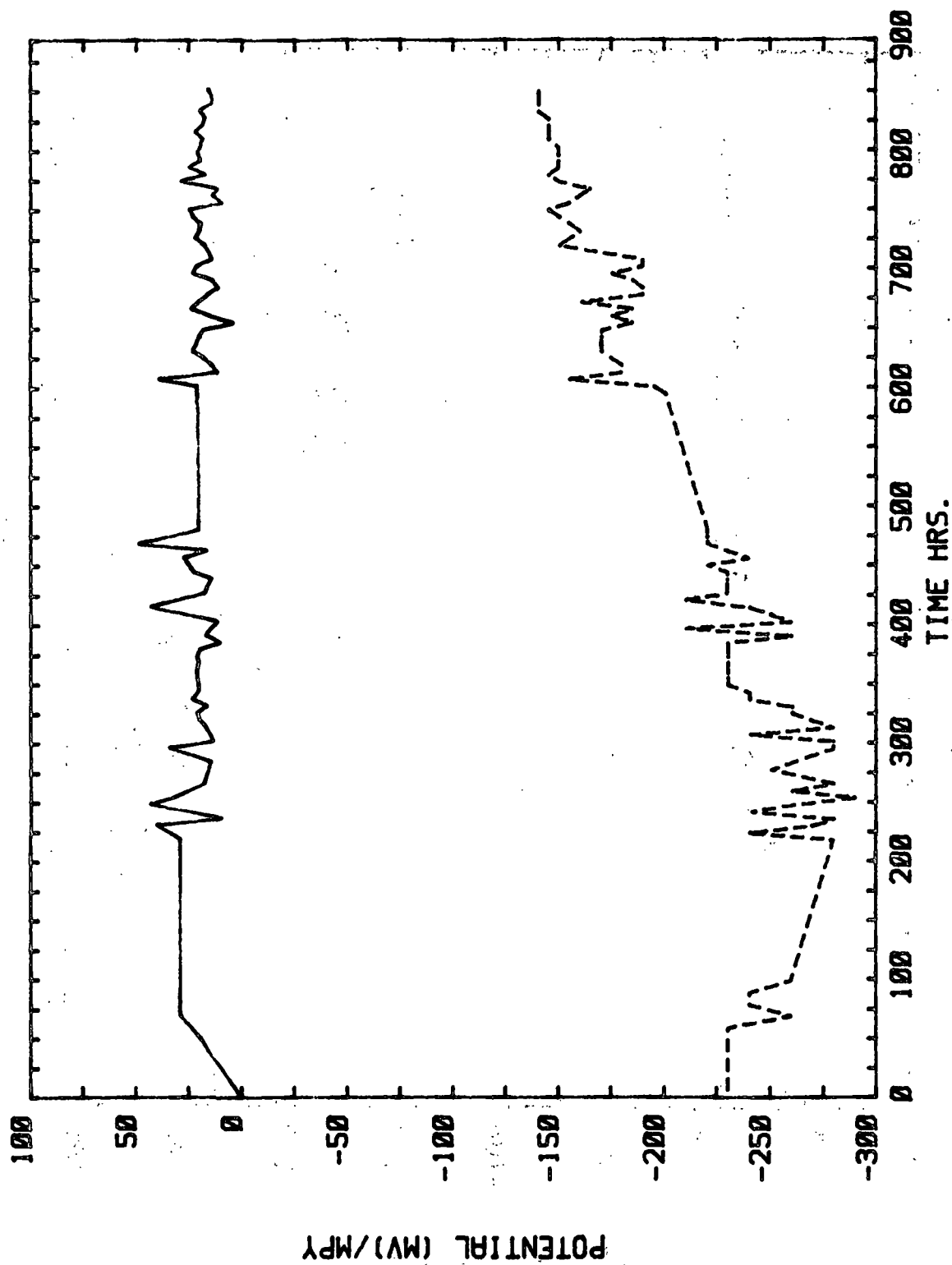


Figure 43. Mill T3. A285C. Anodic LPR. Electrode 2.

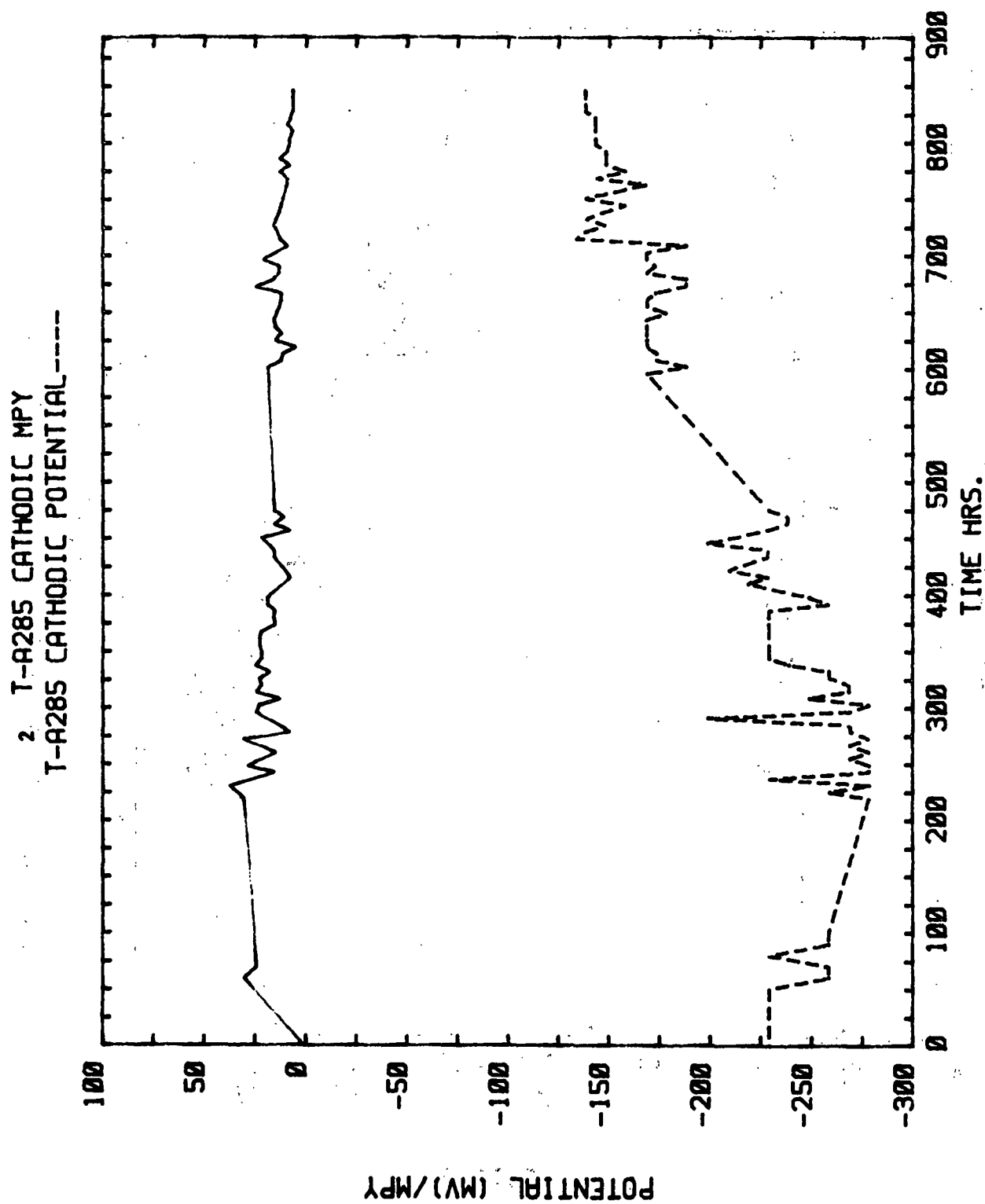


Figure 44. Mill T3. A285C. Cathodic LPR. Electrode 2.

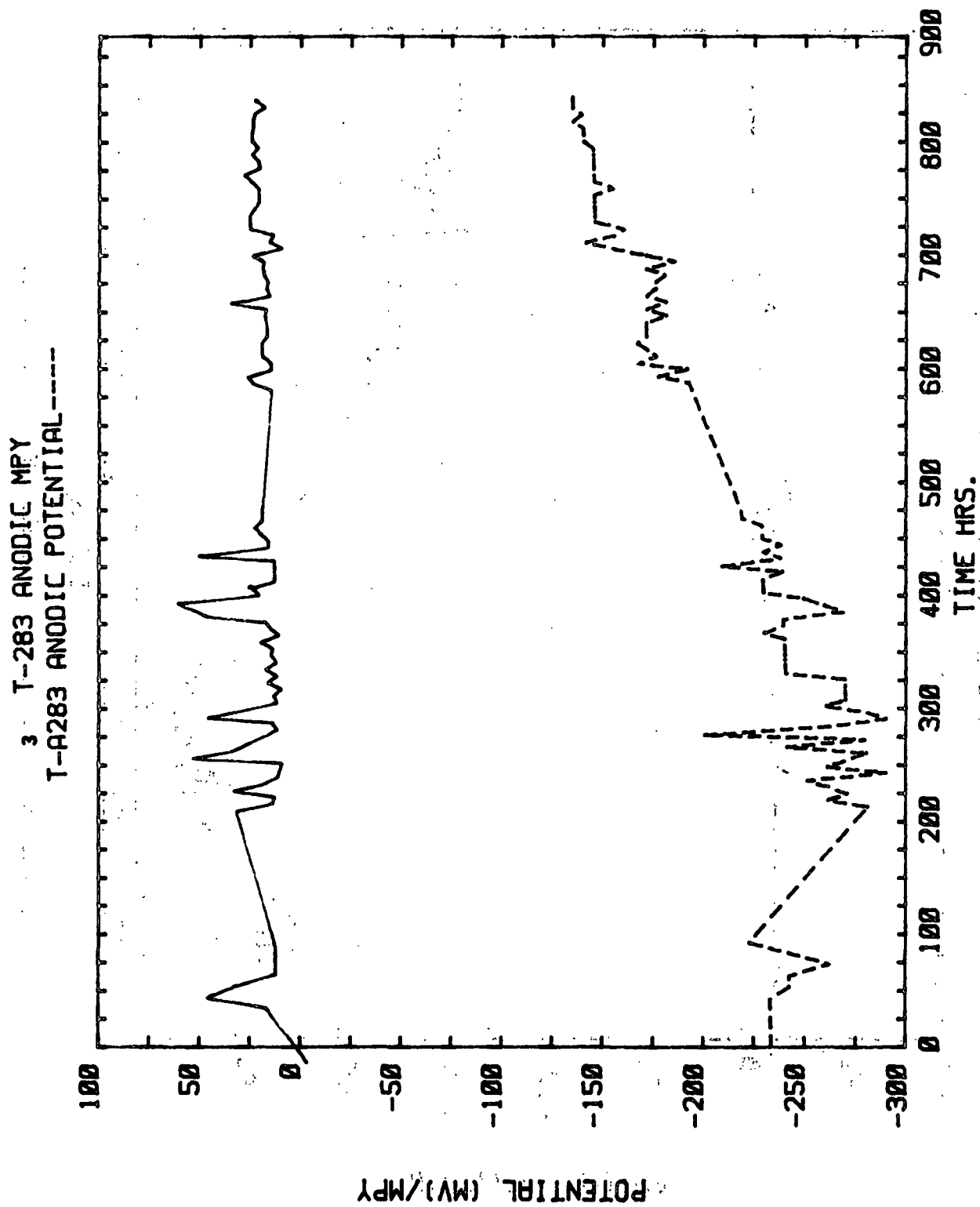


Figure 45. Mill T3. A283. Anodic LPR. Electrode 3.

3 T-283 CATHODIC MPY  
T-283 CATHODIC POTENTIAL-----

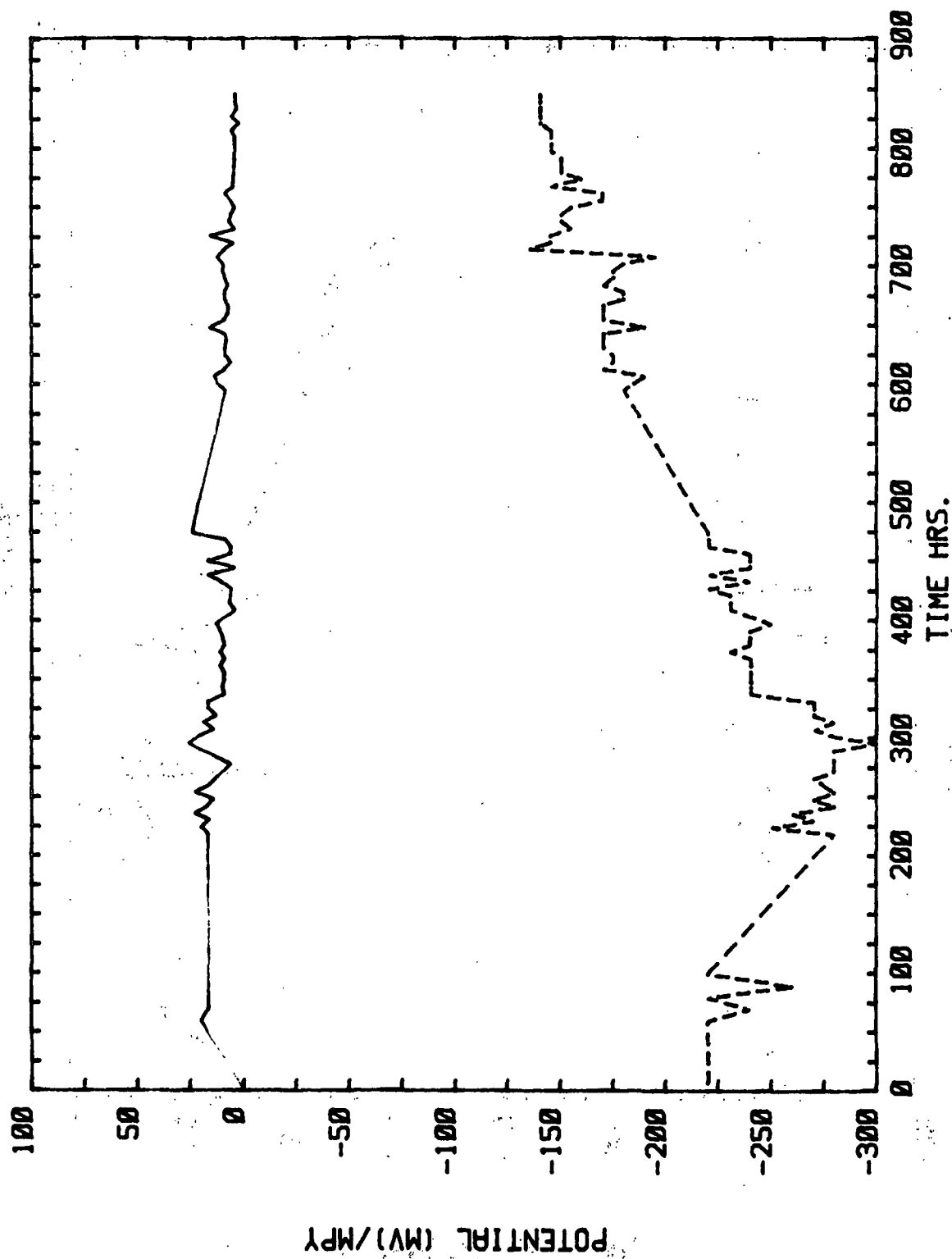


Figure 46. Mill T3. A283. Cathodic LPR. Electrode 3.



4 T-A285 SPECIAL ANODIC MPY  
T-A285 SPECIAL ANODIC POTENTIAL-----

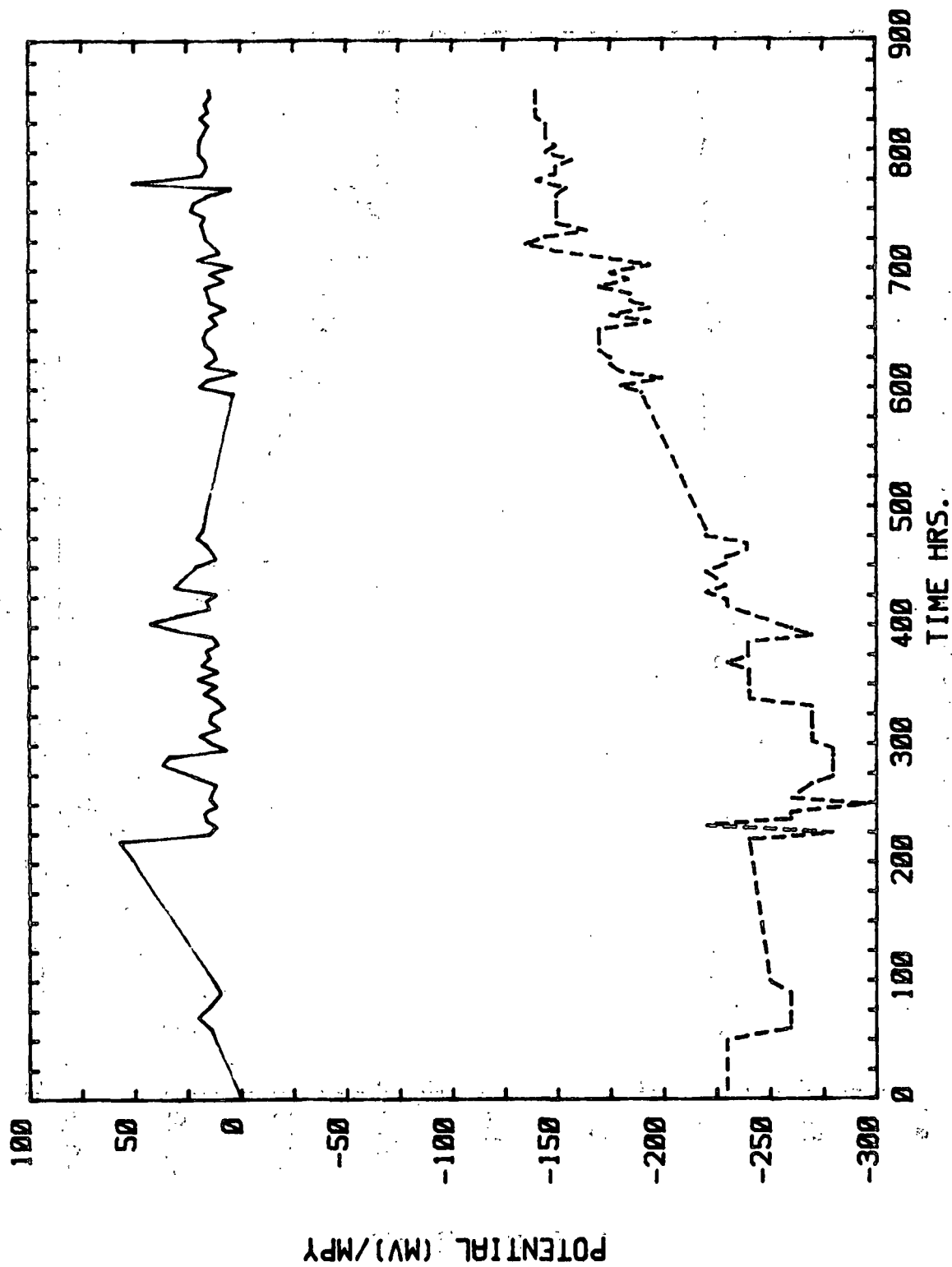


Figure 47. Mill T3. A285-SPEC. Anodic LPR. Electrode 4.

4 T-A285 SPECIAL CATHODIC MPY  
T-A285 SPECIAL CATHODIC POTENTIAL-----

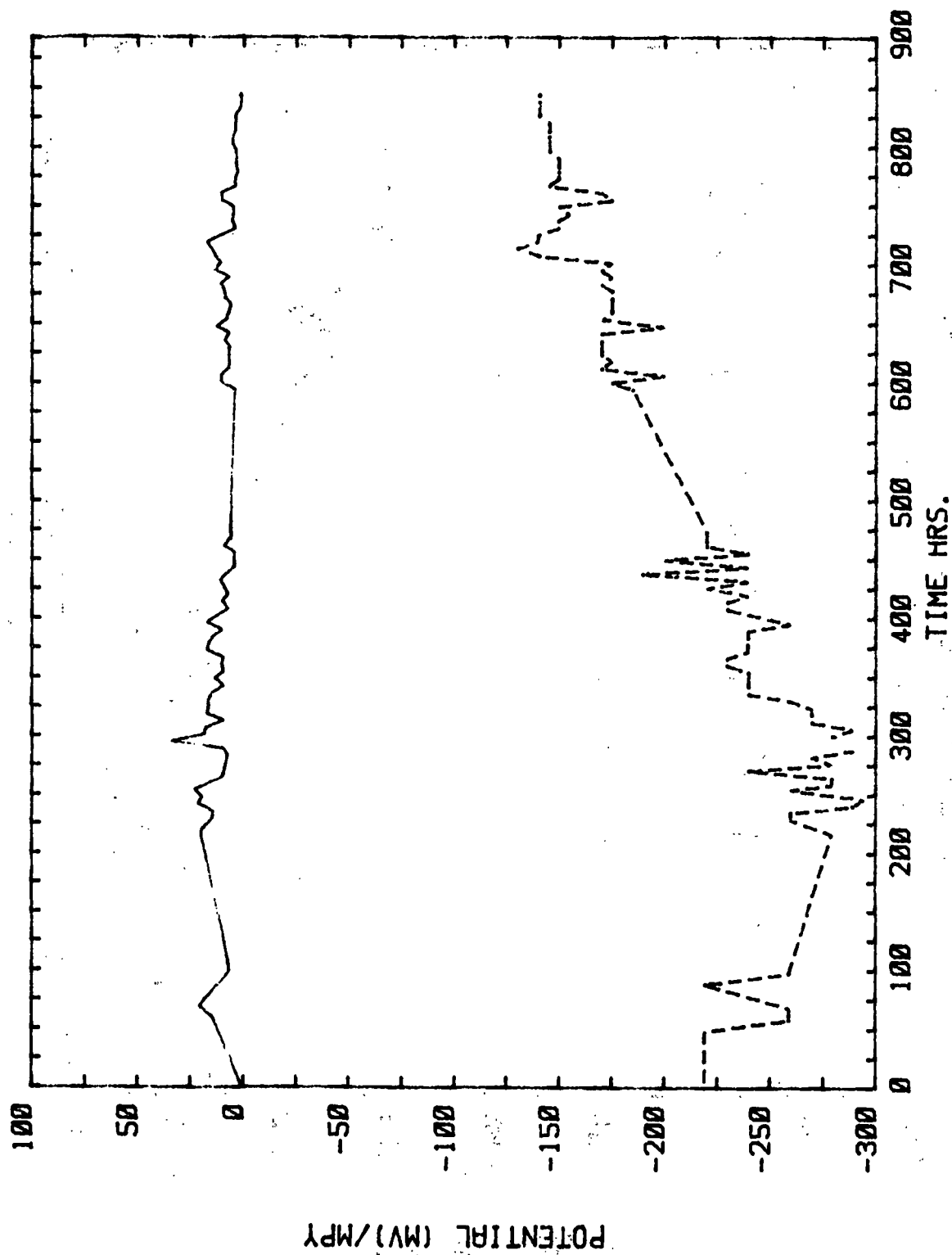


Figure 48. Mill T3. A285-SPEC. Cathodic LPR. Electrode 4.

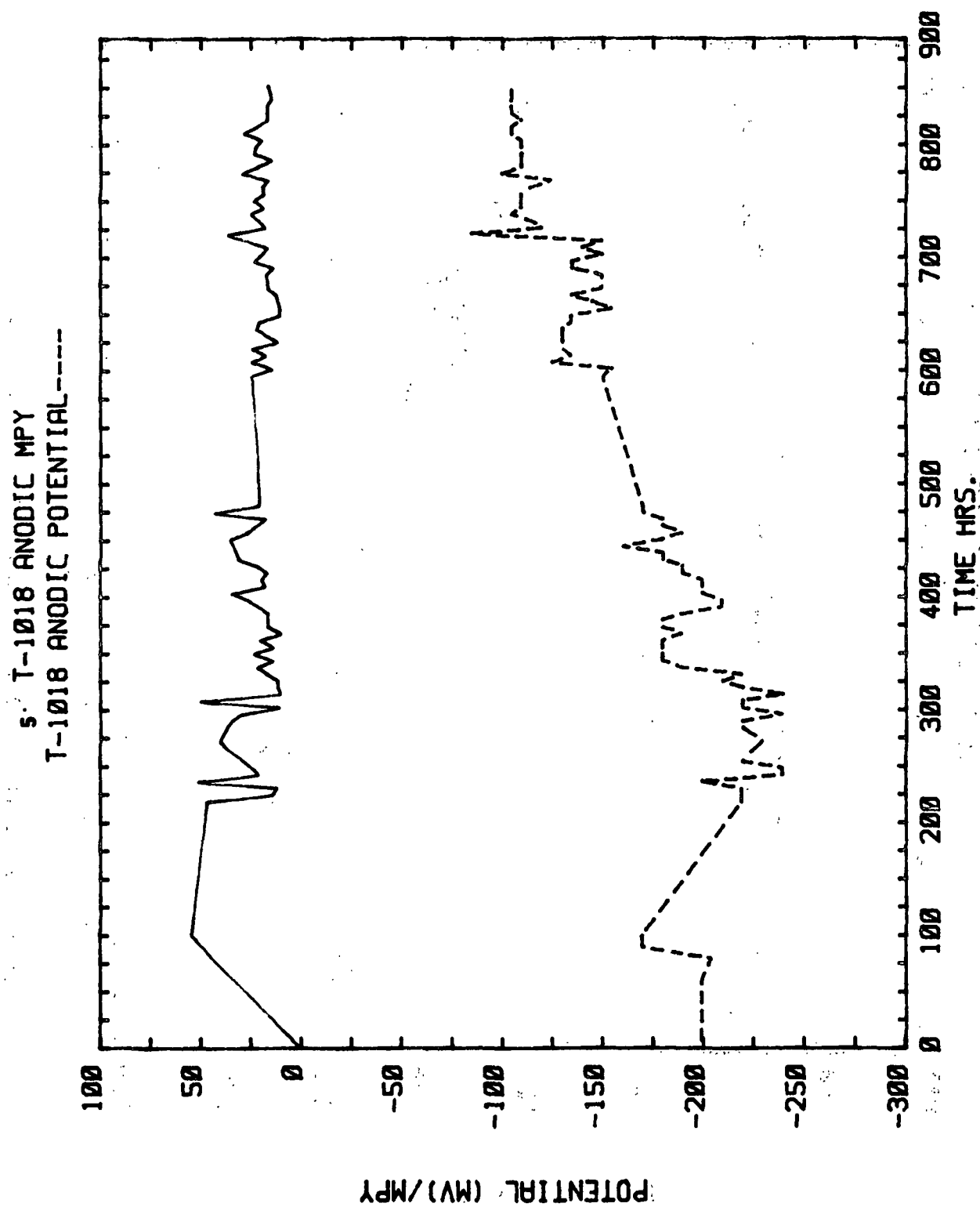


Figure 49. Mill T3. 1018. Anodic LPR. Electrode 5.

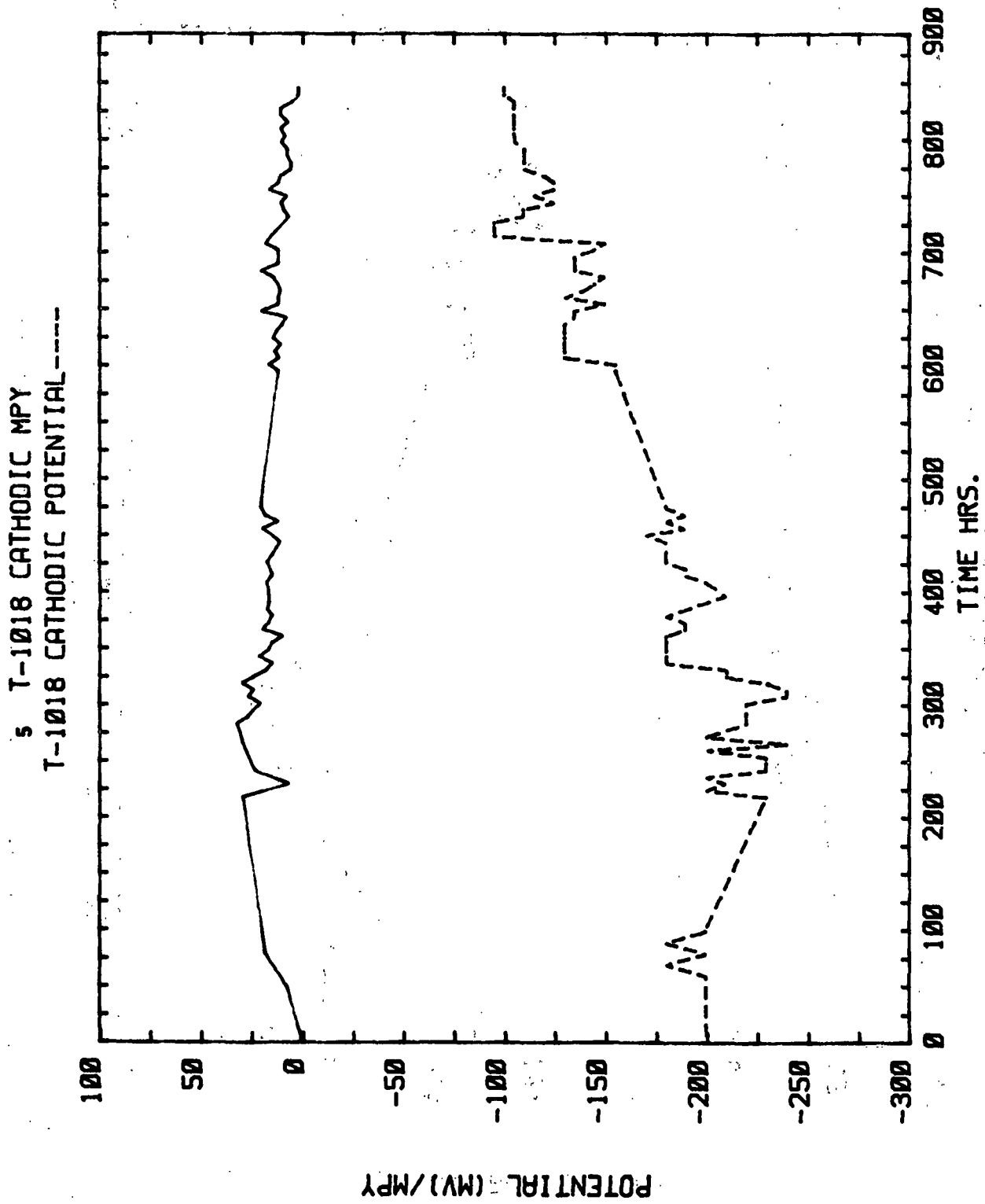


Figure 50. Mill T3. 1018. Cathodic LPR. Electrode 5.

6 T-A285 ANODIC MPY  
T-A285 ANODIC POTENTIAL-----

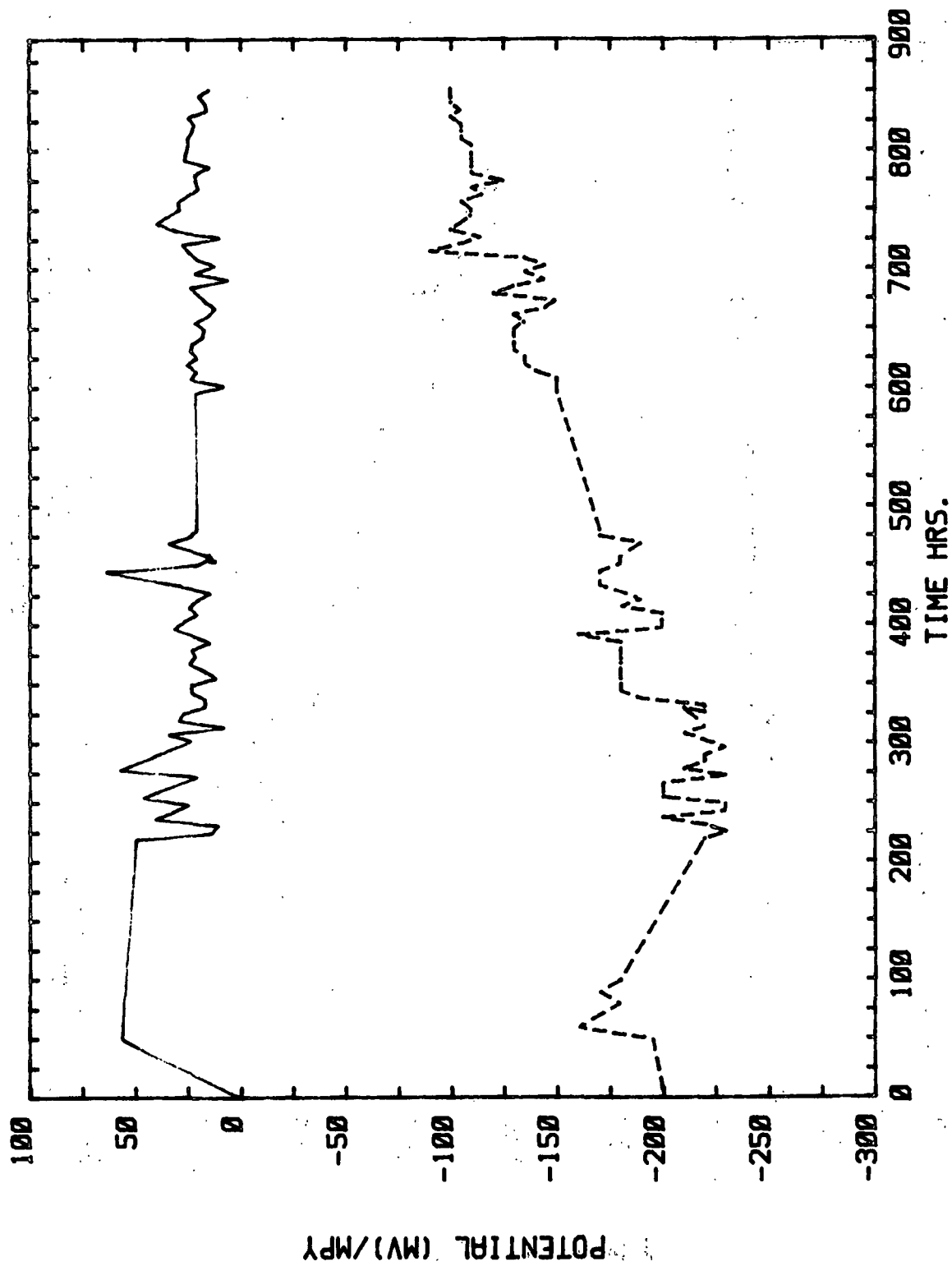


Figure 51. Mill T3. A285C. Anodic LPR. Electrode 6.

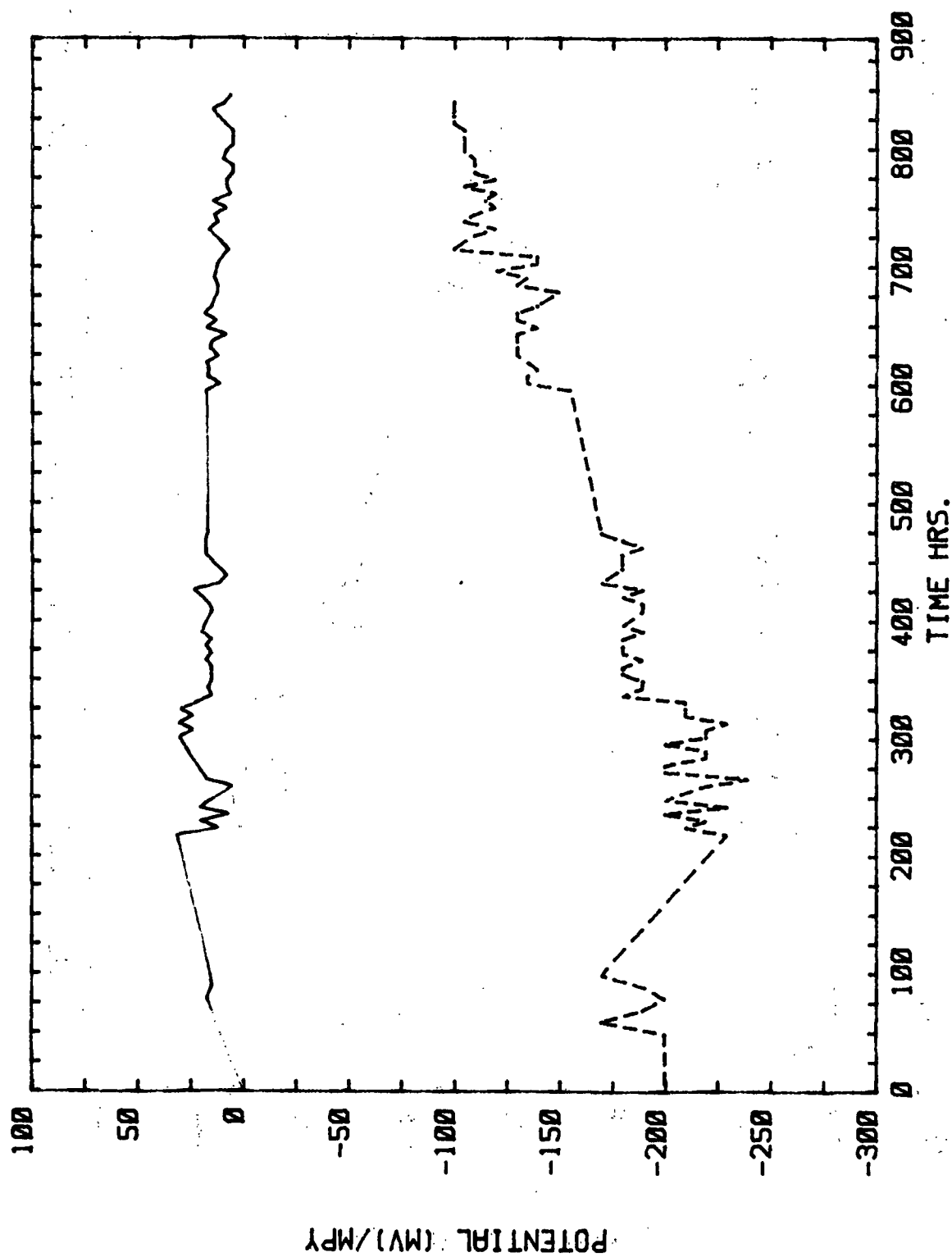


Figure 52. Mill T3. A285C. Cathodic LPR. Electrode 6.

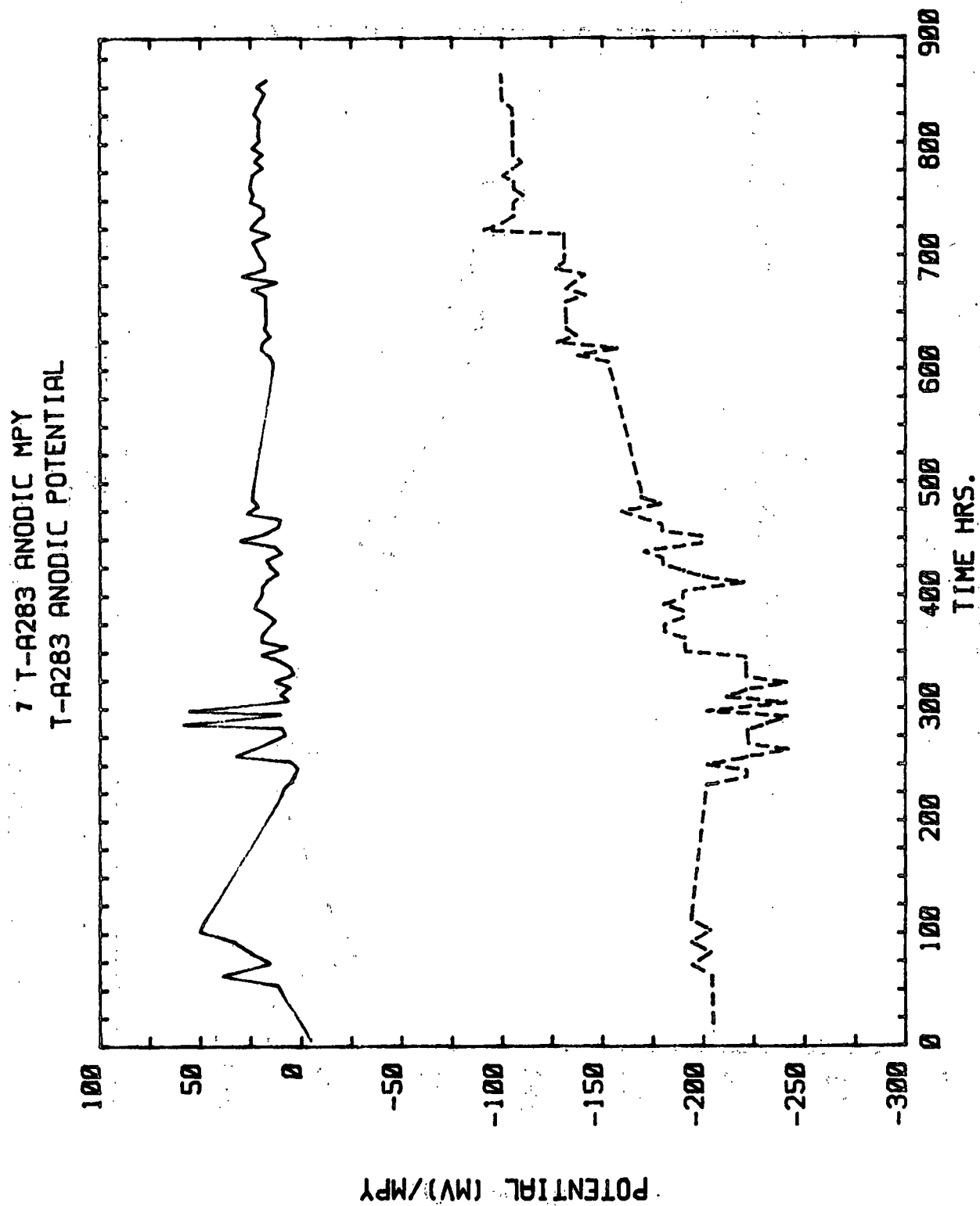


Figure 53. Mill T3. A283. Anodic LPR. Electrode 7.

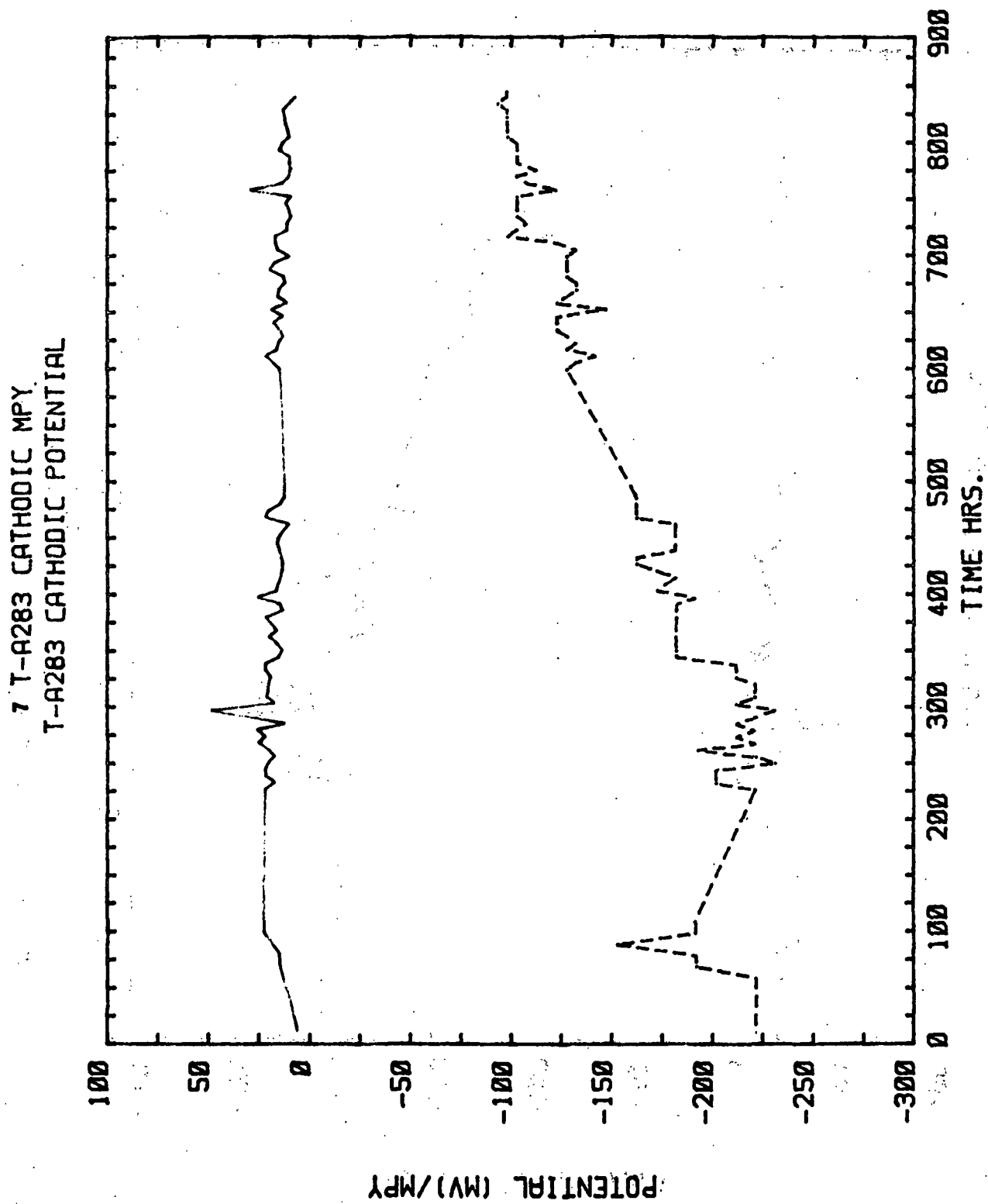


Figure 54. Mill T3. A283. Cathodic LPR. Electrode 7.



8 T-A285 SPECIAL ANODIC MPY  
T-A285 SPECIAL ANODIC POTENTIAL-----

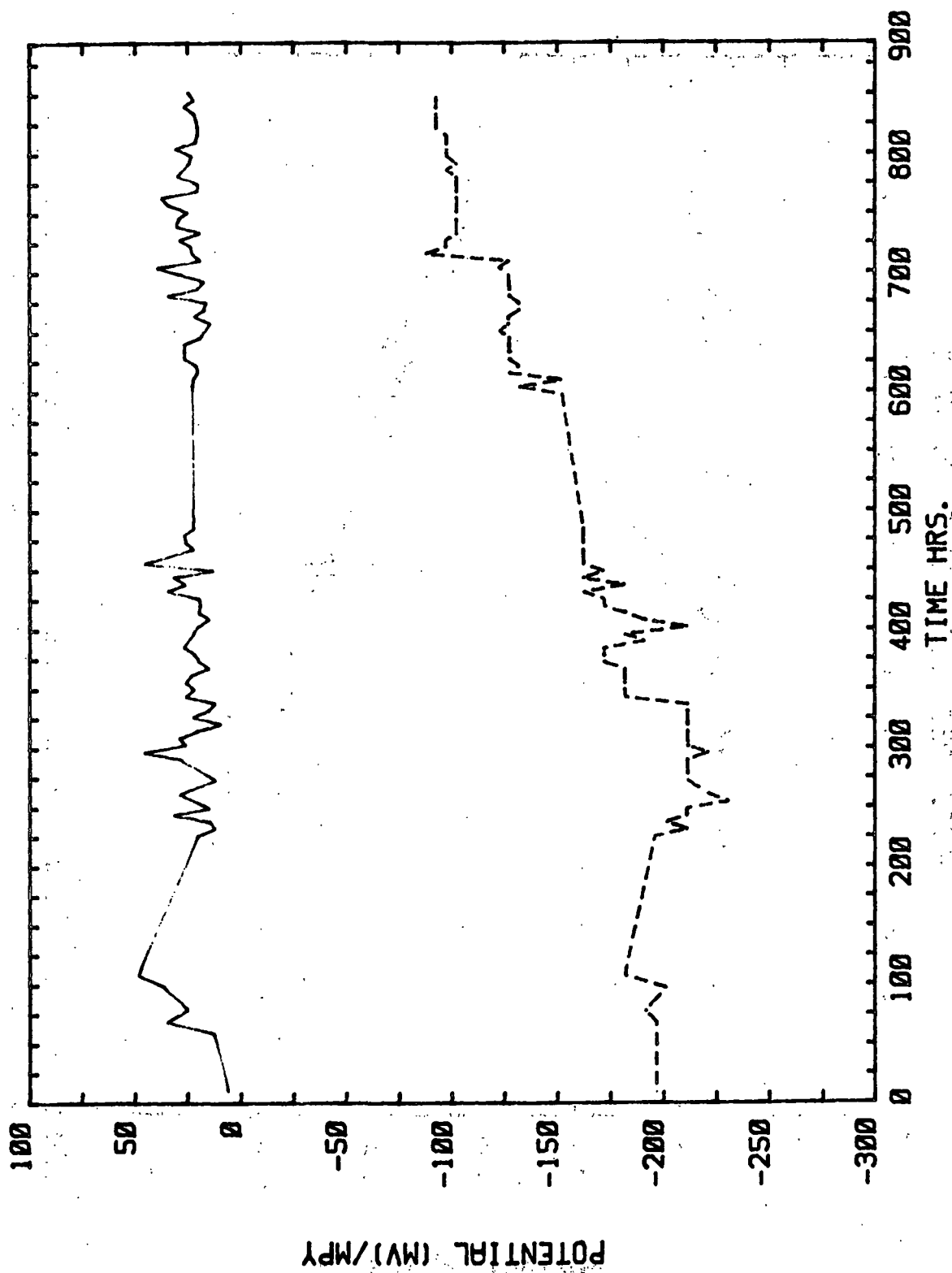


Figure 55. Mill T3: A285-SPEC. Anodic LPR. Electrode 8.

8 T-A285 SPECIAL CATHODIC MPY  
T-A285 SPECIAL CATHODIC POTENTIAL-----

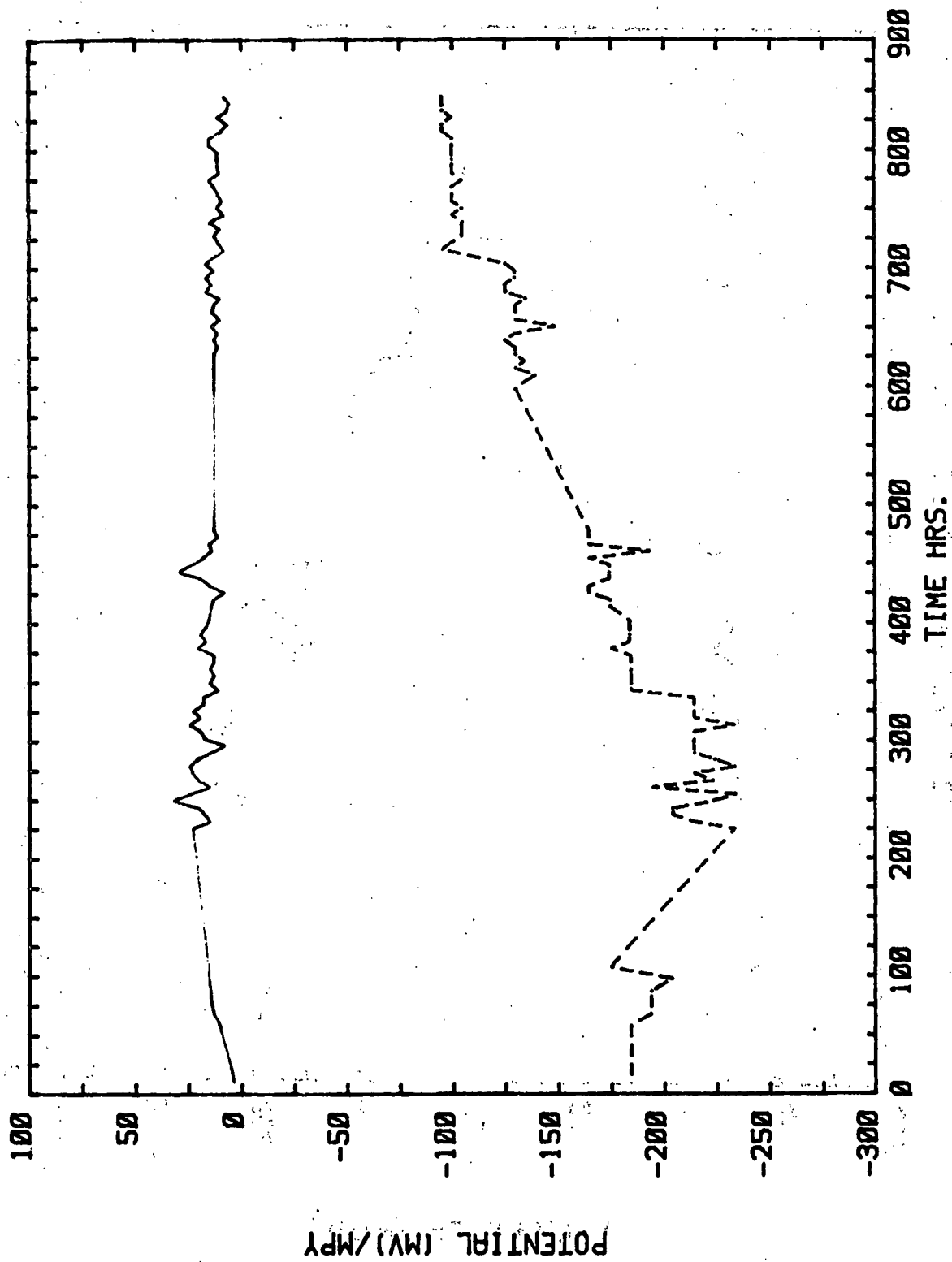


Figure 56. Mill T3. A285-SPEC. Cathodic LPR. Electrode 8.

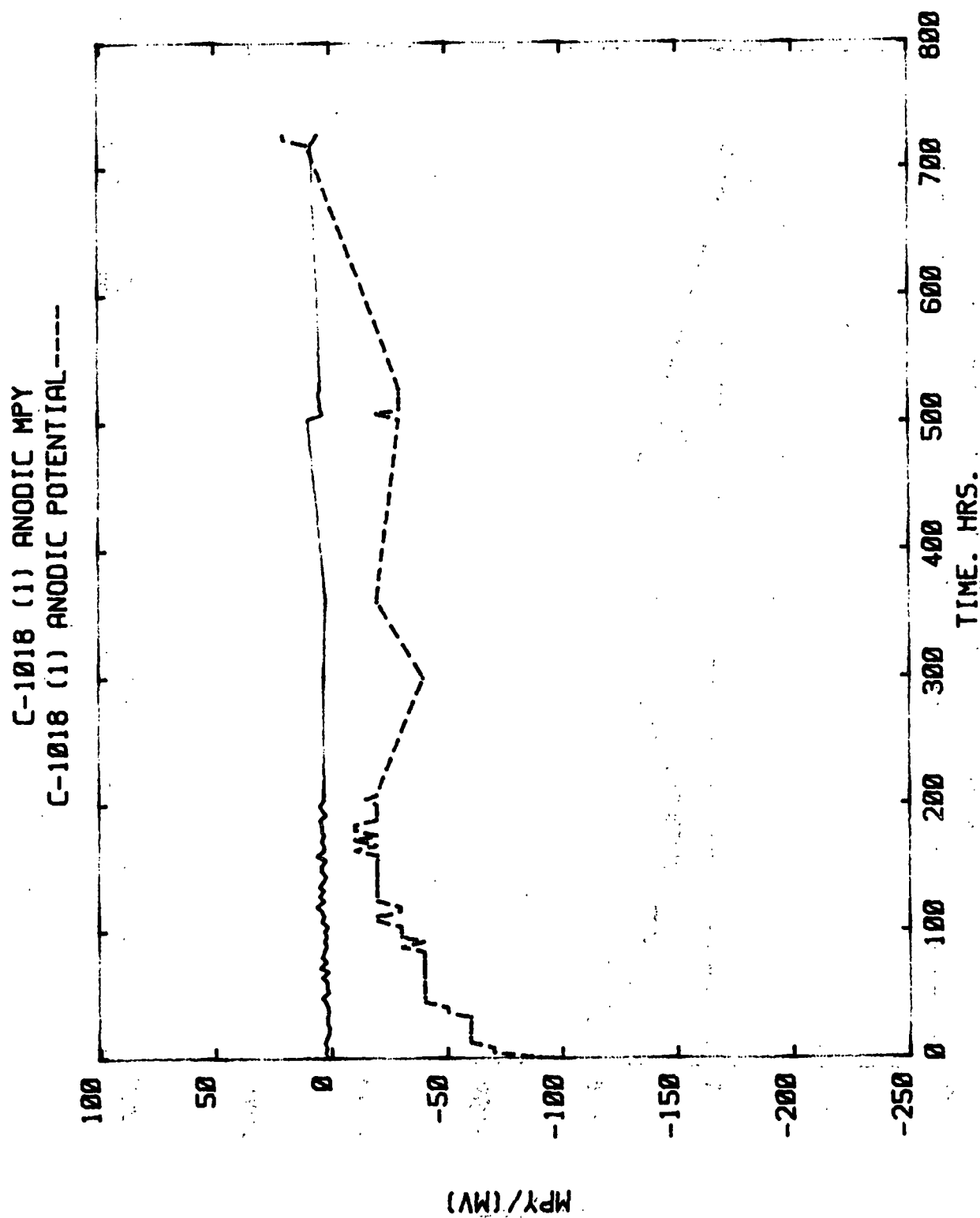


Figure 57. Mill C4. 1018. Anodic LPR. Electrode 1.

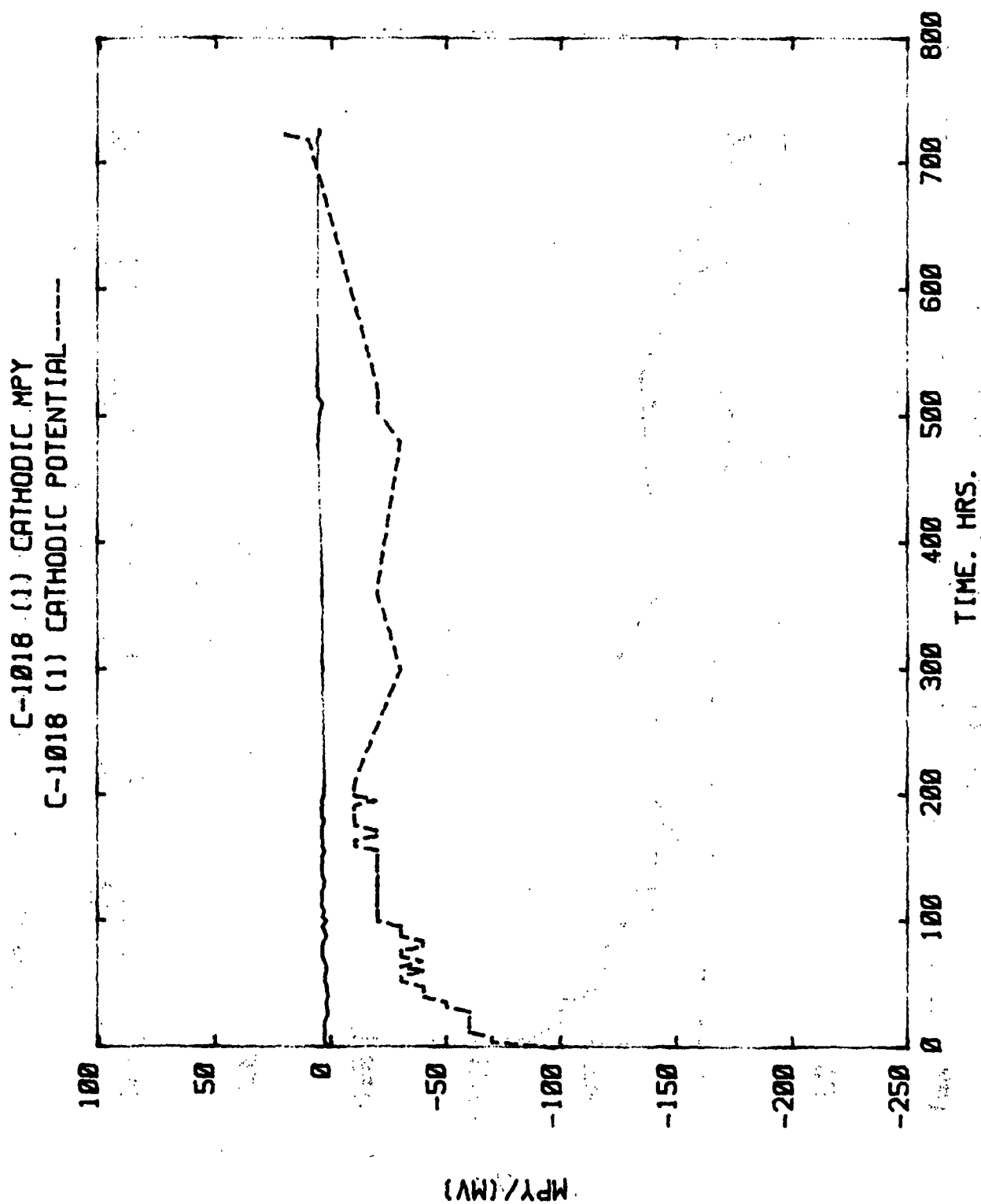


Figure 58. Mill C4. 1018. Cathodic LPR. Electrode 1.

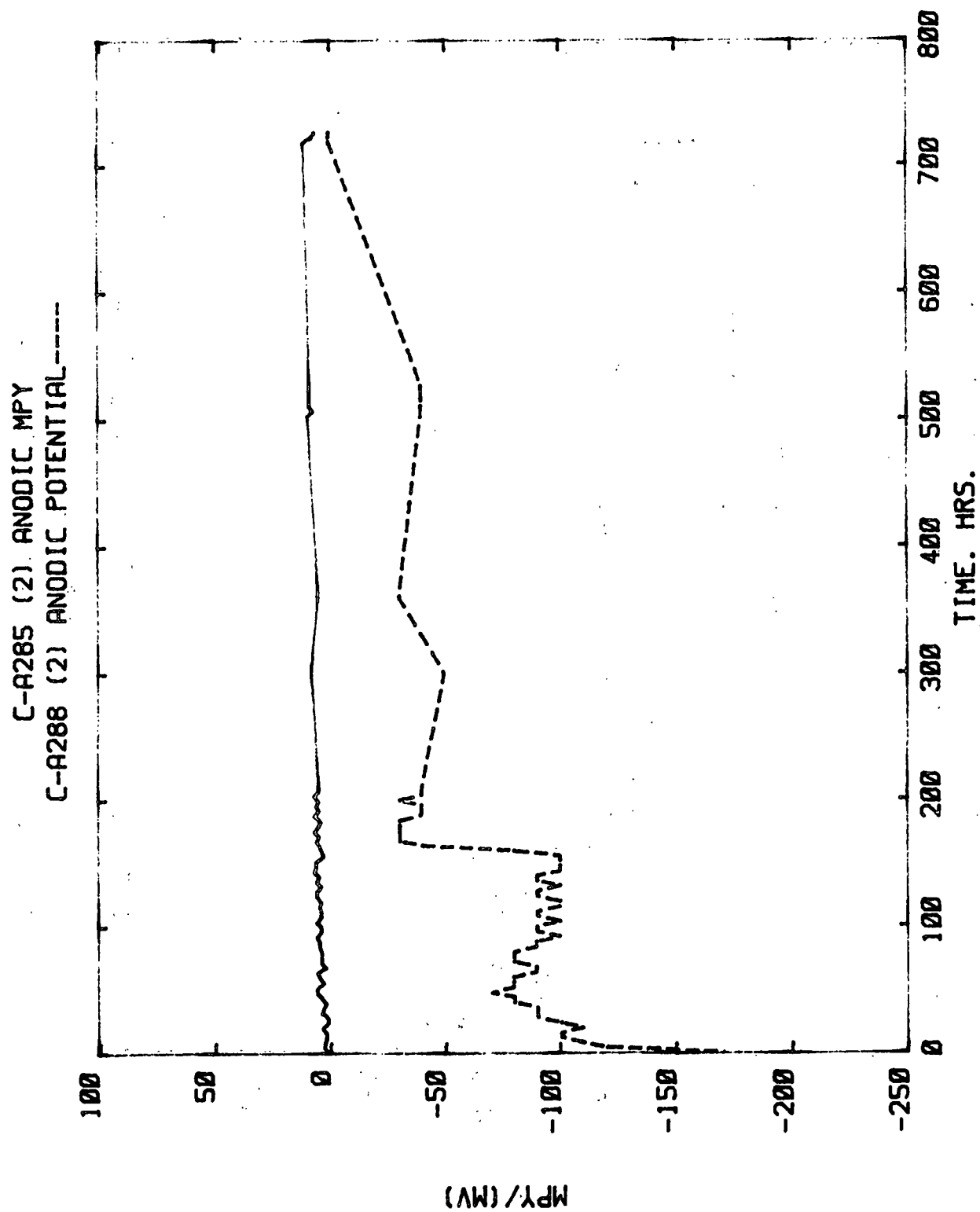


Figure 59. Mill C4. A285C. Anodic LPR. Electrode 2.

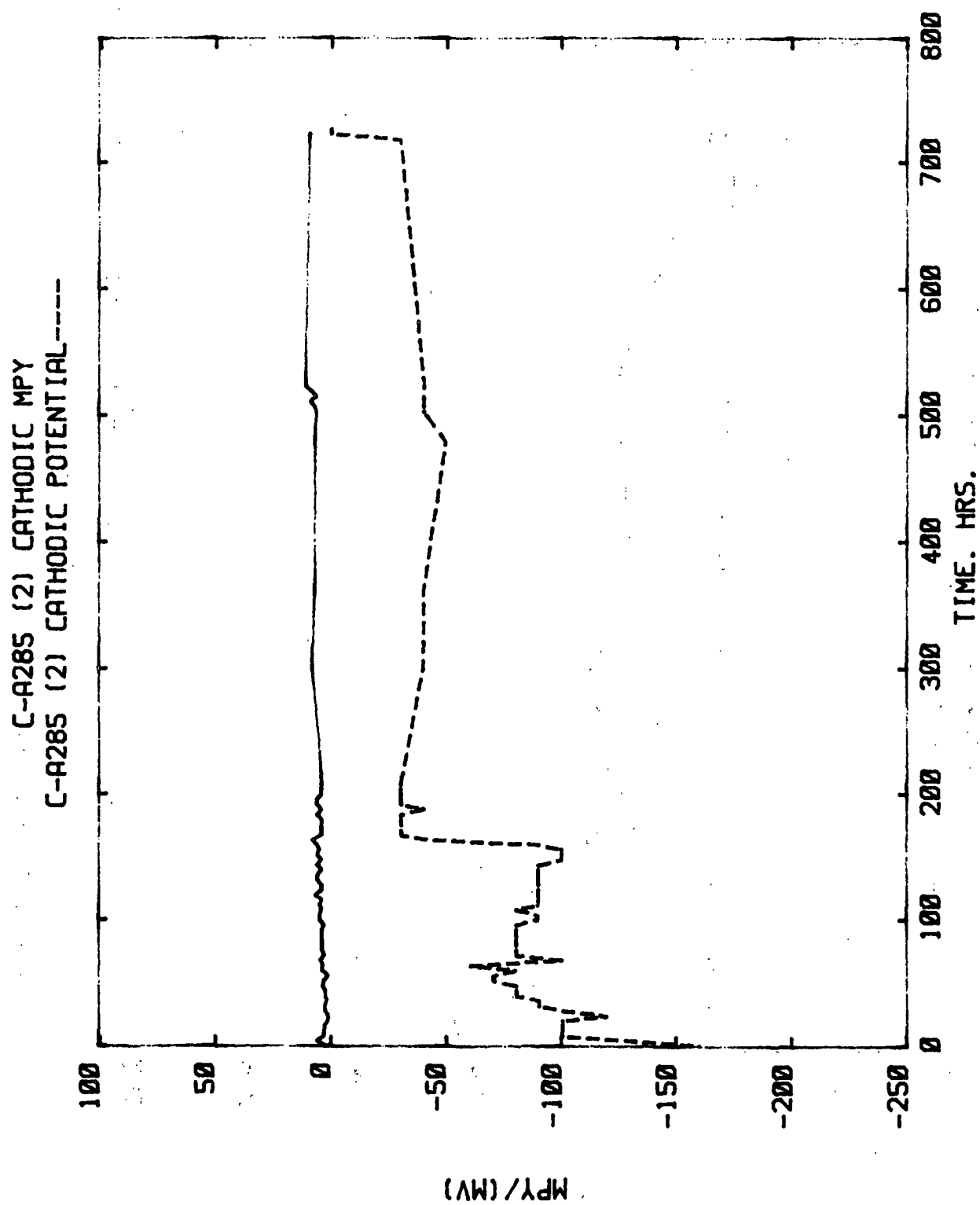


Figure 60. Mill C4. A285C. Cathodic LPR. Electrode 2.

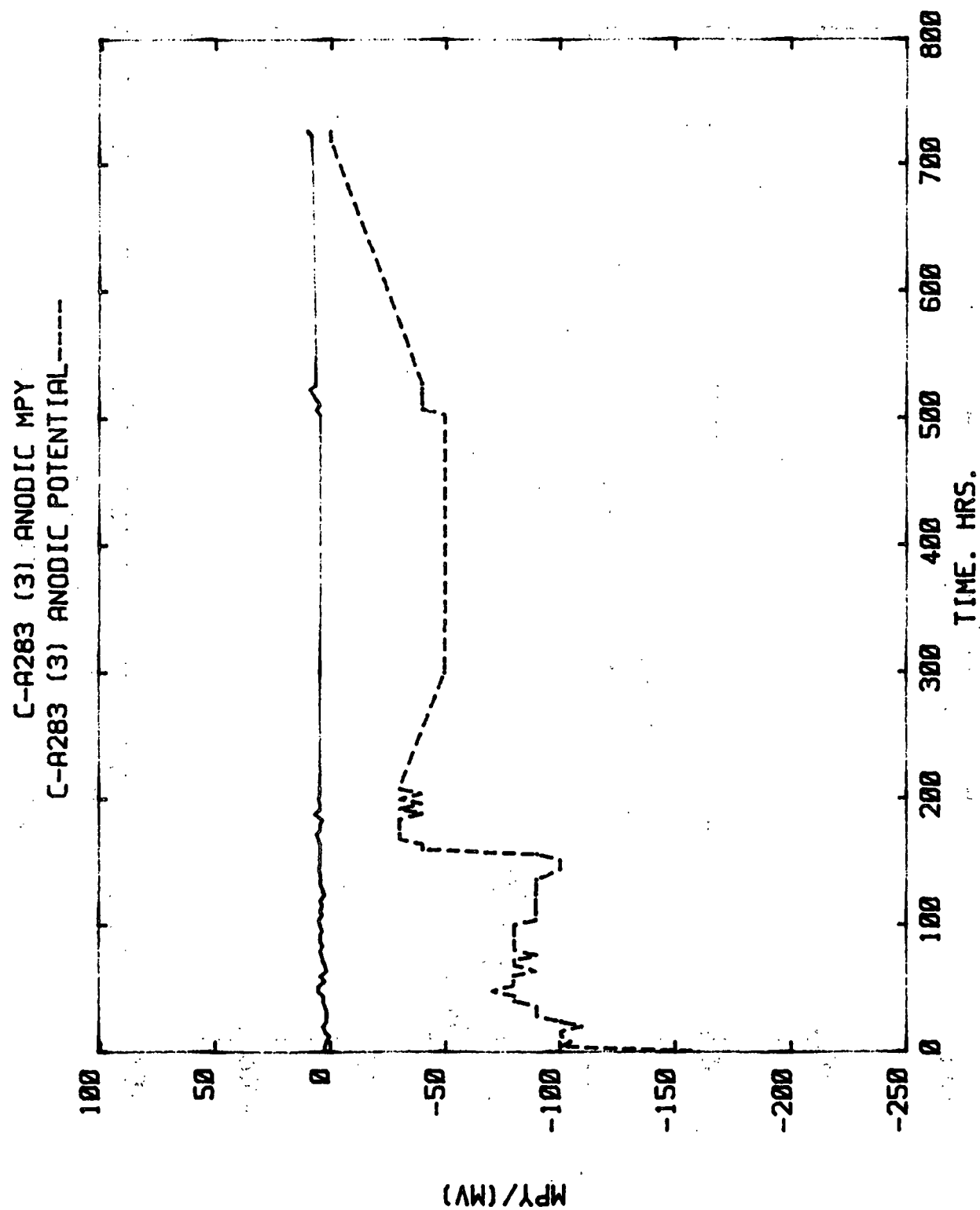


Figure 61. Mill C4. A283. Anodic LPR. Electrode 3.

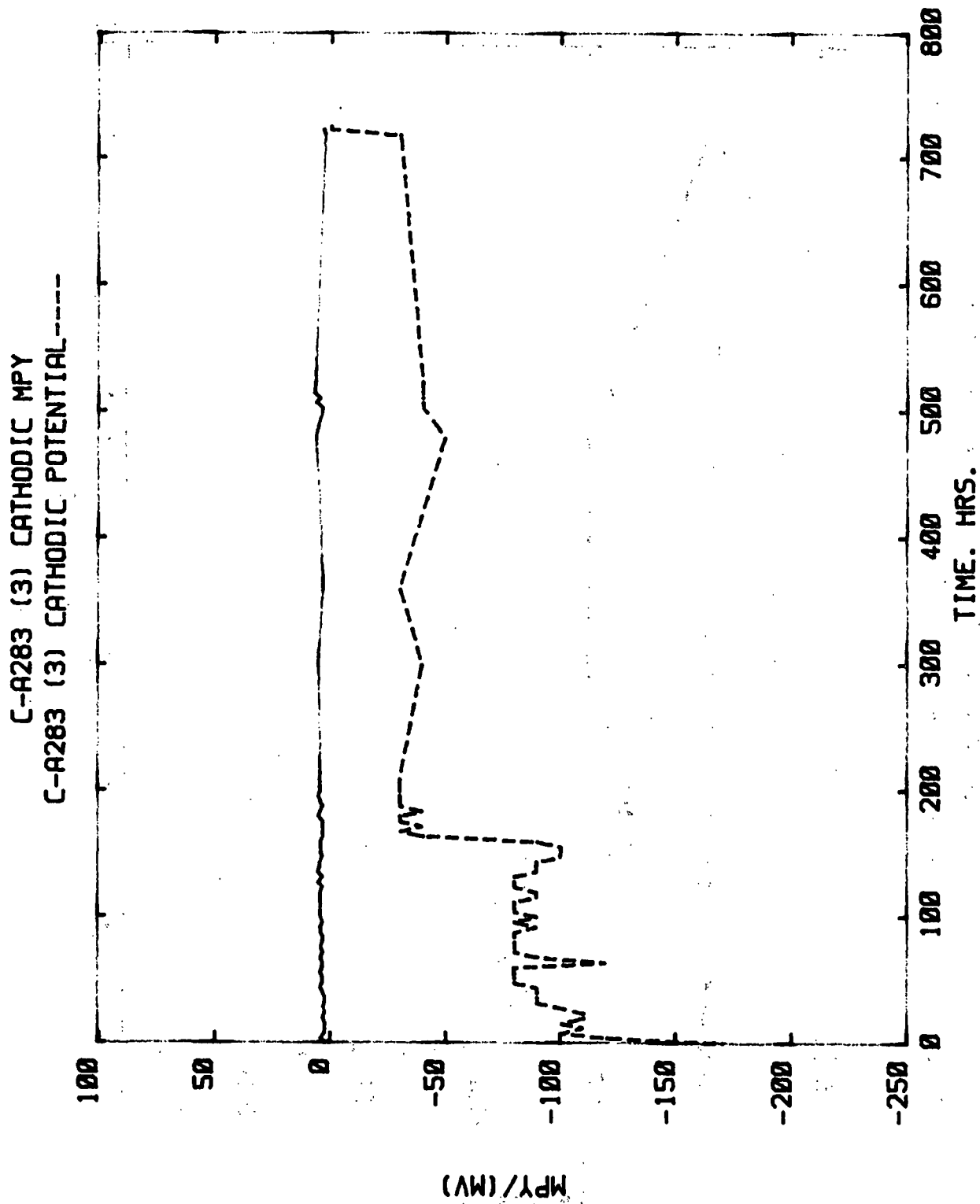


Figure 62. Mill C4. A283. Cathodic LPR. Electrode 3.



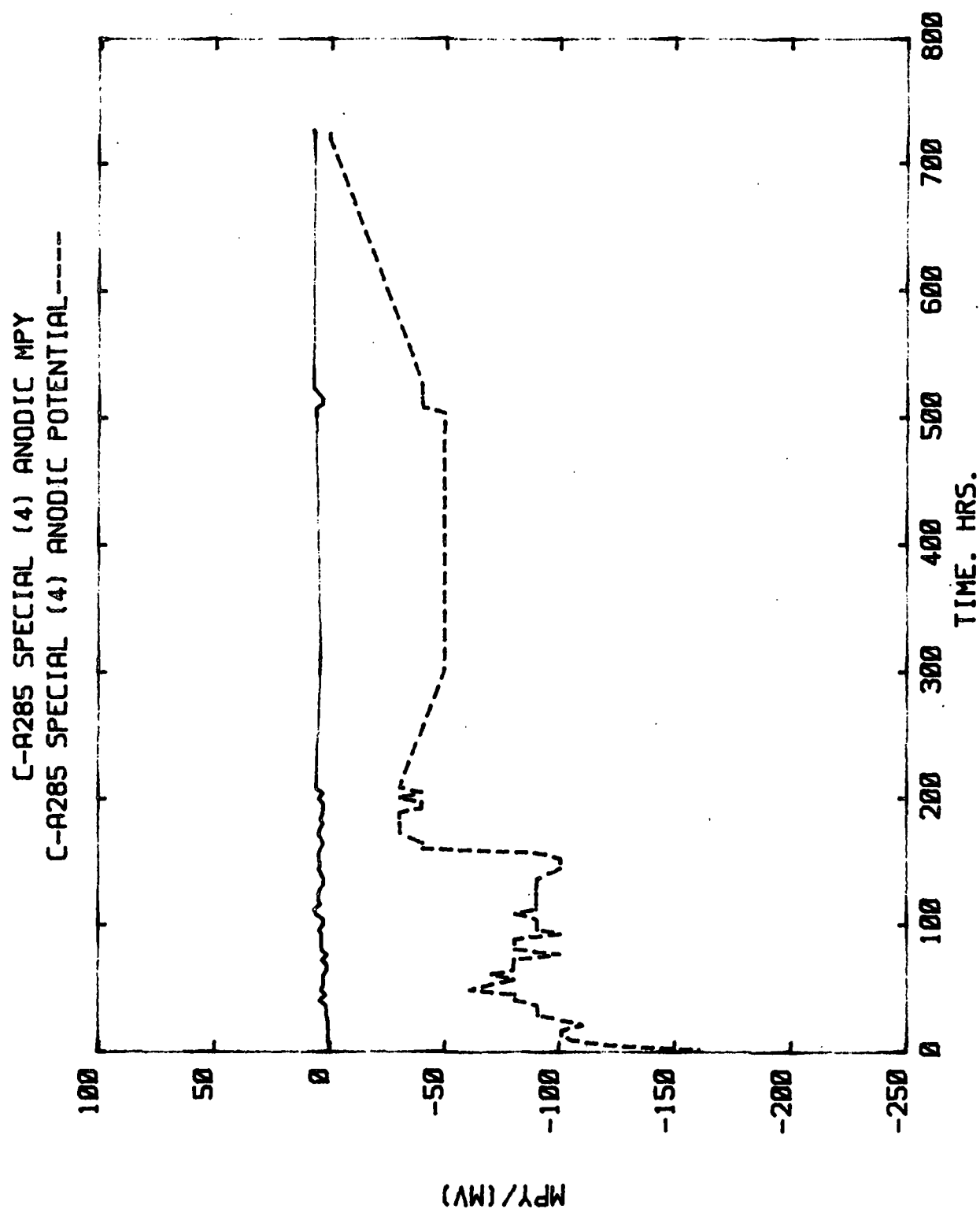


Figure 63. Mill C4. A285-SPEC. Anodic LPR. Electrode 4.

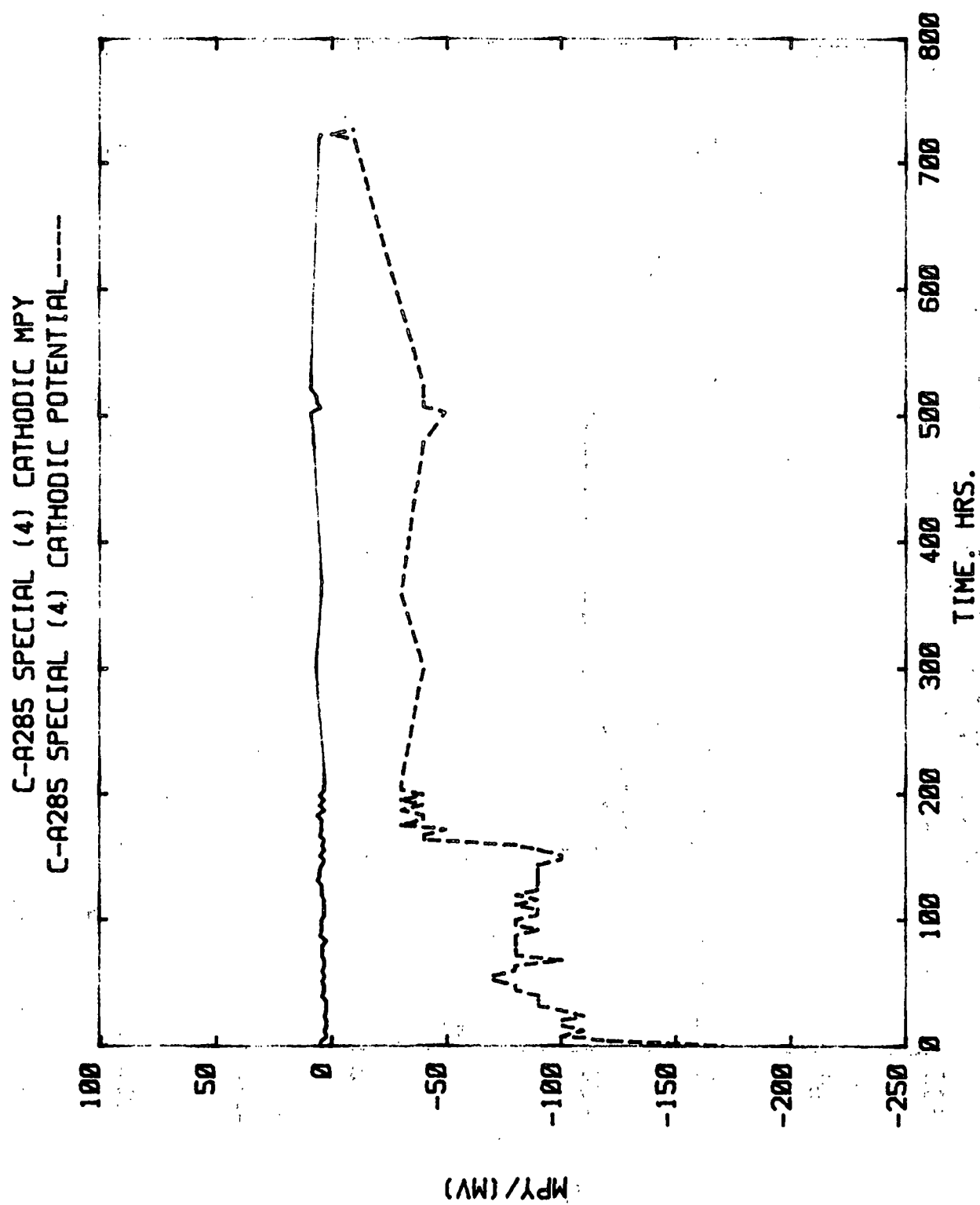


Figure 64. Mill C4. A285-SPEC. Cathodic LPR. Electrode 4.

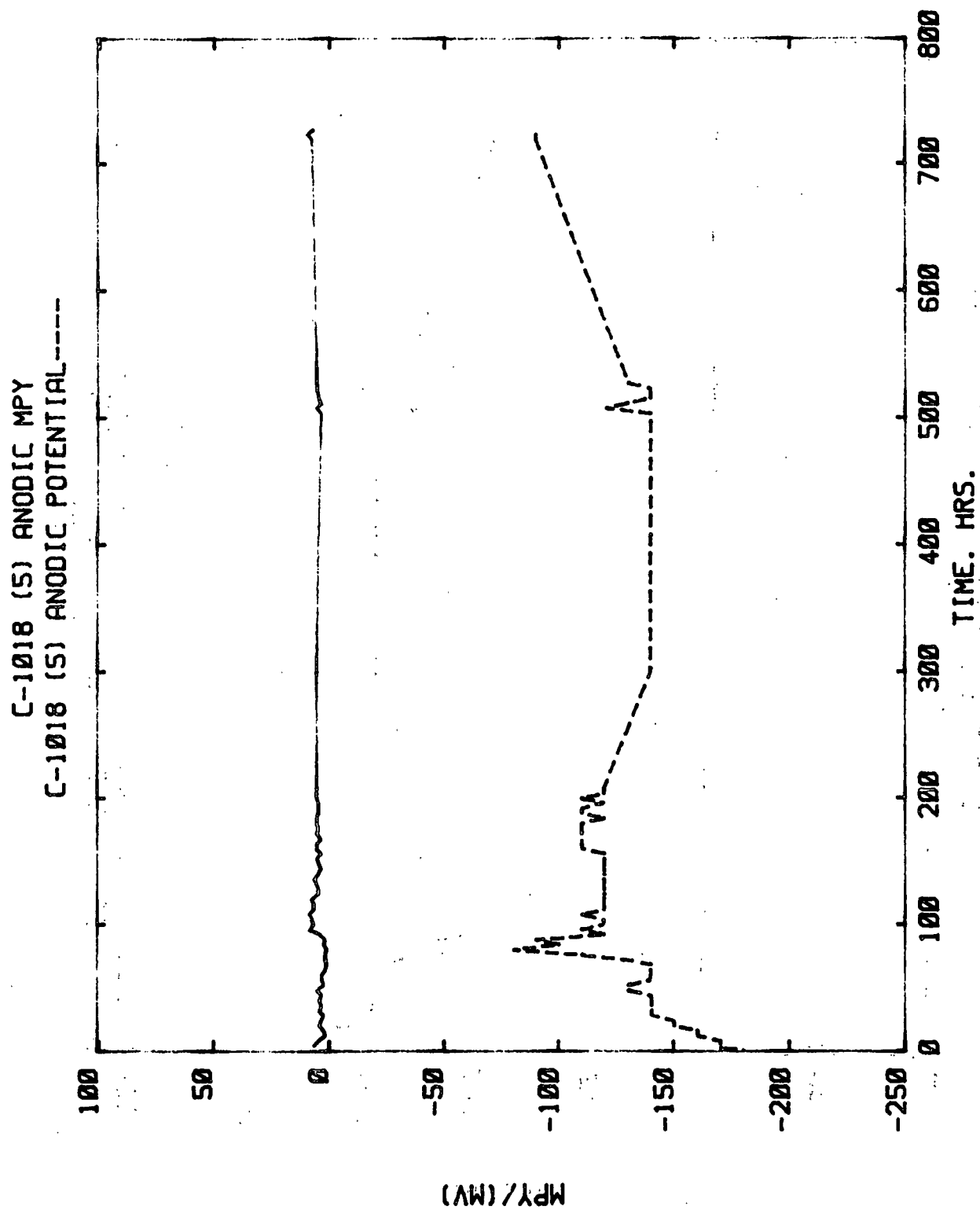


Figure 65. Mill C4. 1018. Anodic LPR. Electrode 5.

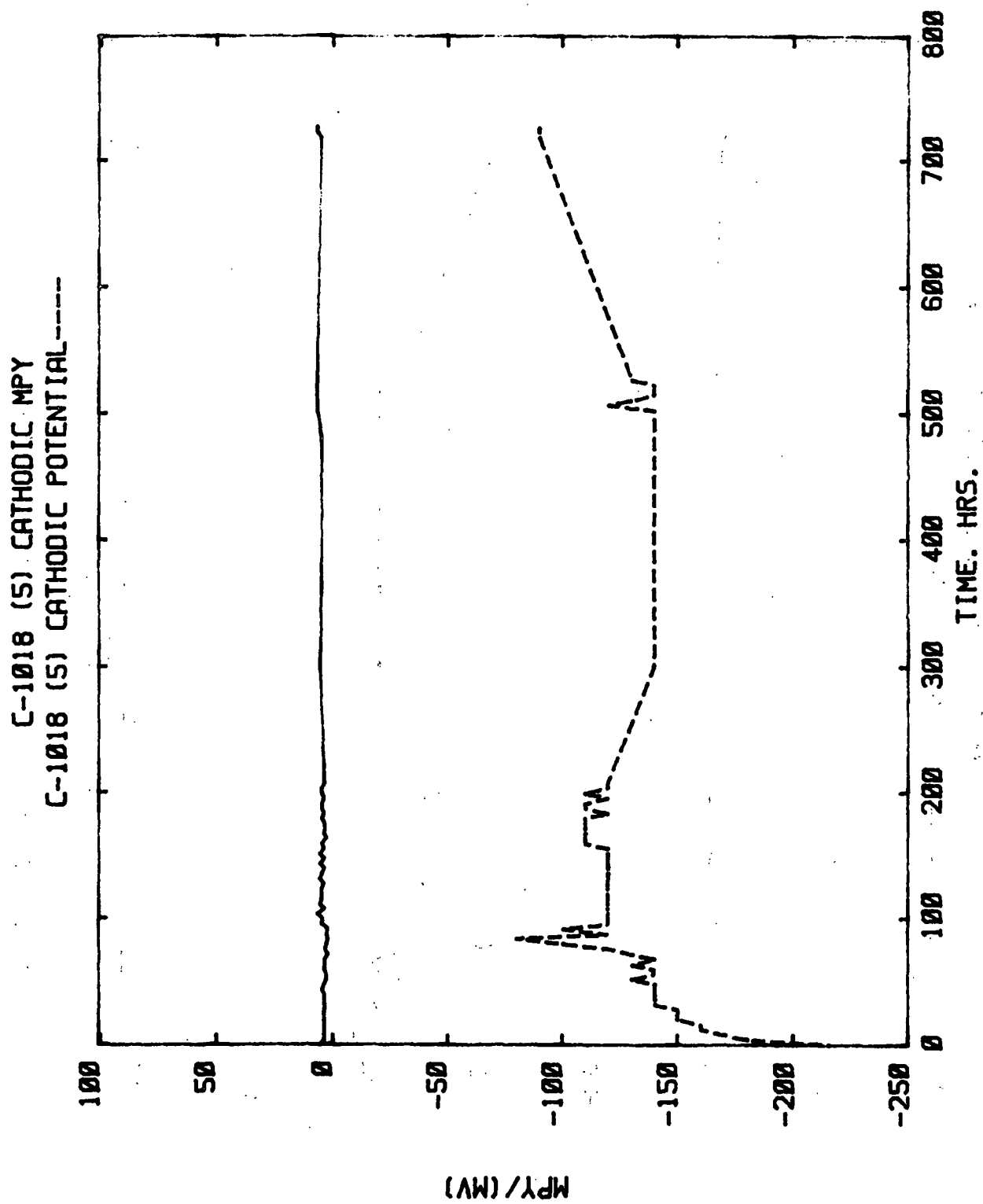


Figure 66. Mill C4. 1018. Cathodic LPR. Electrode 5.

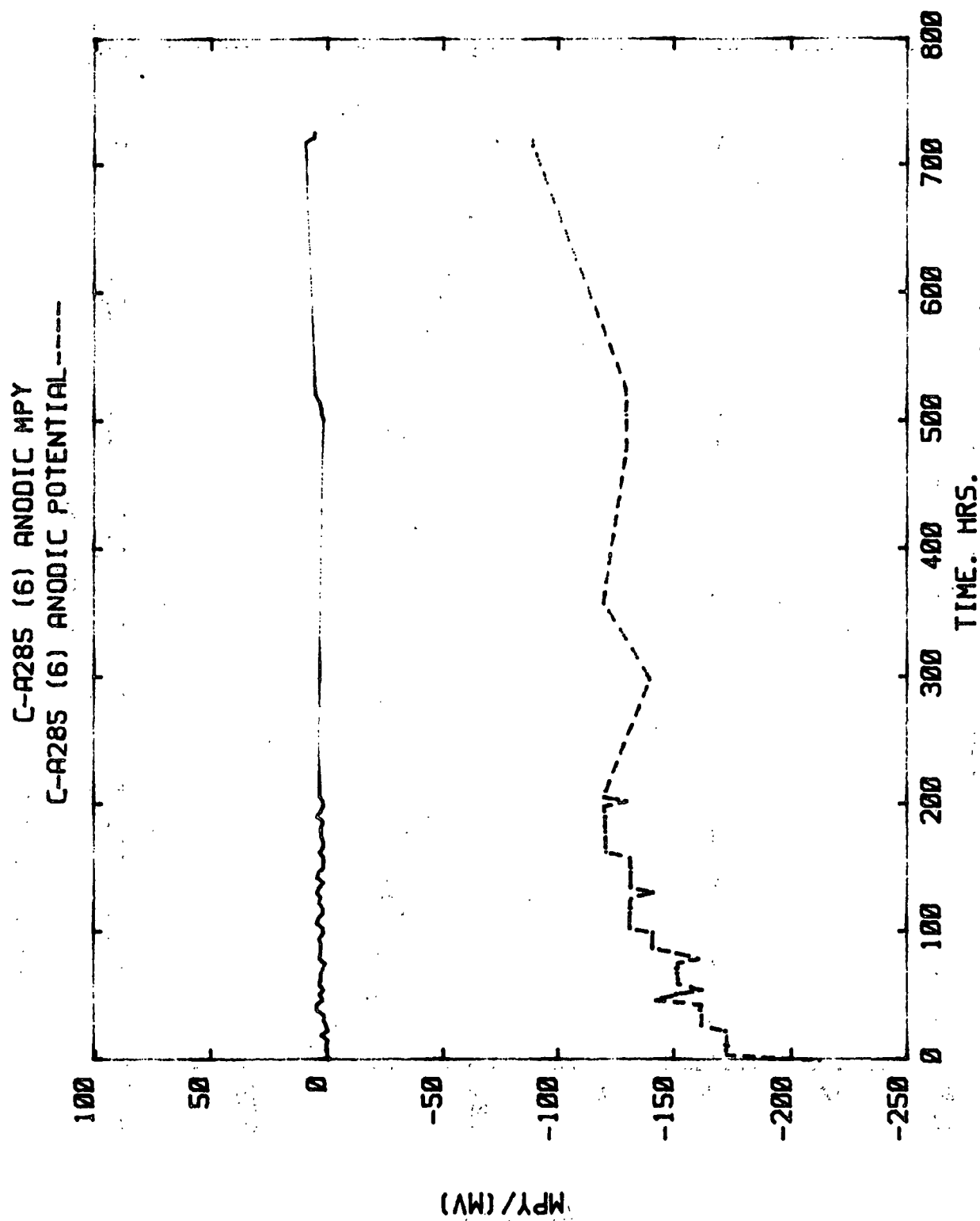


Figure 67. Mill C4. A285C. Anodic LPR. Electrode 6.

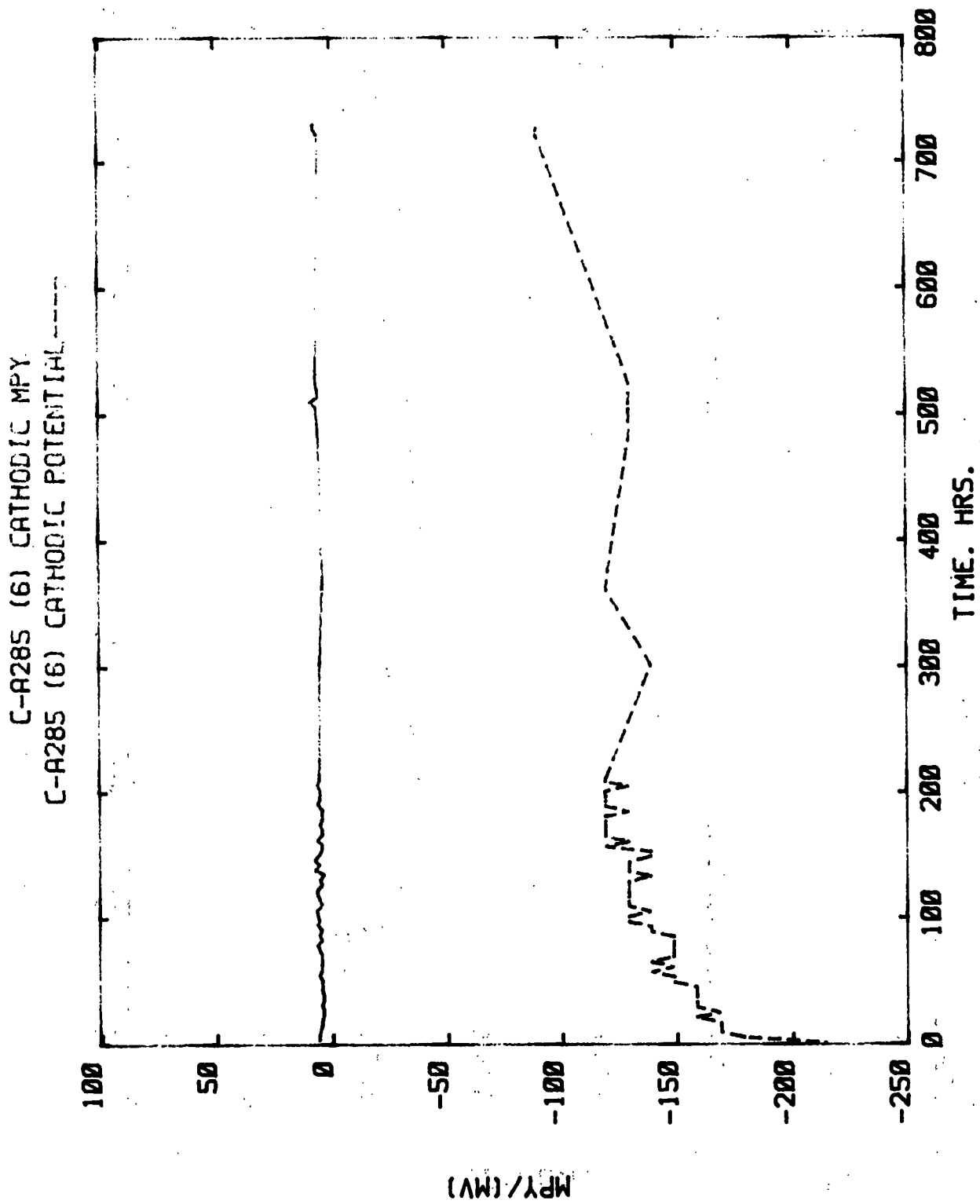


Figure 68. Mill C4. A285C. Cathodic LPR. Electrode 6.

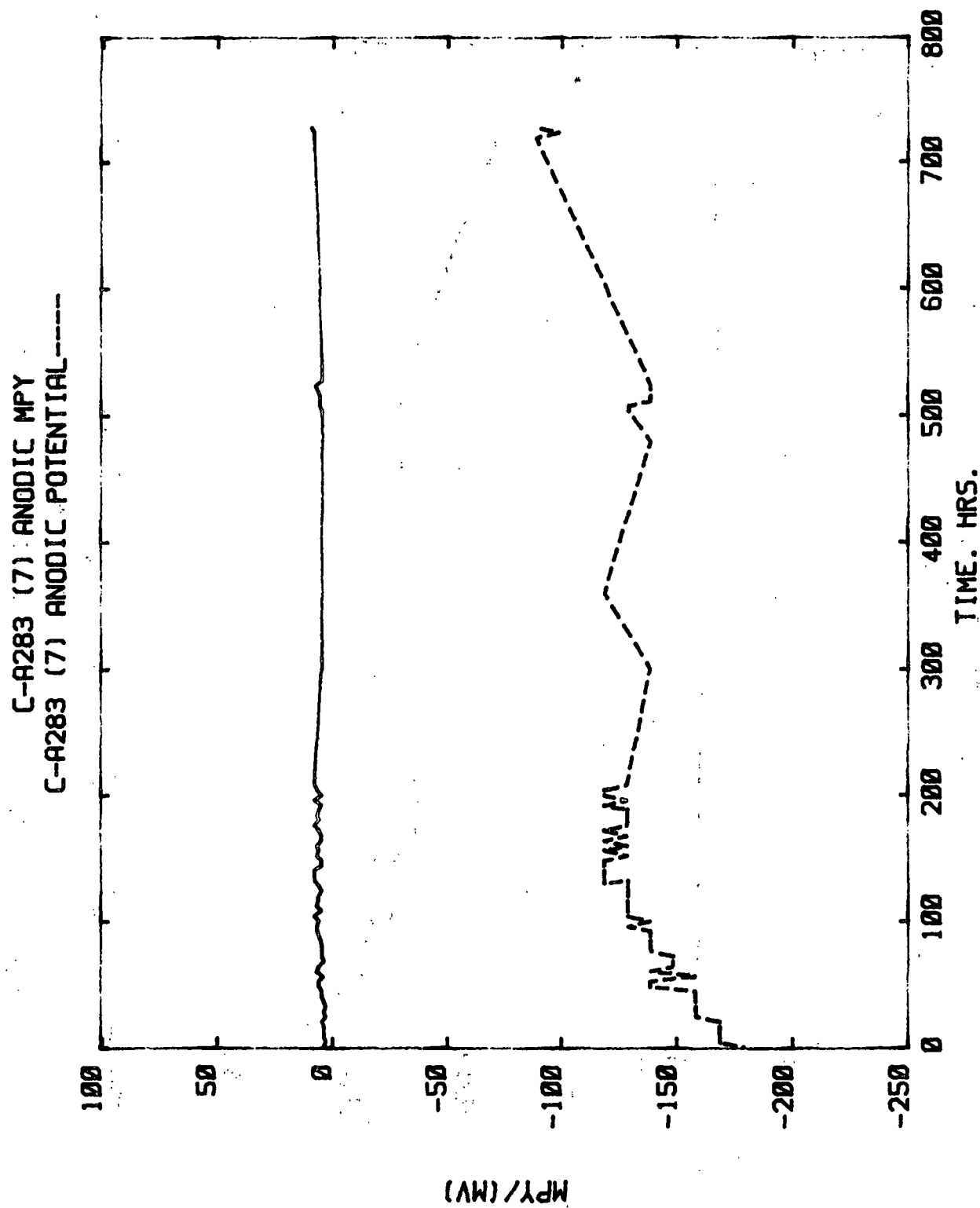


Figure 69. Mill C4. A283. Anodic LPR. Electrode 7.

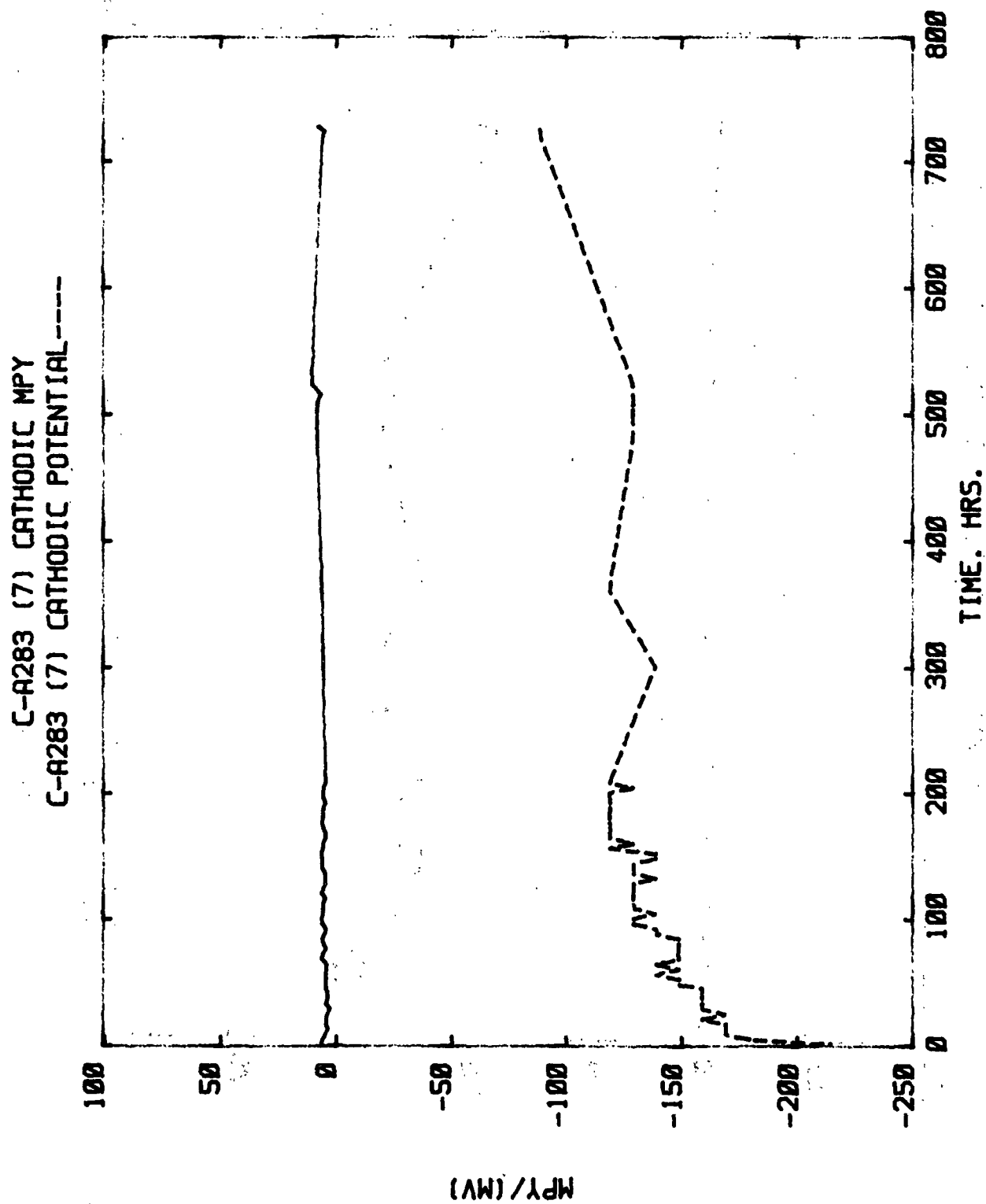


Figure 70. Mill C4. A283. Cathodic LPR. Electrode 7.



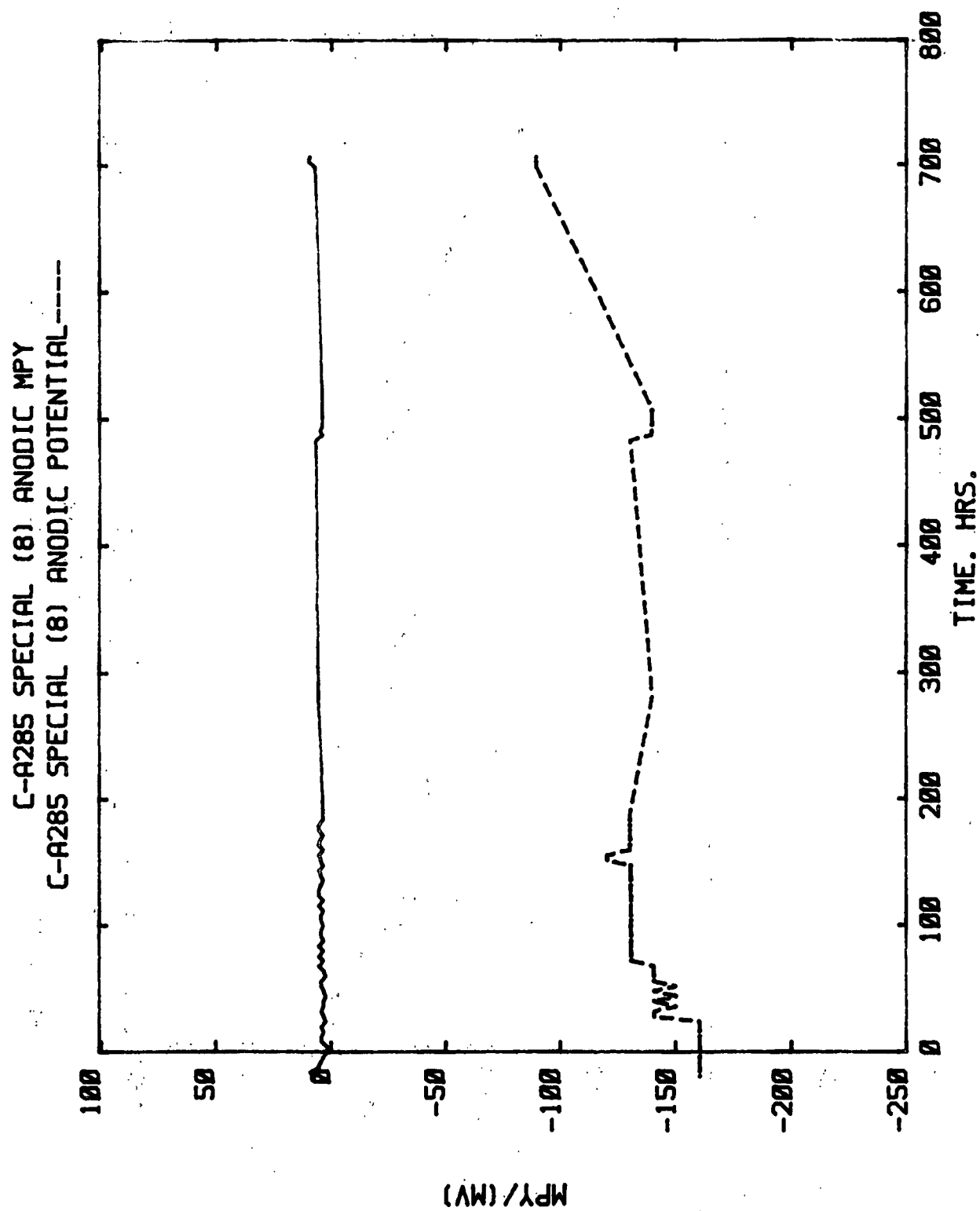


Figure 71. Mill C4. A285-SPEC. Anodic LPR. Electrode 8.

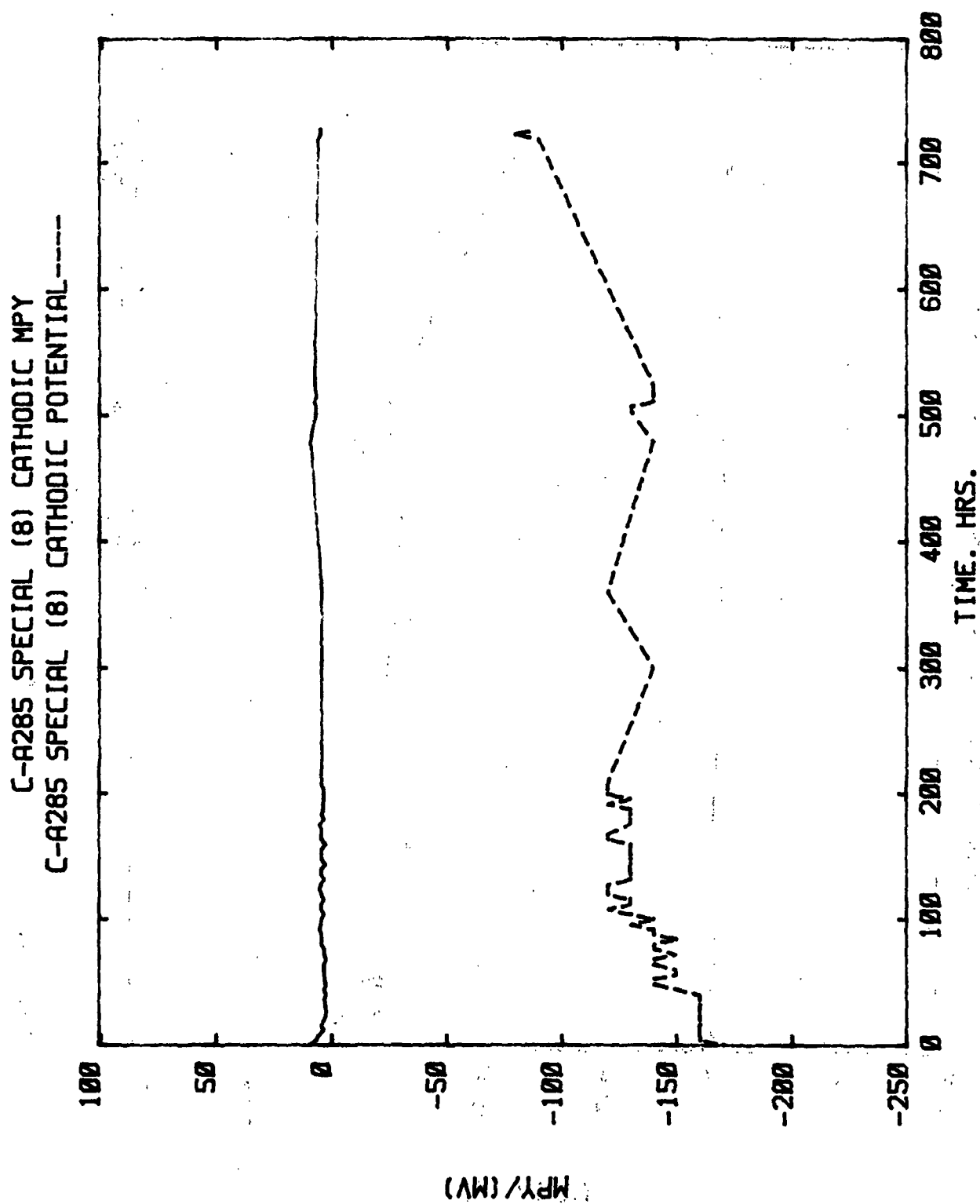


Figure 72. Mill C4. A285-SPEC. Cathodic LPR. Electrode 8.

## APPENDIX II

## POLARIZATION CURVES

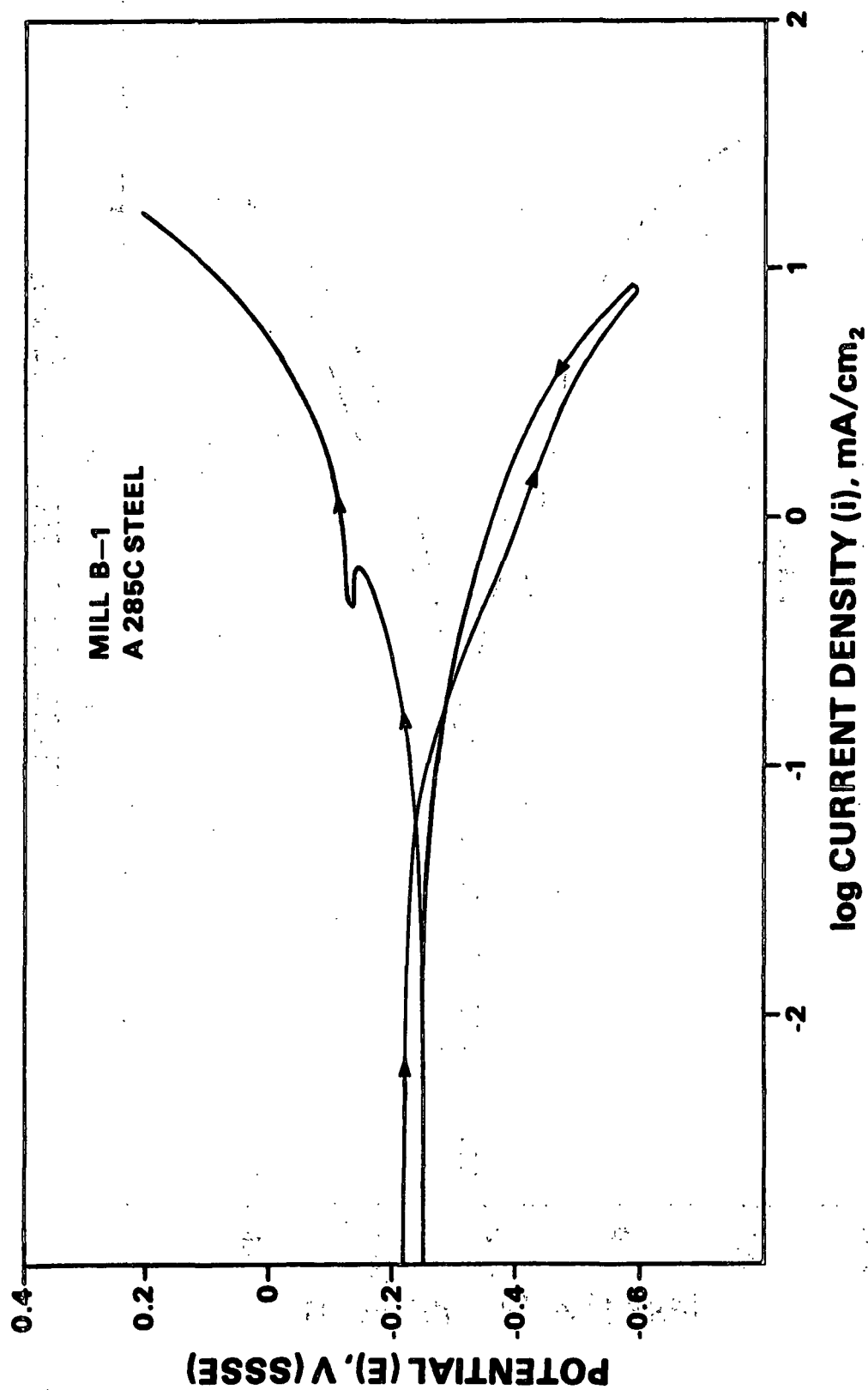


Figure 73. Mill B1. A285C.

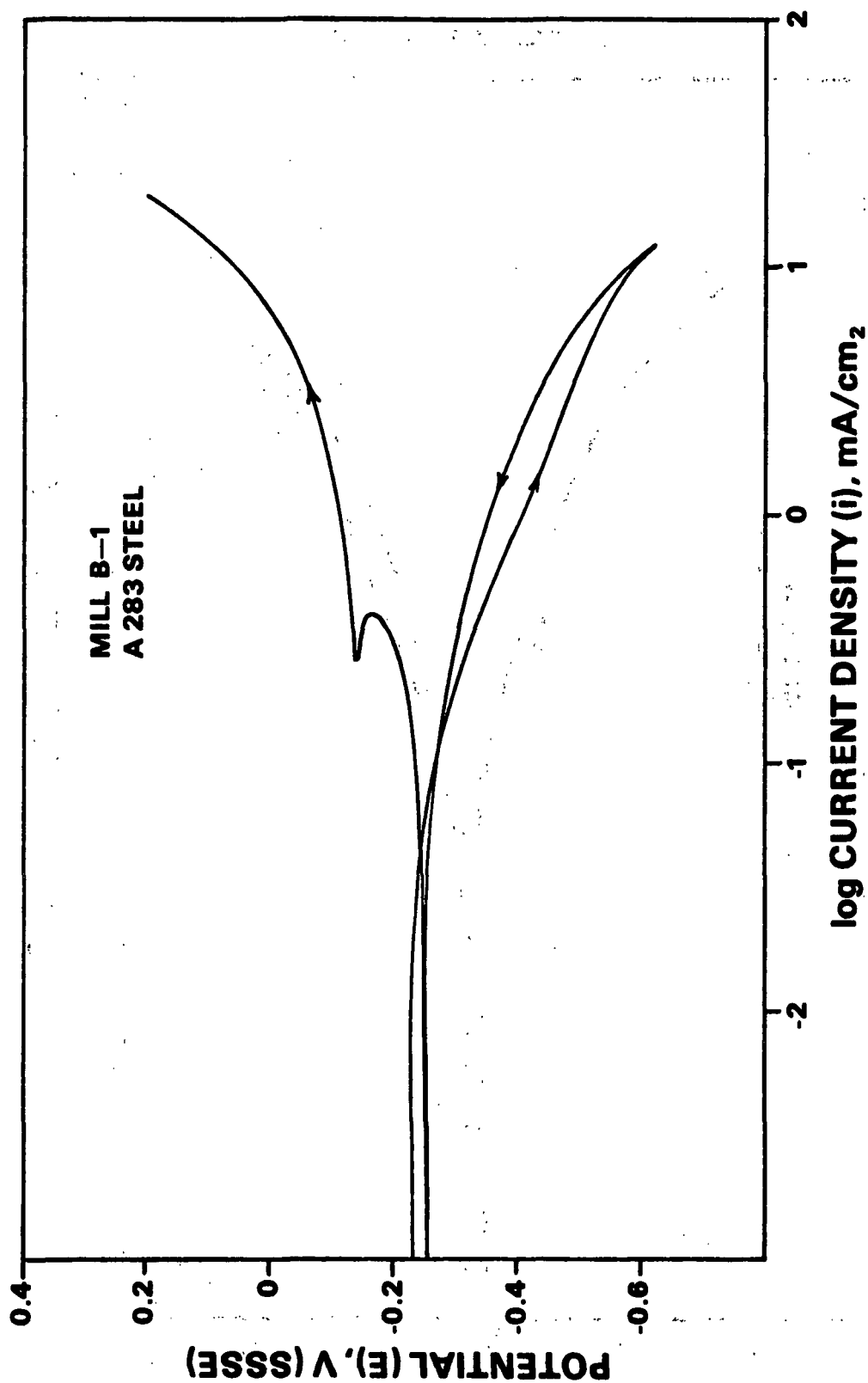


Figure 74. Mill B1. A283.

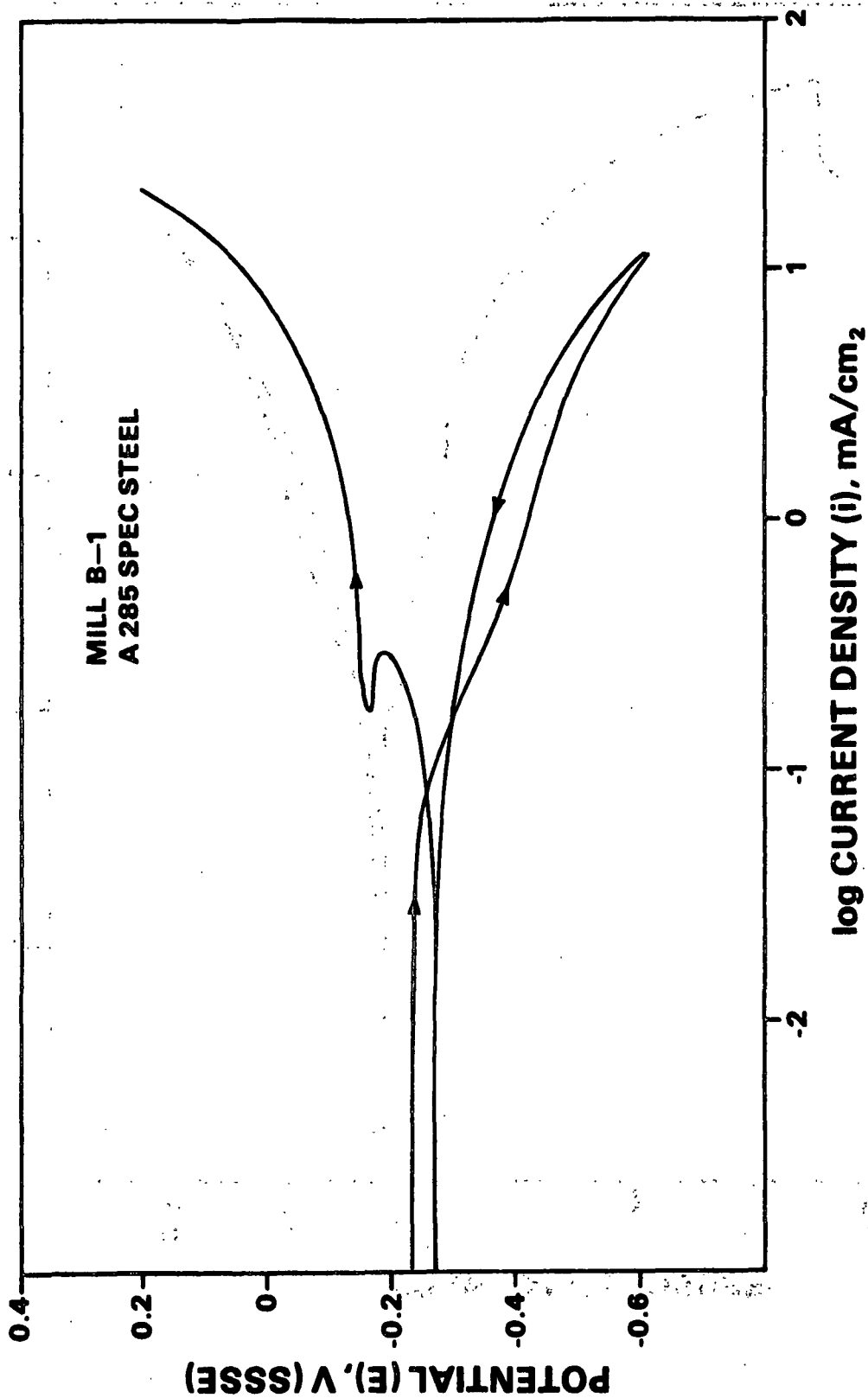


Figure 75. Mill B1. A285-SPECIAL.

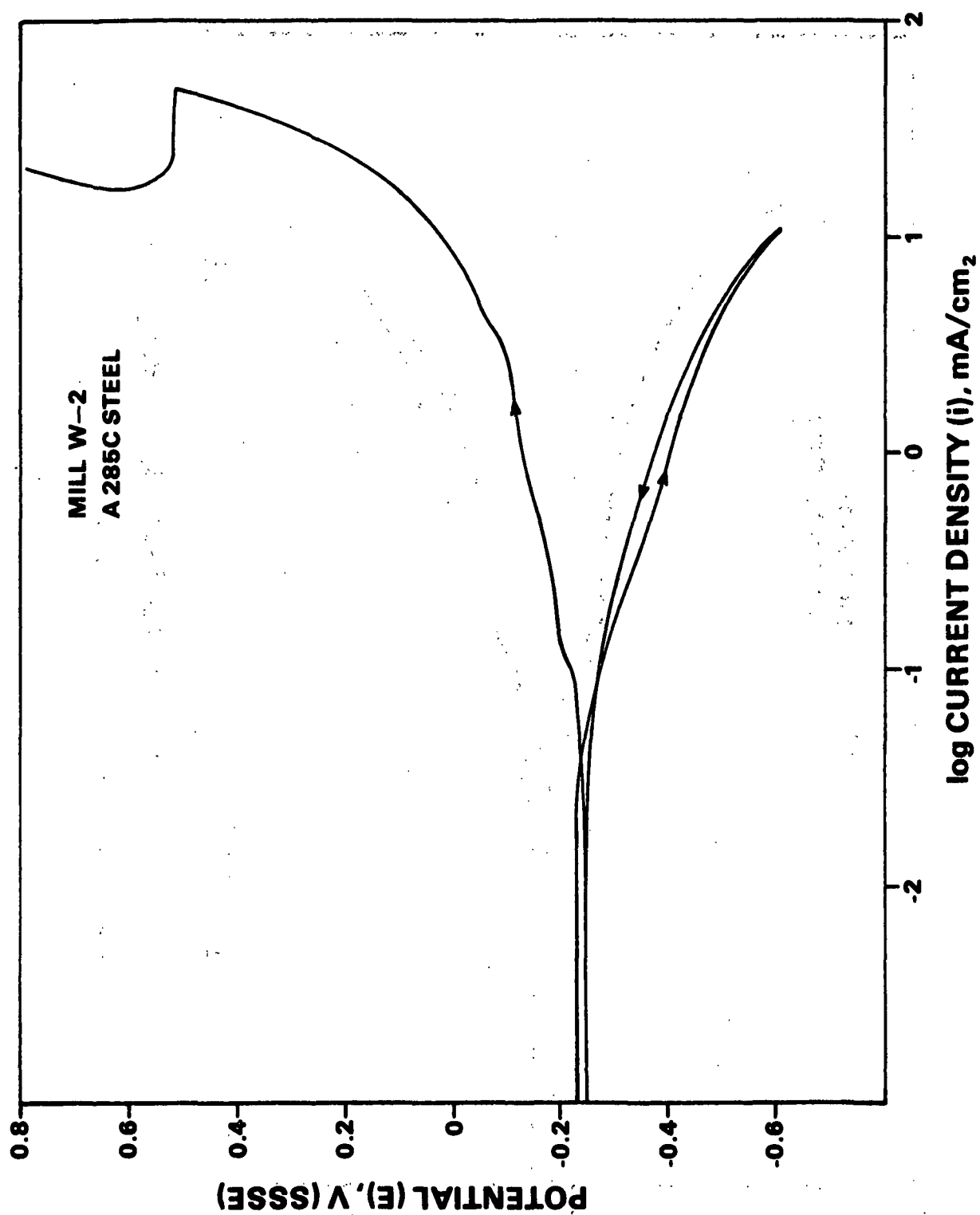


Figure 76. Mill W2. A285C.

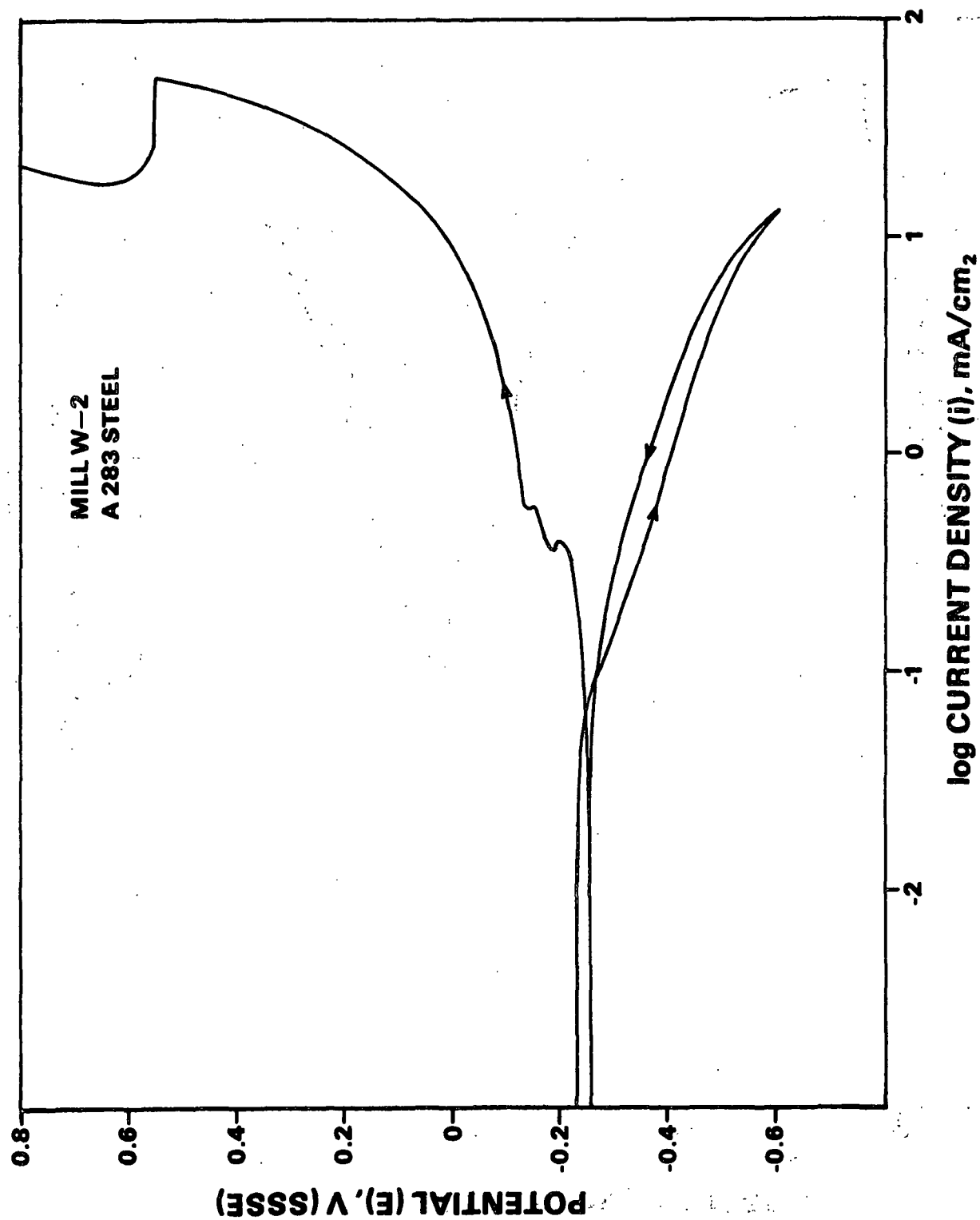


Figure 77. Mill W2. A283.

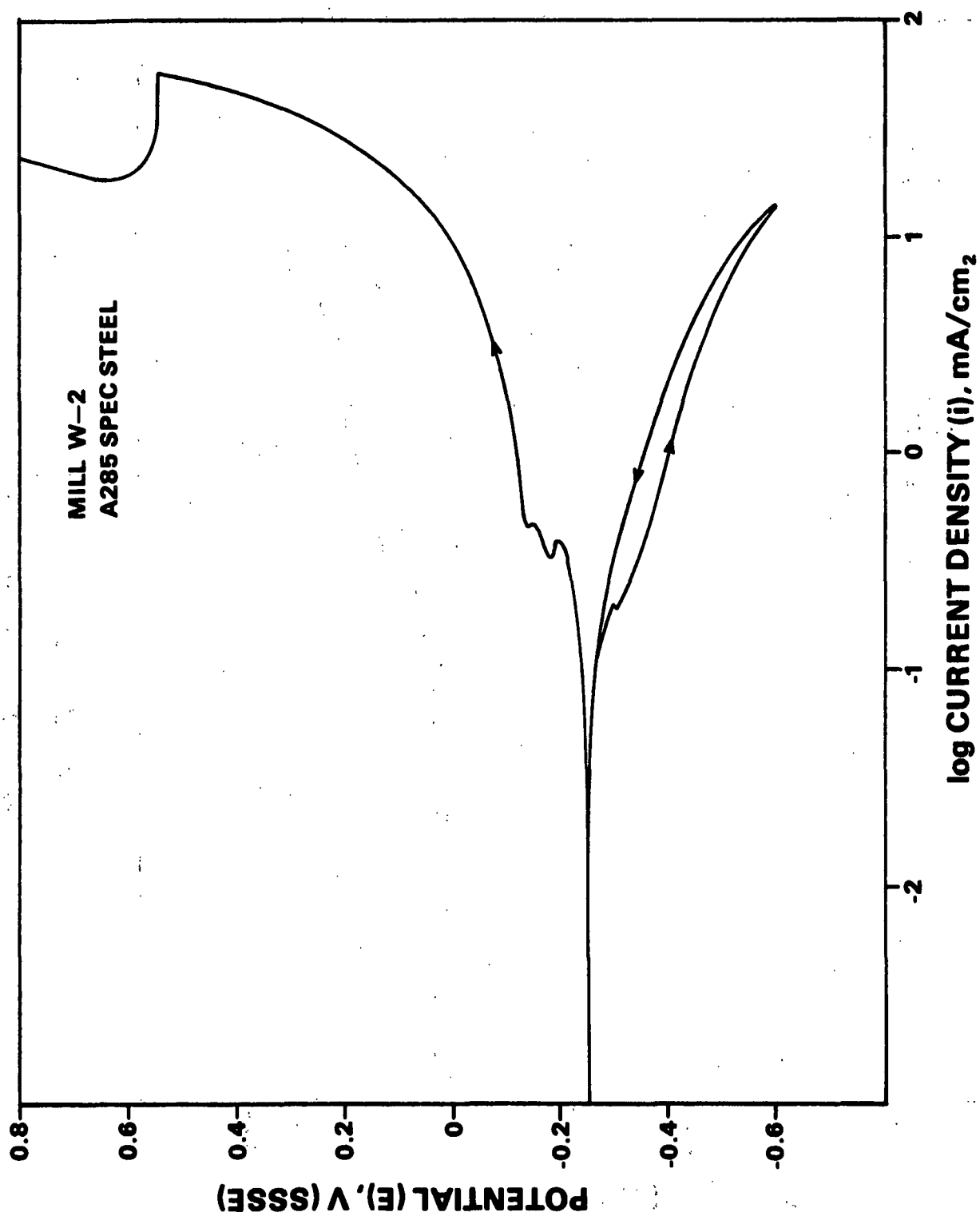


Figure 78. Mill W2. A285-SPECIAL.



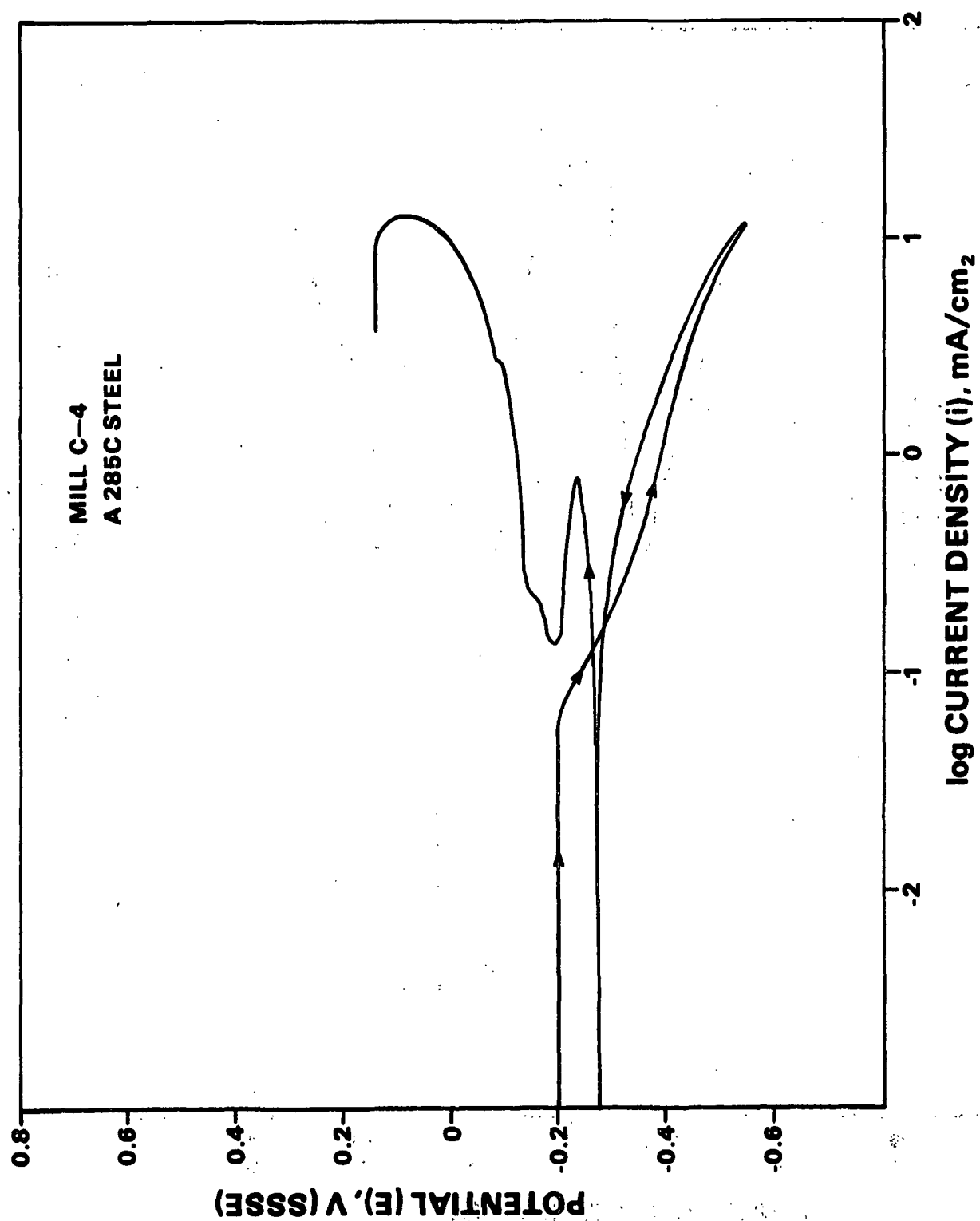


Figure 79. Mill C4. A285C.

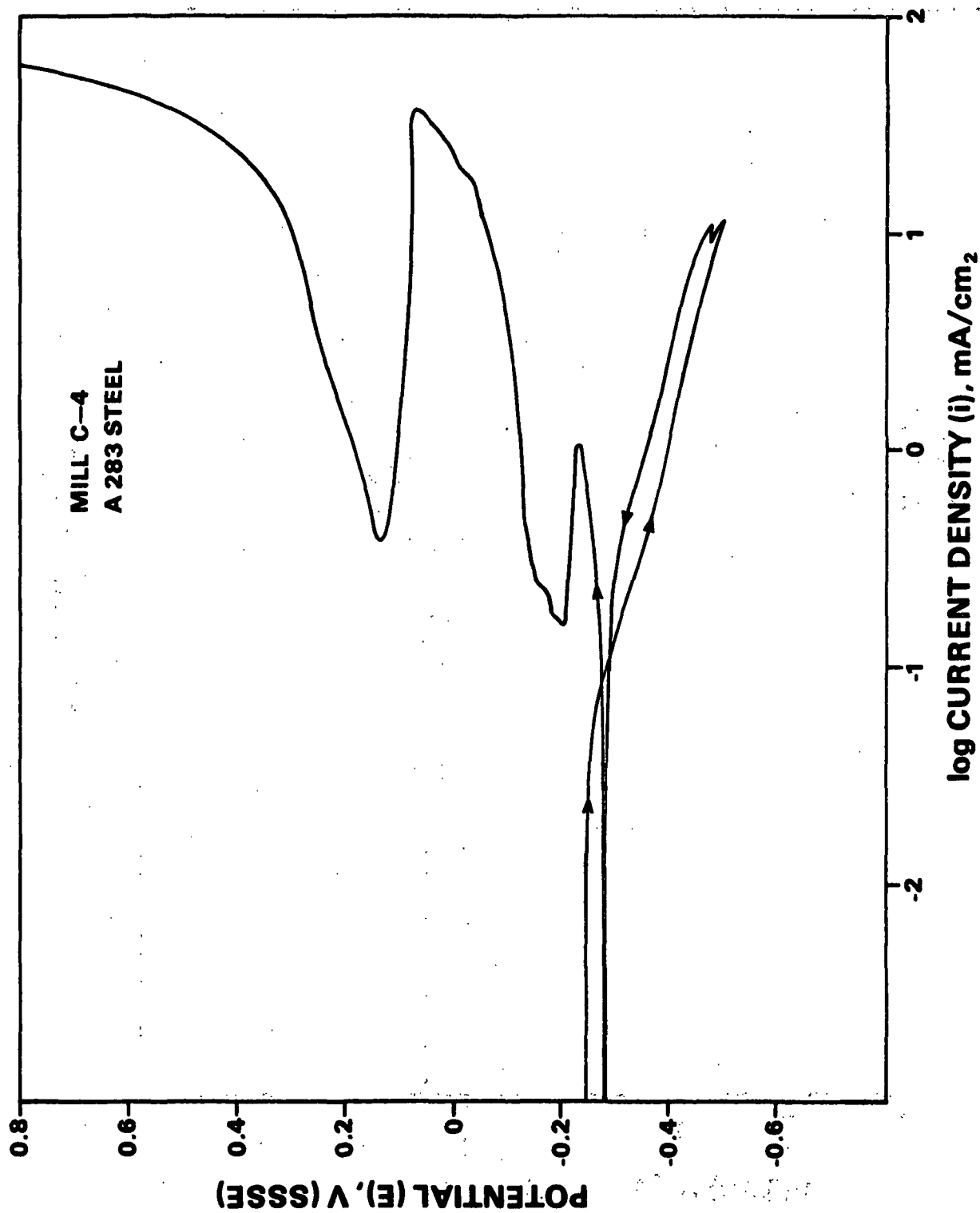


Figure 80. Mill C4. A283.

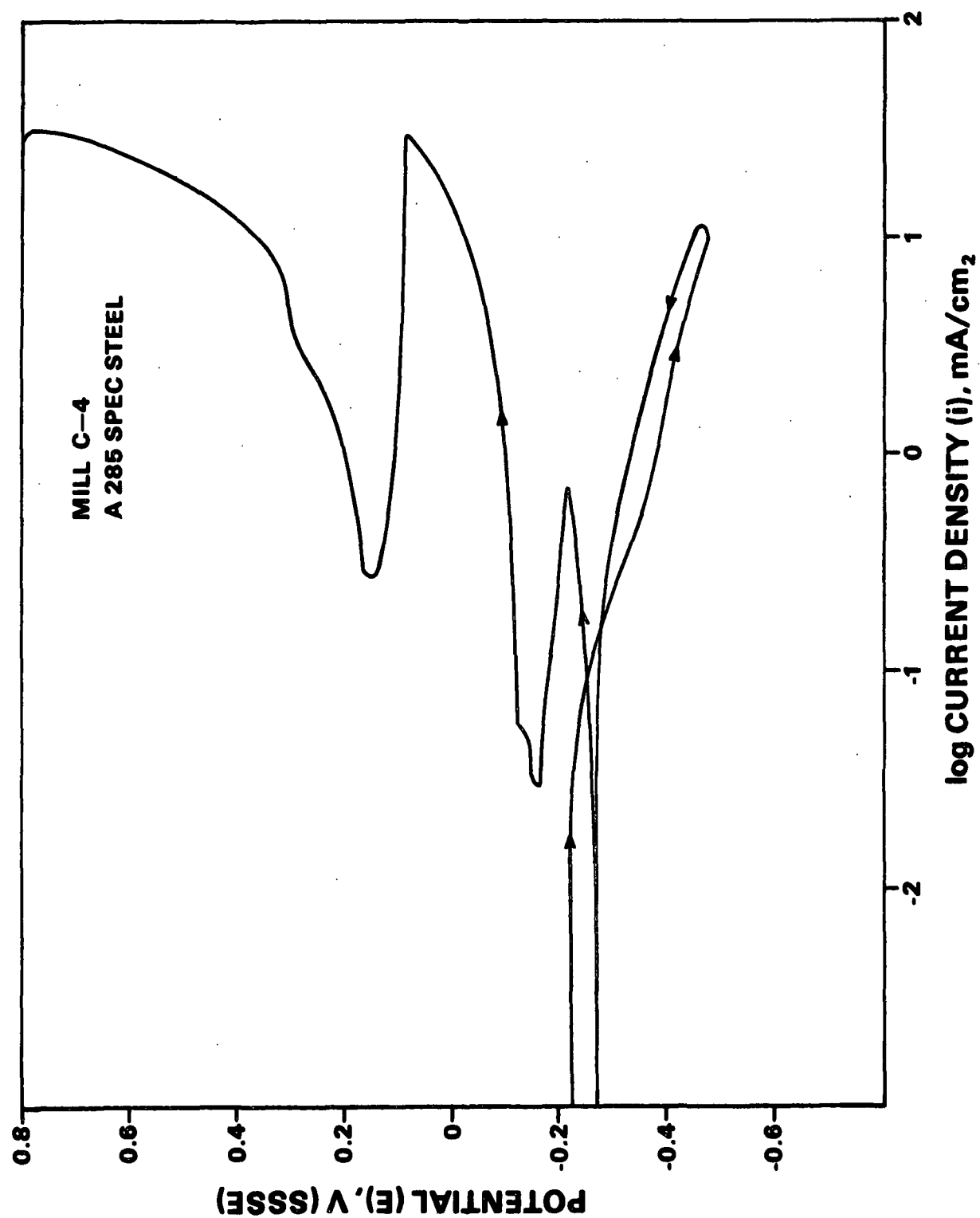


Figure 81. Mill C4. A285-SPECIAL.

IPST HASELTON LIBRARY



5 0602 01057253 7

